Role of Epoxyeicosatrienoic Acids in Protecting Against Ischemic Cardiomyopathy

Theresa Aliwarga

A dissertation
submitted in partial fulfillment of the
requirements for the degree of

Doctor of Philosophy

University of Washington
2018

Reading Committee:
Rheem A. Totah, Chair
Allan E. Rettie
Libin Xu

Program Authorized to Offer Degree:
Medicinal Chemistry

University of Washington

Abstract

Role of Epoxyeicosatrienoic Acids in Protecting Against Ischemic Cardiomyopathy

Theresa Aliwarga

Chair of the Supervisory Committee:
Associate Professor, Rheem A. Totah
Medicinal Chemistry

Epoxyeicosatrienoic acids (EETs) are metabolites of arachidonic acid (AA) epoxidation with important cardioprotective and signaling properties. AA is a twenty carbon ω-6 polyunsaturated fatty acid containing four *cis*-double bonds. Like other PUFAs, both free and membrane-bound AA undergo autoxidation in the presence of initiators such as air, light, heat, and transition metal ions. While autoxidation yields both *cis*- and *trans*-EETs with preference to the later, cytochrome P450 (CYP) epoxygenases, especially CYP2J2, exclusively catalyze the formation of all regioisomer of *cis*-EETs.

The overall goals of this dissertation were to elucidate the formation of enzymatic and non-enzymatic EETs during P450 incubations and in biological systems and determine the protective role EETs play during ischemic cardiomyopathy. To achieve these goals, we used *in*

vitro systems, a mouse model that overexpresses human CYP2J2 in the heart cardiomyocytes, and tissue from diseased and control human subjects. In *in vitro* work, formation of EETs in free radical initiated reactions of AA in benzene and in liposomes exhibited time- and AA concentration-dependence and favored the formation of *trans*-EETs over *cis*-EETs. Experimental conditions were optimized to minimize non-enzymatic EET formation during P450 reactions by adding pyruvate, a hydrogen peroxide scavenger, and an iron chelating agent.

In the *in vivo* mouse model, stressors such as age and disease altered EET levels in transgenic (Tr) mice. EET levels in erythrocyte membranes increased with age while alterations appeared to be regioisomer-specific for cardiac EETs. Effects of acute ischemic cardiac events were evaluated in both a mouse model and human sudden cardiac arrest (SCA) subjects. Acute myocardial infarction in the mouse model increased both erythrocyte membrane and cardiac tissue *cis*- and *trans*-EETs in Tr mice, while human SCA cases had significantly lower EET levels in their erythrocyte membrane compared to the control group.

In ventricular cardiac tissue obtained from patients with cardiovascular disease and controls, EET levels were significantly higher in control tissue compared to diseased. Lower EET levels in diseased cardiac tissue were associated with lower protein expression of CYP2J2, NADPH-Cytochrome P450 oxidoreductase and soluble epoxide hydrolase. Finally, specific activity of CYP2J2 in hydroxylating the probe substrate, terfenadine was shown to be significantly decreased with lower levels of CYP2J2, the main cardiac epoxygenase, in diseased cardiac tissue. These results suggest that higher levels of EETs, specifically *cis*-EETs are cardioprotective, and that erythrocyte membrane of *cis*-EETs could potentially serve as surrogate markers to report on *cis*-EET levels in cardiac tissue.

TABLE OF CONTENTS

LIST OF FIGURES

LIST OF TABLES

ACKNOWLEDGEMENTS

I would like to thank my advisor, Dr. Rheem A. Totah for her guidance throughout my graduate studies. Rheem has been an inspiring mentor and a great advocate for all of her mentees. She has cultivated independence, persistence, and hard work in the training that I received. I am incredibly grateful for the support and the freedom that I was given to investigate interesting scientific observations and to learn from my mistakes. I know it has not been easy and there were many frustrating times working with me and unstable molecules like EETs. Thank you for your patience and understanding.

I would also like to thank past and present members of the Totah lab, Brianne Raccor, Jean Dinh, Eric Evangelista, Ben Maldonato, Christi Cho, Max Zeigler, Julie Denham, Xiaoyun Guo, and Byron Gallis for their help and support. Brianne and Jean have not only been great mentors, but also wonderful friends. I greatly appreciate their help and input. Eric's sassiness, Ben's cheerfulness, Christi's genuineness, and Max's insightfulness with our common interest in science certainly made graduate school experience that much better. I would like to specifically thank Xiaoyun for performing echocardiography and myocardial infarction on our mice. I am very lucky to have had the opportunity to work with so many wonderful and engaging people.

In addition, I would like to thank Dr. Kent L. Kunze, Dr. Allan E. Rettie, Dr. Libin Xu, and Dr. Edward J. Kelly for serving in my committee. I would like to thank Kent for staying on my committee in spite of his retirement. My committee members' thoughtful questions, constructive feedbacks, and advice helped me to scrutinize my data even more, to think outside the box, and to recognize both the limitations and implications of my research.

I would like to thank Dr. Nona Sotoodehnia and Dr. Rozenn Leimatre from Cardiovascular Health Research Unit at University of Washington for giving me access to the sudden cardiac arrest patient samples. I would also like to thank Dr. Qinghang Chris Liu from University of Washington Department of Physiology and Biophysics for his cardiovascular physiology expertise, Dr. Nahush Mokadam for giving us access to diseased cardiac tissues, Dr. Scott Heyward for the control human cardiac tissues, Dr. Darryl C. Zeldin at NIEHS for our transgenic mice.

My work relied heavily on mass spectrometry. Having properly functioning mass spectrometers was crucial. I would like to thank Ross F. Lawrence (retired), Dale Whittington, J Scott Edgar, and Tauri Senn for maintaining, teaching how to use and troubleshoot mass spectrometer machines.

Lastly, I would like to thank my family and friends. Coming from a conservative Chinese-Indonesian family, it is uncommon for a woman to pursue an advanced degree. Despite the ingrained traditional values, my father, Harun Aliwarga, has always been supportive of my academic pursuit. My late paternal grandmother, Kuiheni Wongsowarga, who had never had an official education in her life, but she had taught me a lot about conscientiousness and humility. My amazing siblings, especially my sister, Michelle A. Anderson, my brother, Stanley Aliwarga, and my sister-in-law, Vina Widyanti, who always love, encourage, and support me unconditionally. More importantly, my siblings gave me my nieces, Maddie and Audrey, and my nephew, Jaden, who are the source of my happiness. I am also very lucky to have my American parents, Ron and Kathy Margolis. They have taught, guided, loved, and supported me like their own daughter. I would also like to thank my best friend, Yohanes Putra, who has shared many life's ups and downs with me throughout the years.

DEDICATION

I would like to dedicate this dissertation to:

My two nieces, Claire Madeleine Aliwarga and Audrey Theresa Anderson

My nephew, Marc Jaden Aliwarga

Auntie Tess loves you. You hold very special places in my heart. I hope one day you will be inspired to pursue your dreams.

CHAPTER 1. INTRODUCTION

Human platelets, mononuclear cells, neutrophils, erythrocytes, skeletal muscle, and cardiac tissues contain between 9 and 25% of phospholipid fatty acids as AA (Calder, 2007). Based on its abundance in phospholipid membranes, AA is an important constituent of the cellular membrane. Besides affecting cellular membrane fluidity, AA is an important substrate of multiple enzymes whose products are both autocrine and paracrine mediators with varied biological functions. AA can be metabolized by cyclooxygenases to form prostaglandins and thromboxane, which are key regulators in inflammatory and immune responses, reproductive processes, and maintenance of vascular homeostasis (Jabbour and Sales, 2004; Ricciotti and FitzGerald, 2011). In addition, lipoxygenases can biotransform AA to leukotrienes, which are important for inflammatory and immune responses (Sharma and Mohammed; Liu and Yokomizo, 2015) (Figure 1.1).

Most importantly pertaining to this dissertation project, AA is biotransformed by cytochrome P450 epoxygenases, notably CYP2J2, to generate the cardioprotective epoxyeicosatrienoic acids (EETs). Therefore, it is necessary to understand the physicochemical properties of AA, the function, expression and regulation of CYP2J2 (the main epoxygenase in the heart) in cardiovascular disease (CVD), and the function, localization, and modulation of EETs in CVD.

1.1. PHYSICOCHEMICAL PROPERTIES OF ARACHIDONIC ACID

AA is a twenty carbon ω-6 polyunsaturated fatty acid (PUFA) containing four *cis*-double bonds. The double bonds are homoconjugated resulting in three *bis*-allylic methylene groups. In unactivated human platelets, the concentration of esterified AA was determined to be

approximately 5 mM using a mass per volume calculation (Brash, 2001). In human plasma, free AA ranges from 2.7 to 50 μM (Nishikiori et al., 2015; Wang et al., 2015). Despite the many biological studies focusing on AA, surprisingly, physicochemical properties of AA have not been thoroughly described in the literature. Most of the physicochemical properties of AA have been inferred from computational and experimental studies using linoleic acid (LA), a metabolic precursor of AA. In this subsection, pKa, solubility, partition coefficient (log P), and stability of AA will be described.

Based on a titration study using concentrations greater than 100 μM of LA, the pKa of AA was reported to be around 8 (Glickman and Klinman, 1995; Brash, 2001). This observation is unexpected as the pKa of aliphatic carboxylic acids is typically around 4.5. However, the carbon chain length, degree of unsaturation of fatty acids (FAs), and concentration of FAs have to be taken into consideration because these factors have been shown to affect the pKa of various FAs. Increasing the number of carbon atoms causes FAs to pack tighter onto themselves and subsequently shield the proton on the carboxylic acid, leading to an increase in pKa (Kanicky et al., 2000). Increasing the degree of unsaturation introduces more kinks in the chain, which prevent FAs from tight packing and lead to a decrease in pKa (Kanicky and Shah, 2002). In a similar titration study of LA, pKa values of LA decreased at concentrations lower than 100 μM (Glickman and Klinman, 1995).

AA is highly soluble in ethanol, dimethyl sulfoxide, and dimethyl formamide up to 100 mg/mL (328 mM) and up to 50 mg/mL (164 mM) in chloroform, and methanol, respectively (Sigma-Aldrich). However, AA, just like other FAs, is poorly soluble in water. It is a challenge to determine the solubility of FAs because FAs tend to associate with themselves either by forming monolayers or micelles. In summary data compiled by the Environmental Protection

Agency, the predicted water solubility of AA ranges between 0.1 to 72 μM (Agency). Depending on the carbon chain length, temperature, ionic environment, pH, FA concentration, and presence of proteins or lipoproteins, aqueous solubility of FAs varies widely. A study on saturated fatty acids in subcritical water showed that longer carbon chain length led to a decrease in aqueous solubility (Khuwijitjaru et al., 2002). In the same study, higher temperature improved solubility of FAs while pressure did not significantly affect the solubility. The presence of other ions in solution can affect the solubility of FAs, which are quite soluble in aqueous solution as their sodium or potassium salts. The sodium salt of AA, in particular, is soluble in water up to 16.4 mM (Sigma-Aldrich). However, precipitation of AA was observed in the presence of relatively high calcium ion concentrations (Brash, 2001). In addition, the solution pH and solute concentration affect solubility. The ionization state of the carboxylic acid on FAs will depend upon the pH of the solution. As described in the LA study, a lower concentration of LA led to decreased pKa. Therefore at physiological concentrations and pH, it would be expected that FAs would be increasingly soluble.

FAs have been shown to bind to human serum albumin, the most abundant protein in whole blood, as well as to fatty acid binding protein (FABP). When the molar ratio of AA to serum albumin was two or less, AA bound to serum albumin tightly (Purdon and Rao, 1989). The equilibrium dissociation constant of AA from human serum albumin has not been determined; however, one study reported that equilibrium dissociation constant of AA from bovine serum albumin at 38ºC to be approximately 25 μM (Bojesen and Bojesen, 1994). FABP is ubiquitously expressed in tissues that are actively involved in FA metabolism. FABP makes up approximately one to five percent of total soluble cytosolic proteins. FABP3, which is also known as Heart-FABP (H-FABP), is the most abundant cardiac FABP in mammalian heart

(Smathers and Petersen, 2011). While rat FABP3 has high affinity towards AA (K_d = 0.05 μM) (Widstrom et al., 2001), human FABP3 was reported to have a much lower K_d (0.37 μM) (Veerkamp et al., 1999). Another binding partner of AA is low density lipoprotein (LDL). LDL shuttles AA to platelets for further oxidation (Dobner and Engelmann, 1998). Binding to either serum albumin or FABP or LDL reduced the likelihood of AA to form micelles and improved delivery of AA to different tissue compartments for signaling, metabolism, membrane synthesis, storage, and activation of nuclear receptors (Smathers and Petersen, 2011),which implies an increase in apparent AA solubility under these conditions.

The partition coefficient of AA can also affect its solubility. Log P values are used as a measure of lipophilicity of small molecules. The more positive a log P value is, the more a molecule prefers to partition into lipophilic environment. Log P values of small molecules are usually used to predict absorption and ability to penetrate lipophilic barriers within the human body. Being an amphipathic molecule, the log P of AA, determined using liquid chromatography, is 6.98 (D'Amboise and Hanai, 1982). Based on this value, it is not surprising that AA is mostly found in phospholipid membranes. A ten-minute incubation of tritiated AA in human endothelial cells led to 83% incorporation of radioactive AA into the phospholipids with preference for phosphatidylcholine (about 50%) (Thomas et al., 1984).

Like other PUFAs, both free and membrane-bound AA undergoes autoxidation in the presence of initiators such as air, light, heat, and transition metal ions (Porter et al., 1979; Terao and Matsushita, 1981; Trotta et al., 1982; Nawar, 1984; Nakamura et al., 1997; Refsgaard et al., 2000). This process occurs via a free radical chain mechanism.

Free radical oxidation proceeds in three steps; initiation, propagation, and termination. An extensive description of each step is available (Yin et al., 2011). Briefly, both lipid and

initiator radicals are generated during the initiation step. During the propagation step, addition of molecular oxygen to the carbon radical on the lipid generates peroxyl radicals, which further propagates the chain by abstraction of a hydrogen atom from another lipid, or addition to a double bond. In the termination step, the lipid radicals can react with one another to form non radical products. Autoxidation of AA has been reported to produce a mixture of hydroperoxides and cyclic peroxides following the general mechanism depicted in Figure 1.2 (Yin et al., 2011). Six hydroperoxides were identified as the primary products of AA autoxidation; 15-hydroperoxyeicosatetraenoic acid (15-HPETE) (40%), 5-HPETE (27%), 11-HPETE (11%), 9-HPETE (9 %), 8-HPETE (7%), and 12-HPETE (6%) (Porter 1984). These HPETEs can then be further reduced to their alcohol derivatives, hydroxyeicosatetraenoic acids (HETEs). One group of cyclic peroxides formed during AA autoxidation is bicyclic endoperoxides generated through two steps of 5-*exo* cyclization of the lipid peroxyl radical. Further reduction of these bicyclic endoperoxides led to formation of isoprostanes, one of the major oxidation products of AA (Yin et al., 2007) (Figure 1.3).

Besides exogenous sources of free radicals such as tobacco smoke, pesticides, environmental pollutants, drugs like acetaminophen and radiation, several cellular organs and diseases are known to generate endogenous reactive oxygen species (ROS). Generally the cellular organs that produce ROS, such as mitochondria, peroxisomes, and endoplasmic reticulum (ER), consume a lot of oxygen in their cellular processes (Phaniendra et al., 2015). The ER contains cytochrome P450 enzymes (CYP) and uncoupling of the CYP catalytic cycle is known to produce ROS (Vaz et al., 1991). In particular, CYP2C isozymes have been suggested to be ROS generators in coronary endothelial cells (Fleming, 2001; Yang et al., 2001). In addition, CVD, diabetes, cancer, and neurodegenerative injury have been reported to be

associated with elevated levels of ROS (Flaherty and Weisfeldt, 1988; Lucas and Szweda, 1998; Davì et al., 2005; Shao and Heinecke, 2009; Barrera, 2012; Abeti et al., 2015).

1.2. CYP2J2 FUNCTION, EXPRESSION, AND REGULATION IN CVD

The CYP superfamily of membrane-bound NADPH-dependent heme-containing monooxygenases catalyzes the oxidation of both xenobiotics and endogenous compounds by inserting an oxygen atom from molecular oxygen into their products. The CYP2J2 gene contains nine exons and eight introns that span approximately 40.3 kilobases (kb), including about 6 kb of 5'- flanking region and about 1 kb of 3'-untranslated region (GenBank accession number AF272142) (King et al., 2002). This gene encodes 502 amino acids, which translates to approximately a protein of ~58 kDa. CYP2J2 is the only member of the human CYP2J family and one of the main epoxygenases alongside the CYP2C family. CYP2J2 catalyzes metabolism of AA to produce, exclusively, four regioisomers of *cis*-EETs (Wu et al., 1996).

CYP2J2 is mainly expressed in the heart, and to a lesser degree, in liver, kidney, skeletal muscle, lung, brain, pancreas, gastrointestinal tract, monocytes and macrophages (Wu et al., 1996; King et al., 2002; Dutheil et al., 2009; Bystrom et al., 2013). Protein expression of CYP2J2 in human livers does not vary as much as in human hearts (Wu et al., 1996). In a non-diseased human heart, CYP2J2 protein was found, via immunohistochemical staining, in cardiomyocytes and endothelium of blood vessels (Delozier et al., 2007). In a separate study, CYP2J2 was also found in both small and large human coronary arteries (Node et al., 1999). Overexpression of CYP2J2 has been reported to be protective in several disease states, including CVD. In monocrotaline-induced pulmonary hypertensive Sprague-Dawley rats, CYP2J2 gene therapy attenuated vascular remodeling and development of pulmonary arterial hypertension (Zheng et al., 2010). Overexpression of cardiac CYP2J2 in a C57/BL6 mouse model has also

been shown to lower arrhythmia susceptibility in cardiac hypertrophy and to improve left ventricular recovery post ischemic-reperfusion injury (Seubert et al., 2004; Westphal et al., 2013).

Expression of CYP2J2 can be regulated by xenobiotics, changes associated with disease states, microRNA and single nucleotide polymorphisms (SNPs). Expression of CYP2J2 was not altered with typical CYP inducers in primary adult ventricular myocytes (Evangelista et al., 2013). However, increases in CYP2J2 transcript after four hours and protein after 24 hours were observed in human peripheral blood mononuclear cells (PBMC) exposed to bacterial lipopolysaccharides (LPS)(Bystrom et al., 2013). An elevated level of tumor necrosis factor -α (TNF-α), an inflammatory cytokine produced by macrophages during acute inflammation, was shown to induce expression of CYP2J2 in the human first trimester trophoblast-derived cell line, SGHP-4 (Herse et al., 2012). In a murine model, modest upregulation of cardiac CYP2J2 was observed in cocaine-treated mice (Wang et al., 2002). In human pulmonary squamous cancer cells, expression of CYP2J2 was reported to be inversely proportional to expression of let-7b, a highly conserved microRNA across many species (Chen et al., 2012). Recently, microRNAs have received more attention for their contribution to the regulation of gene expression. Several different microRNAs have been reported to be involved in cardiac development and to be modulated in CVD pathologies. Upregulation of these microRNAs including let-7, miR-19, miR-20 to name a few, has been shown in CVDs including myocardial infarction (MI), ischemic cardiomyopathy, and dilated cardiomyopathy (Ikeda et al., 2007; Luo et al., 2010).

Similar to other CYP isozymes, CYP2J2 is polymorphically expressed throughout the population. The polymorphisms of CYP2J2 identified to date are rare, and are ethnic group specific, with the exception of *CYP2J2*7.* This allele represents a G>T substitution in the

promoter region (-50 bp), which results in reduced binding of transcription factor Sp1 (King et al., 2002). *CYP2J2*7* was found in different ethnic groups with allelic frequencies ranging from 1.1-17% (King et al., 2002; Polonikov et al., 2007). In a Caucasian population, studies have shown that the *CYP2J2*7* allele has about 40% lower protein expression without any significant change in enzyme activity (Yamazaki et al., 2006). The presence of the CYP2J2*7 allele in the African-American population was associated with a significantly lower risk of CAD, while an increased risk of CAD was observed in the Caucasian population (Spiecker et al., 2004; Lee et al., 2007). Another study in high risk cardiovascular patients in Germany did not find a significant association between CYP2J2*7 and the risk of developing MI (Börgel et al., 2008). However, there were two different studies that found *CYP2J2*7* allele increased risk of developing premature MI in the Taiwanese population and MI in a predominantly Caucasian population (Liu et al., 2007; Marciante et al., 2008). The association of the CYP2J2*7 allele and CVD risk in various ethnic groups is summarized in Table 1.

1.3. LOCALIZATION AND FUNCTIONS OF EETS AND ALTERATION OF EET LEVELS IN CVD

Phospholipase A_2 (PLA_2) catalyzes the hydrolysis of phospholipids at the *sn*-2 position, leading to free fatty acids and lysophospholipids. According to structure, catalytic mechanism and localization, six families of PLA_2 are recognized. Found only in vertebrates and widely expressed in mammalian cells, the cytosolic $PLA_2\alpha$ group IVA has been identified as the major PLA_2 that releases AA from the membrane (Murakami et al., 2011). Following binding of calcium ion to the C2 domain of PLA_2, the enzyme is translocated to the perinuclear membrane where it is further activated by phosphorylation on several of its serine residues, including

serine-505 and serine-515 by extracellular regulated kinase 1/2 (ERK 1/2) and serine-727 mitogen-activated protein kinase (MAPK) interacting kinase-1 (Hefner et al., 2000; Pavicevic et al., 2008). Upon activation of PLA_2, AA is released and metabolized through various pathways, including cyclooxygenases, lipoxygenases and CYPs (Bellien et al., 2011)(Figure 1.1). Through the CYP pathway, and primarily by CYP2C and CYP2J subfamilies, AA is metabolized to four bioactive regioisomers of *cis*-EETs (Capdevila et al., 2000). *Cis*-EETs are rapidly hydrolyzed to less biologically active dihydroxyeicosatrienoic acids (DHETs) by soluble epoxide hydrolase (sEH) *in vivo* (Yu et al., 2000). Like AA, EETs can be re-esterified back into the membrane via an acyl-coenzyme A-dependent mechanism (Weintraub et al., 1997). *Cis*-EETs can also circulate in erythrocyte membranes, plasma phospholipid and be bound to plasma lipoproteins and FABP (Karara et al., 1992; Fang et al., 1995; Jiang et al., 2005; Jiang et al., 2010). The erythrocyte membrane has been suggested as a reservoir for both *cis*- and *trans*-EETs and to be the predominant source of plasma EETs (Jiang et al., 2005). In two male adults, half of the EETs in circulating lipoprotein were bound to HDL (49%) followed by LDL (28%), and VLDL (23%) (Karara et al., 1992). EETs also bind to FABP with a 7.4 to 34 fold lower affinities compared to AA (Widstrom et al., 2001). Due to the intrinsic instability of EETs, the binding of EETs to FABP may maintain intracellular retention of EETs as well as prevent hydrolysis by sEH, thereby prolonging the duration of EETs' biological activity (Widstrom et al., 2001).

In order to exert EETs' physiological effects, EETs are putatively believed to bind to and stimulate a receptor(s) activating signaling cascades. These signaling cascades include the MAPK-associated pathways, such as JNK/c-Jun (Ma et al., 2012) and the PI3K/Akt (Yang et al., 2007). There have been several attempts to identify the endogenous EET receptor to date, with a few studies showing EET activation of PPARα (Ng et al., 2007; Wray et al., 2009) and therefore

control over PPARα regulated genes. Recent work by Park et al. identified the G-protein coupled receptor GPR40, also known as free fatty acid receptor 1 (FFA1), as a possible target for EETs in the vascular system (Park et al., 2018). Specifically, they were able to show that EETs can alter the Ca^{2+} flux in HEK293 cells expressing GPR40 and mediate the relaxation of bovine arteries and affect the whole cell potassium currents of HUVEC cells expressing GPR40. Additionally, treatment with GPR40 antagonist mitigated EETs' ability to increase intracellular calcium concentration in both cell systems (Park et al., 2018). GPR40 is expressed primarily in the pancreas and the brain, at both the mRNA and protein levels (Stoddart et al., 2008; Mancini and Poitout, 2013), as well as in the liver, heart, and skeletal muscle at an mRNA level (Kotarsky et al., 2003; Stoddart et al., 2008). While this finding is exciting and the first report identifying an "EET receptor" more work is needed to determine if the GPR40 is also the receptor for EETs in cardiomyocytes.

Pleiotropic effects of *cis*-EETs have been widely reported in the literature. Some of physiological functions of EETs in the vascular system include modulation of vascular tone, anti-inflammatory properties, migratory and proliferative of vascular endothelial and smooth muscle cells, as well as anti-platelet aggregation properties (Sudhahar et al., 2010). In contrast, studies on the function of *trans*-EETs are scarce. Lipid peroxidation *in vitro* is reported to generate both *cis*- and *trans*- EETs with a preference for *trans*-EETs (Aliwarga et al., 2017). Indeed an *ex vivo* study reported that *trans*-14,15-EET is approximately 10-fold more potent than *cis*-14,15-EET in relaxing rat preconstricted arcuate arteries (Jiang et al., 2011). Ultimately, EETs protect the cardiovascular system through different mechanisms, but the importance of *cis*- vs. *trans*-EETs has not been elucidated.

In humans, several disease states have been shown to affect EET levels. Both obese and non-obese CAD patients were reported to have significantly higher total EET levels compared to healthy volunteers (Theken et al., 2012). In contrast, another study by the same group reported that there were significantly lower total plasma EETs in obstructive CAD patients than in healthy volunteers (Oni-Orisan et al., 2016). These authors suggested that the contradictory results in their studies were due to significant differences in the soluble epoxide hydrolase activity, as indicated by the ratio of 14,15-EET to DHET.

1.4. HYPOTHESES AND SPECIFIC AIMS

The main goal of this study is to elucidate the protective role of EETs in ischemic cardiomyopathy. Understanding and validating formation of enzymatic and non-enzymatic EETs were undertaken in this dissertation project. An emphasis is placed on the optimization of *in vitro* AA incubations in reconstituted recombinant CYP2J2, which highlights the difficulty in accurately diluting AA and limiting non-enzymatic products. To evaluate how ischemia-associated cardiac events affect EET levels in both human and mouse models, levels of EET were quantified and compared from RBC of control and sudden cardiac arrest patients and from RBC and heart tissue of wild-type (WT) and cardiac-specific overexpressing CYP2J2 transgenic (Tr) mice that were subjected to sham or MI surgery. In addition, the effect of age on EET levels and the correlation between EET levels in the RBC membrane and cardiac tissue of WT and Tr mice were assessed. Finally, protein levels involved in biotransformation and degradation of EETs were measured, which provided insight of how CVD affect the regulation of those enzymes. The hypotheses for this dissertation project and the specific aims to test them are as follows:

1. CYP2J2 exclusively forms *cis*-EETs, while both *cis*- and *trans*-EETs are generated through autoxidation.
2. Higher levels of circulating EETs are protective against ischemia-associated cardiac events.

The two hypotheses will be addressed in six aims that encompass both *in vitro* and *in vivo* studies:

Aim 1. Determine (A) the time- and (B) the AA concentration-dependence of *cis*- and *trans*-EET formation due to free radical oxidation in benzene and liposomes (Chapter 2)

Aim 2. (A) Demonstrate that CYP2J2 produces *cis*-EETs, but not *trans*-EETs. (B) Optimize *in vitro* incubation conditions using recombinant CYP2J2 to minimize autoxidation and *trans*-EET formation (Chapter 2).

Aim 3. (A) Determine the EET levels in heart and RBC membrane of WT and Tr mice that overexpress human CYP2J2 in their cardiac tissue. (B) Determine if a correlation exists between the endogenous EETs in the cardiac tissue and RBC membranes of WT and Tr mice (C) Determine the effect of age on EET levels in heart and RBC membranes of WT and Tr mice (Chapter 3).

Aim 4. Subject WT and Tr mice to acute MI. (A) Determine levels of ROS, extent of fibrosis and apoptosis, and changes in cardiac structure and function using echocardiography between the two groups. (B) Measure EET levels in heart tissue and RBC membrane of sham vs MI groups (Chapter 3).

Aim 5. Compare *cis*- and *trans*-EET levels in RBC membranes of SCA patients and controls (Chapter 3).

Aim 6. (A) Determine the levels of sEH, POR and CYP2J2 in healthy vs. diseased human hearts. (B) Measure the levels of EETs in healthy vs. diseased hearts and correlate with the activity of CYP2J2 using terfenadine as a probe substrate (Chapter 4).

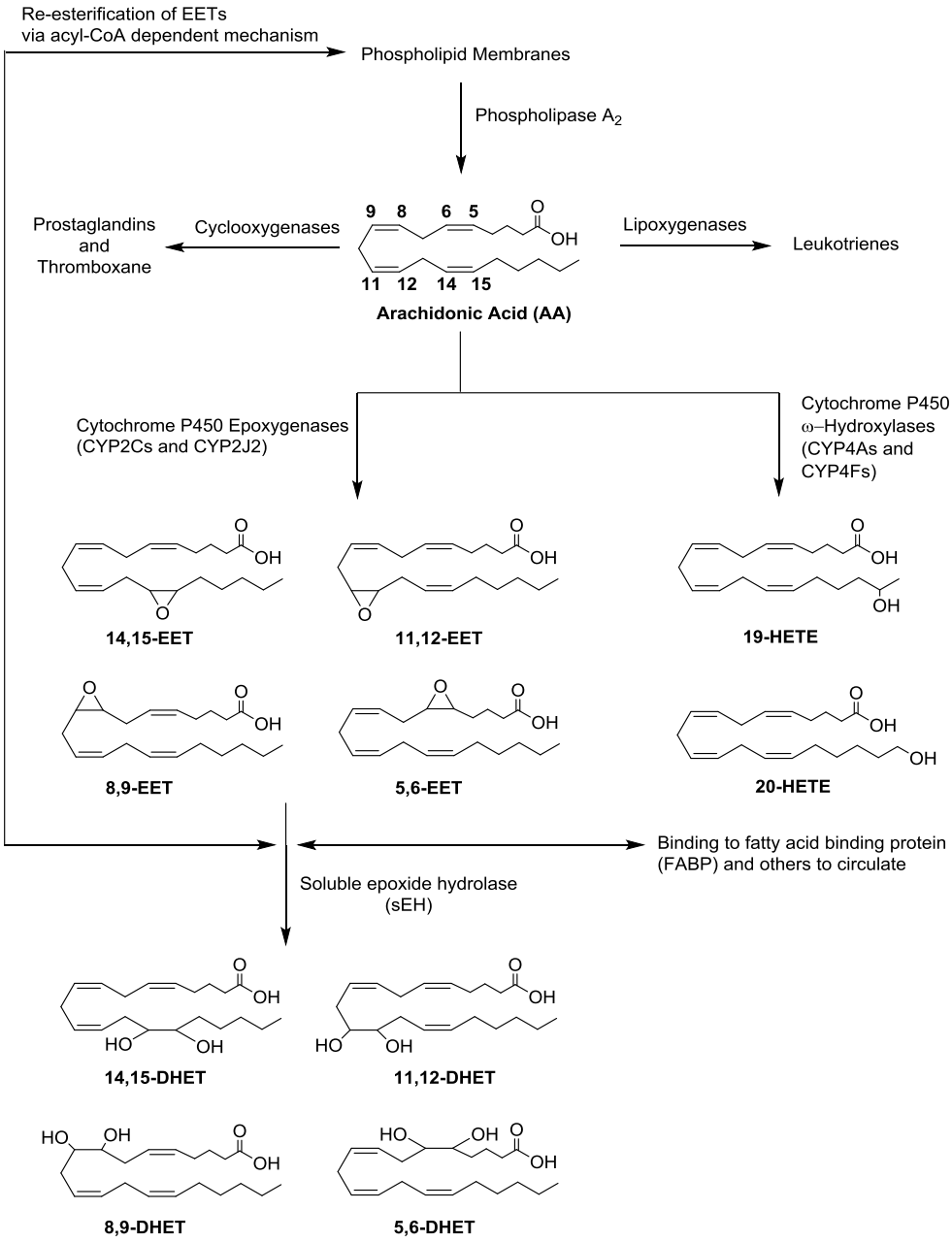

Figure 1.1. AA metabolic pathway focusing on the formation of CYP mediated eicosanoids. Upon activation of phospholipase A_2, AA is released from the phospholipid membrane. AA can be metabolized by cyclooxygenases to generate prostaglandins and thromboxanes or by lipoxygenases to form leukotrienes. The CYP ω–hydroxylases, notably the CYP4A and CYP4F sub-families, will convert AA to either 19- or 20-HETE, while CYP epoxygenases, namely CYP2Cs and CYP2J2, will mediate biotransformation of AA exclusively to four regioisomers of *cis*-EETs. Once formed, EETs can either be incorporated back into the phospholipid membrane via acyl-CoA dependent mechanism or bound to other proteins to circulate, or be hydrolyzed by sEH to generate DHETs.

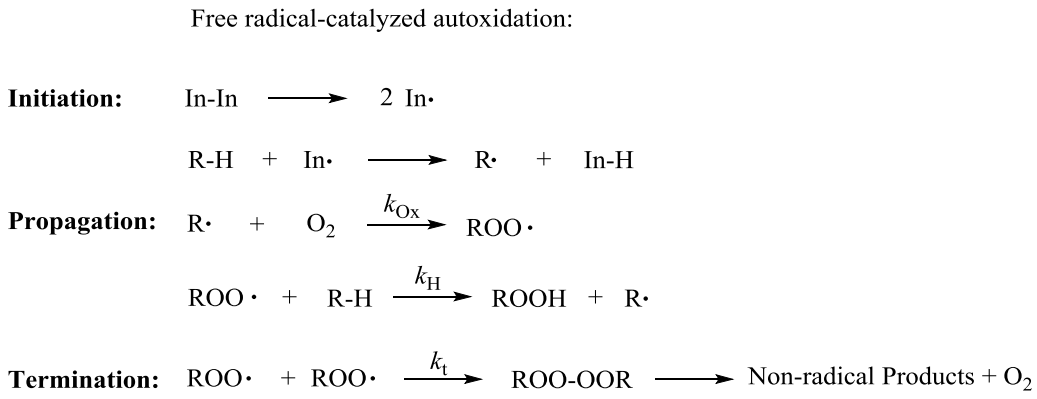

Figure 1.2. General scheme of free radical chain oxidation reaction mechanism.

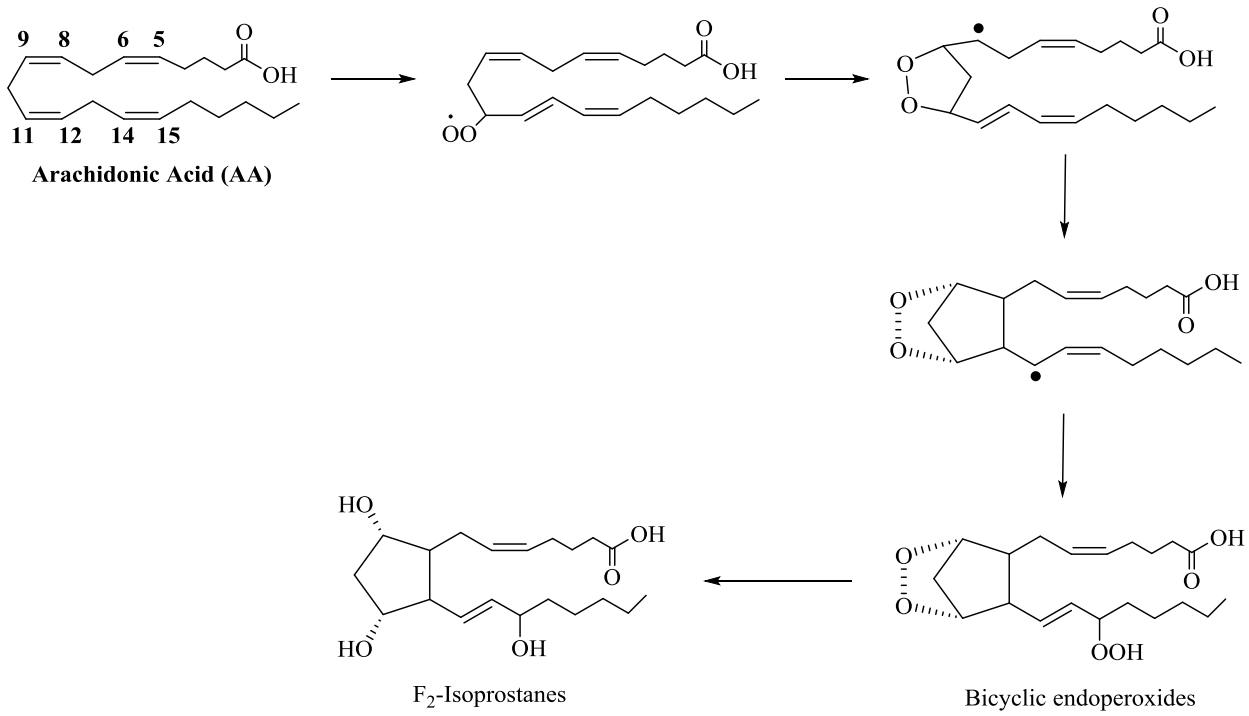

Figure 1.3. Generation of bicyclic endoperoxides through two steps of 5-*exo* cyclization of lipid peroxyl radical and conversion to isoprostanes through subsequent reduction.

Table 1.1. Summary of the effect of *CYP2J2*7* in altering the risk associated with developing cardiovascular dysfunction in different ethnic groups.

Disease state	Population	Risk	Significant association	References
Premature myocardial infarction	Taiwanese	Increased	Yes	(Liu et al., 2007)
Myocardial infarction (MI)	Germanic	None	No	(Börgel et al., 2008)
	Caucasian in Western Washington state	Increased	Yes	(Marciante et al., 2008)
	South Indian	Increased	Yes	(Arun Kumar et al., 2015)
Ischemic stroke	Chinese Han	Increased	Yes	(Li et al., 2015; Wang et al., 2017)
Atherosclerosis	African-American	Decreased	Yes	(Lee et al., 2007)
	Caucasian from central Germany	Increased	Yes	(Spiecker et al., 2004)

REFERENCES

Abeti R, Uzun E, Renganathan I, Honda T, Pook MA, and Giunti P (2015) Targeting lipid peroxidation and mitochondrial imbalance in Friedreich's ataxia. *Pharmacol Res* **99:**344-350.

Agency USEP Arachidonic acid.

Aliwarga T, Raccor BS, Lemaitre RN, Sotoodehnia N, Gharib SA, Xu L, and Totah RA (2017) Enzymatic and free radical formation of cis- and trans- epoxyeicosatrienoic acids in vitro and in vivo. *Free Radic Biol Med* **112:**131-140.

Arun Kumar AS, Kumar SS, Umamaheswaran G, Kesavan R, Balachandar J, and Adithan C (2015) Association of CYP2C8, CYP2C9 and CYP2J2 gene polymorphisms with myocardial infarction in South Indian population. *Pharmacol Rep* **67:**97-101.

Barrera G (2012) Oxidative stress and lipid peroxidation products in cancer progression and therapy. *ISRN Oncol* **2012:**137289.

Bellien J, Joannides R, Richard V, and Thuillez C (2011) Modulation of cytochrome-derived epoxyeicosatrienoic acids pathway: a promising pharmacological approach to prevent endothelial dysfunction in cardiovascular diseases? *Pharmacol Ther* **131:**1-17.

Bojesen IN and Bojesen E (1994) Binding of arachidonate and oleate to bovine serum albumin. *J Lipid Res* **35:**770-778.

Brash AR (2001) Arachidonic acid as a bioactive molecule. *J Clin Invest* **107:**1339-1345.

Bystrom J, Thomson SJ, Johansson J, Edin ML, Zeldin DC, Gilroy DW, Smith AM, and Bishop-Bailey D (2013) Inducible CYP2J2 and its product 11,12-EET promotes bacterial phagocytosis: a role for CYP2J2 deficiency in the pathogenesis of Crohn's disease? *PLoS One* **8:**e75107.

Börgel J, Bulut D, Hanefeld C, Neubauer H, Mügge A, Epplen JT, Holland-Letz T, and Spiecker M (2008) The CYP2J2 G-50T polymorphism and myocardial infarction in patients with cardiovascular risk profile. *BMC Cardiovasc Disord* **8:**41.

Calder PC (2007) Dietary arachidonic acid: harmful, harmless or helpful? *Br J Nutr* **98:**451-453.

Capdevila JH, Falck JR, and Harris RC (2000) Cytochrome P450 and arachidonic acid bioactivation. Molecular and functional properties of the arachidonate monooxygenase. *J Lipid Res* **41:**163-181.

Chen F, Chen C, Yang S, Gong W, Wang Y, Cianflone K, Tang J, and Wang DW (2012) Let-7b inhibits human cancer phenotype by targeting cytochrome P450 epoxygenase 2J2. *PLoS One* **7:**e39197.

D'Amboise M and Hanai T (1982) Hydrophobicity and retention in reversed phase liquid chromatography. *Journal of Liquid Chromatography* **5:**229-244.

Davì G, Falco A, and Patrono C (2005) Lipid peroxidation in diabetes mellitus. *Antioxid Redox Signal* **7:**256-268.

Delozier TC, Kissling GE, Coulter SJ, Dai D, Foley JF, Bradbury JA, Murphy E, Steenbergen C, Zeldin DC, and Goldstein JA (2007) Detection of human CYP2C8, CYP2C9, and CYP2J2 in cardiovascular tissues. *Drug Metab Dispos* **35:**682-688.

Dobner P and Engelmann B (1998) Low-density lipoproteins supply phospholipid-bound arachidonic acid for platelet eicosanoid production. *Am J Physiol* **275:**E777-784.

Dutheil F, Dauchy S, Diry M, Sazdovitch V, Cloarec O, Mellottée L, Bièche I, Ingelman-Sundberg M, Flinois JP, de Waziers I, Beaune P, Declèves X, Duyckaerts C, and Loriot MA (2009) Xenobiotic-metabolizing enzymes and transporters in the normal human brain: regional and cellular mapping as a basis for putative roles in cerebral function. *Drug Metab Dispos* **37:**1528-1538.

Evangelista EA, Kaspera R, Mokadam NA, Jones JP, and Totah RA (2013) Activity, inhibition, and induction of cytochrome P450 2J2 in adult human primary cardiomyocytes. *Drug Metab Dispos* **41:**2087-2094.

Fang X, VanRollins M, Kaduce TL, and Spector AA (1995) Epoxyeicosatrienoic acid metabolism in arterial smooth muscle cells. *J Lipid Res* **36:**1236-1246.

Flaherty JT and Weisfeldt ML (1988) Reperfusion injury. *Free Radic Biol Med* **5:**409-419.

Fleming I (2001) Cytochrome p450 and vascular homeostasis. *Circ Res* **89:**753-762.

Glickman MH and Klinman JP (1995) Nature of rate-limiting steps in the soybean lipoxygenase-1 reaction. *Biochemistry* **34:**14077-14092.

Hefner Y, Borsch-Haubold AG, Murakami M, Wilde JI, Pasquet S, Schieltz D, Ghomashchi F, Yates JR, Armstrong CG, Paterson A, Cohen P, Fukunaga R, Hunter T, Kudo I, Watson SP, and Gelb MH (2000) Serine 727 phosphorylation and activation of cytosolic phospholipase A2 by MNK1-related protein kinases. *J Biol Chem* **275:**37542-37551.

Herse F, Lamarca B, Hubel CA, Kaartokallio T, Lokki AI, Ekholm E, Laivuori H, Gauster M, Huppertz B, Sugulle M, Ryan MJ, Novotny S, Brewer J, Park JK, Kacik M, Hoyer J, Verlohren S, Wallukat G, Rothe M, Luft FC, Muller DN, Schunck WH, Staff AC, and Dechend R (2012) Cytochrome P450 subfamily 2J polypeptide 2 expression and circulating epoxyeicosatrienoic metabolites in preeclampsia. *Circulation* **126:**2990-2999.

Ikeda S, Kong SW, Lu J, Bisping E, Zhang H, Allen PD, Golub TR, Pieske B, and Pu WT (2007) Altered microRNA expression in human heart disease. *Physiol Genomics* **31:**367-373.

Jabbour HN and Sales KJ (2004) Prostaglandin receptor signalling and function in human endometrial pathology. *Trends Endocrinol Metab* **15:**398-404.

Jiang H, Anderson GD, and McGiff JC (2010) Red blood cells (RBCs), epoxyeicosatrienoic acids (EETs) and adenosine triphosphate (ATP). *Pharmacol Rep* **62:**468-474.

Jiang H, Quilley J, Doumad AB, Zhu AG, Falck JR, Hammock BD, Stier CT, and Carroll MA (2011) Increases in plasma trans-EETs and blood pressure reduction in spontaneously hypertensive rats. *Am J Physiol Heart Circ Physiol* **300:**H1990-1996.

Jiang H, Quilley J, Reddy LM, Falck JR, Wong PY, and McGiff JC (2005) Red blood cells: reservoirs of cis- and trans-epoxyeicosatrienoic acids. *Prostaglandins Other Lipid Mediat* **75:**65-78.

Kanicky JR, Poniatowski AF, Mehta NR, and Shah DO (2000) Cooperativity among molecules at interfaces in relation to various technological processes: effect of chain length on the pKa. *Langmuir* **16:**172-177.

Kanicky JR and Shah DO (2002) Effect of degree, type, and position of unsaturation on the pKa of long-chain fatty acids. *J Colloid Interface Sci* **256:**201-207.

Karara A, Wei S, Spady D, Swift L, Capdevila JH, and Falck JR (1992) Arachidonic acid epoxygenase: structural characterization and quantification of epoxyeicosatrienoates in plasma. *Biochem Biophys Res Commun* **182:**1320-1325.

Khuwijitjaru P, Adachi S, and Matsuno R (2002) Solubility of saturated fatty acids in water at elevated temperatures. *Biosci Biotechnol Biochem* **66:**1723-1726.

King LM, Ma J, Srettabunjong S, Graves J, Bradbury JA, Li L, Spiecker M, Liao JK, Mohrenweiser H, and Zeldin DC (2002) Cloning of CYP2J2 gene and identification of functional polymorphisms. *Mol Pharmacol* **61:**840-852.

Kotarsky K, Nilsson NE, Flodgren E, Owman C, and Olde B (2003) A human cell surface receptor activated by free fatty acids and thiazolidinedione drugs. *Biochem Biophys Res Commun* **301:**406-410.

Lee CR, North KE, Bray MS, Couper DJ, Heiss G, and Zeldin DC (2007) CYP2J2 and CYP2C8 polymorphisms and coronary heart disease risk: the Atherosclerosis Risk in Communities (ARIC) study. *Pharmacogenet Genomics* **17:**349-358.

Li Q, Zhao JH, Ma PJ, Su LL, Tao SB, and Ji SB (2015) Association of CYP2J2 gene polymorphisms with ischemic stroke. *Int J Clin Exp Med* **8:**8163-8167.

Liu M and Yokomizo T (2015) The role of leukotrienes in allergic diseases. *Allergol Int* **64:**17-26.

Liu PY, Li YH, Chao TH, Wu HL, Lin LJ, Tsai LM, and Chen JH (2007) Synergistic effect of cytochrome P450 epoxygenase CYP2J2*7 polymorphism with smoking on the onset of premature myocardial infarction. *Atherosclerosis* **195:**199-206.

Lucas DT and Szweda LI (1998) Cardiac reperfusion injury: aging, lipid peroxidation, and mitochondrial dysfunction. *Proc Natl Acad Sci U S A* **95:**510-514.

Luo X, Zhang H, Xiao J, and Wang Z (2010) Regulation of human cardiac ion channel genes by microRNAs: theoretical perspective and pathophysiological implications. *Cell Physiol Biochem* **25:**571-586.

Ma J, Zhang L, Han W, Shen T, Ma C, Liu Y, Nie X, Liu M, Ran Y, and Zhu D (2012) Activation of JNK/c-Jun is required for the proliferation, survival, and angiogenesis induced by EET in pulmonary artery endothelial cells. *J Lipid Res* **53:**1093-1105.

Mancini AD and Poitout V (2013) The fatty acid receptor FFA1/GPR40 a decade later: how much do we know? *Trends Endocrinol Metab* **24:**398-407.

Marciante KD, Totah RA, Heckbert SR, Smith NL, Lemaitre RN, Lumley T, Rice KM, Hindorff LA, Bis JC, Hartman B, and Psaty BM (2008) Common variation in cytochrome P450 epoxygenase genes and the risk of incident nonfatal myocardial infarction and ischemic stroke. *Pharmacogenet Genomics* **18:**535-543.

Murakami M, Taketomi Y, Miki Y, Sato H, Hirabayashi T, and Yamamoto K (2011) Recent progress in phospholipase A_2 research: from cells to animals to humans. *Prog Lipid Res* **50:**152-192.

Nakamura T, Bratton DL, and Murphy RC (1997) Analysis of epoxyeicosatrienoic and monohydroxyeicosatetraenoic acids esterified to phospholipids in human red blood cells by electrospray tandem mass spectrometry. *J Mass Spectrom* **32:**888-896.

Nawar WW (1984) Chemical changes in lipids produced by thermal processing. *Journal of Chemical Education* **61:**299-302.

Ng VY, Huang Y, Reddy LM, Falck JR, Lin ET, and Kroetz DL (2007) Cytochrome P450 eicosanoids are activators of peroxisome proliferator-activated receptor alpha. *Drug Metab Dispos* **35:**1126-1134.

Nishikiori M, Iizuka H, Ichiba H, Sadamoto K, and Fukushima T (2015) Determination of free fatty acids in human serum by HPLC with fluorescence detection. *J Chromatogr Sci* **53:**537-541.

Node K, Huo Y, Ruan X, Yang B, Spiecker M, Ley K, Zeldin DC, and Liao JK (1999) Anti-inflammatory properties of cytochrome P450 epoxygenase-derived eicosanoids. *Science* **285:**1276-1279.

Oni-Orisan A, Edin ML, Lee JA, Wells MA, Christensen ES, Vendrov KC, Lih FB, Tomer KB, Bai X, Taylor JM, Stouffer GA, Zeldin DC, and Lee CR (2016) Cytochrome P450-derived epoxyeicosatrienoic acids and coronary artery disease in humans: a targeted metabolomics study. *J Lipid Res* **57:**109-119.

Park SK, Herrnreiter A, Pfister SL, Gauthier KM, Falck BA, Falck JR, and Campbell WB (2018) GPR40 is a low-affinity epoxyeicosatrienoic acid receptor in vascular cells. *J Biol Chem* **293:**10675-10691.

Pavicevic Z, Leslie CC, and Malik KU (2008) cPLA2 phosphorylation at serine-515 and serine-505 is required for arachidonic acid release in vascular smooth muscle cells. *J Lipid Res* **49:**724-737.

Phaniendra A, Jestadi DB, and Periyasamy L (2015) Free radicals: properties, sources, targets, and their implication in various diseases. *Indian J Clin Biochem* **30:**11-26.

Polonikov AV, Ivanov VP, Solodilova MA, Khoroshaya IV, Kozhuhov MA, and Panfilov VI (2007) Promoter polymorphism G-50T of a human CYP2J2 epoxygenase gene is associated with common susceptibility to asthma. *Chest* **132:**120-126.

Porter NA, Wolf RA, Yarbro EM, and Weenen H (1979) The autoxidation of arachidonic acid: formation of the proposed SRS-A intermediate. *Biochem Biophys Res Commun* **89:**1058-1064.

Purdon AD and Rao AK (1989) Interaction of albumin, arachidonic acid and prostanoids in platelets. *Prostaglandins Leukot Essent Fatty Acids* **35:**213-218.

Refsgaard HH, Tsai L, and Stadtman ER (2000) Modifications of proteins by polyunsaturated fatty acid peroxidation products. *Proc Natl Acad Sci U S A* **97:**611-616.

Ricciotti E and FitzGerald GA (2011) Prostaglandins and inflammation. *Arterioscler Thromb Vasc Biol* **31:**986-1000.

Seubert J, Yang B, Bradbury JA, Graves J, Degraff LM, Gabel S, Gooch R, Foley J, Newman J, Mao L, Rockman HA, Hammock BD, Murphy E, and Zeldin DC (2004) Enhanced postischemic functional recovery in CYP2J2 transgenic hearts involves mitochondrial ATP-sensitive K+ channels and p42/p44 MAPK pathway. *Circ Res* **95:**506-514.

Shao B and Heinecke JW (2009) HDL, lipid peroxidation, and atherosclerosis. *J Lipid Res* **50:**599-601.

Sharma JN and Mohammed LA The role of leukotrienes in the pathophysiology of inflammatory disorders: Is there a case for revisiting leukotrienes as therapeutic targets?

Sigma-Aldrich Arachidonic acid, St. Louis, MO.

Smathers RL and Petersen DR (2011) The human fatty acid-binding protein family: evolutionary divergences and functions. *Hum Genomics* **5:**170-191.

Spiecker M, Darius H, Hankeln T, Soufi M, Sattler AM, Schaefer JR, Node K, Börgel J, Mügge A, Lindpaintner K, Huesing A, Maisch B, Zeldin DC, and Liao JK (2004) Risk of coronary artery disease associated with polymorphism of the cytochrome P450 epoxygenase CYP2J2. *Circulation* **110:**2132-2136.

Stoddart LA, Smith NJ, and Milligan G (2008) International Union of Pharmacology. LXXI. Free fatty acid receptors FFA1, -2, and -3: pharmacology and pathophysiological functions. *Pharmacol Rev* **60:**405-417.

Sudhahar V, Shaw S, and Imig JD (2010) Epoxyeicosatrienoic acid analogs and vascular function. *Curr Med Chem* **17:**1181-1190.

Terao J and Matsushita S (1981) The isomeric compositions of hydroperoxides produced by oxidation of arachidonic acid with singlet oxygen. *Agricultural and Biological Chemistry* **45:**587-593.

Theken KN, Schuck RN, Edin ML, Tran B, Ellis K, Bass A, Lih FB, Tomer KB, Poloyac SM, Wu MC, Hinderliter AL, Zeldin DC, Stouffer GA, and Lee CR (2012) Evaluation of cytochrome P450-derived eicosanoids in humans with stable atherosclerotic cardiovascular disease. *Atherosclerosis* **222:**530-536.

Thomas JM, Hullin F, Chap H, and Douste-Blazy L (1984) Phosphatidylcholine is the major phospholipid providing arachidonic acid for prostacyclin synthesis in thrombin-stimulated human endothelial cells. *Thromb Res* **34:**117-123.

Trotta RJ, Sullivan SG, and Stern A (1982) Lipid peroxidation and haemoglobin degradation in red blood cells exposed to t-butyl hydroperoxide. Effects of the hexose monophosphate shunt as mediated by glutathione and ascorbate. *Biochem J* **204:**405-415.

Vaz ADN, Roberts EA, and Coon MJ (1991) Olefin formation in the oxidative deformylation of aldehydes by cytochrome-P450. Mechanistic implications for catalysis by oxygen-derived peroxide. *J Am Chem Soc* **113:**5886-5887.

Veerkamp JH, van Moerkerk HT, Prinsen CF, and van Kuppevelt TH (1999) Structural and functional studies on different human FABP types. *Mol Cell Biochem* **192:**137-142.

Wang JF, Yang Y, Sullivan MF, Min J, Cai J, Zeldin DC, Xiao YF, and Morgan JP (2002) Induction of cardiac cytochrome p450 in cocaine-treated mice. *Exp Biol Med (Maywood)* **227:**182-188.

Wang SY, Xing PF, Zhang CY, and Deng BQ (2017) Association of CYP2J2 gene polymorphisms with ischemic stroke and stroke subtypes in Chinese population. *Medicine (Baltimore)* **96:**e6266.

Wang W, Qin S, Li L, Chen X, Wang Q, and Wei J (2015) An Optimized High Throughput Clean-Up Method Using Mixed-Mode SPE Plate for the Analysis of Free Arachidonic Acid in Plasma by LC-MS/MS. *Int J Anal Chem* **2015:**374819.

Weintraub NL, Fang X, Kaduce TL, VanRollins M, Chatterjee P, and Spector AA (1997) Potentiation of endothelium-dependent relaxation by epoxyeicosatrienoic acids. *Circ Res* **81:**258-267.

Westphal C, Spallek B, Konkel A, Marko L, Qadri F, DeGraff LM, Schubert C, Bradbury JA, Regitz-Zagrosek V, Falck JR, Zeldin DC, Müller DN, Schunck WH, and Fischer R (2013) CYP2J2 overexpression protects against arrhythmia susceptibility in cardiac hypertrophy. *PLoS One* **8:**e73490.

Widstrom RL, Norris AW, and Spector AA (2001) Binding of cytochrome P450 monooxygenase and lipoxygenase pathway products by heart fatty acid-binding protein. *Biochemistry* **40:**1070-1076.

Wray JA, Sugden MC, Zeldin DC, Greenwood GK, Samsuddin S, Miller-Degraff L, Bradbury JA, Holness MJ, Warner TD, and Bishop-Bailey D (2009) The epoxygenases CYP2J2 activates the nuclear receptor PPARalpha in vitro and in vivo. *PLoS One* **4:**e7421.

Wu S, Moomaw CR, Tomer KB, Falck JR, and Zeldin DC (1996) Molecular cloning and expression of CYP2J2, a human cytochrome P450 arachidonic acid epoxygenase highly expressed in heart. *J Biol Chem* **271:**3460-3468.

Yamazaki H, Okayama A, Imai N, Guengerich FP, and Shimizu M (2006) Inter-individual variation of cytochrome P4502J2 expression and catalytic activities in liver microsomes from Japanese and Caucasian populations. *Xenobiotica* **36:**1201-1209.

Yang B, Graham L, Dikalov S, Mason RP, Falck JR, Liao JK, and Zeldin DC (2001) Overexpression of cytochrome P450 CYP2J2 protects against hypoxia-reoxygenation injury in cultured bovine aortic endothelial cells. *Mol Pharmacol* **60:**310-320.

Yang S, Lin L, Chen JX, Lee CR, Seubert JM, Wang Y, Wang H, Chao ZR, Tao DD, Gong JP, Lu ZY, Wang DW, and Zeldin DC (2007) Cytochrome P-450 epoxygenases protect endothelial cells from apoptosis induced by tumor necrosis factor-alpha via MAPK and PI3K/Akt signaling pathways. *Am J Physiol Heart Circ Physiol* **293:**H142-151.

Yin H, Brooks JD, Gao L, Porter NA, and Morrow JD (2007) Identification of novel autoxidation products of the omega-3 fatty acid eicosapentaenoic acid in vitro and in vivo. *J Biol Chem* **282:**29890-29901.

Yin H, Xu L, and Porter NA (2011) Free radical lipid peroxidation: mechanisms and analysis. *Chem Rev* **111:**5944-5972.

Yu Z, Xu F, Huse LM, Morisseau C, Draper AJ, Newman JW, Parker C, Graham L, Engler MM, Hammock BD, Zeldin DC, and Kroetz DL (2000) Soluble epoxide hydrolase regulates hydrolysis of vasoactive epoxyeicosatrienoic acids. *Circ Res* **87:**992-998.

Zheng C, Wang L, Li R, Ma B, Tu L, Xu X, Dackor RT, Zeldin DC, and Wang DW (2010) Gene delivery of cytochrome p450 epoxygenase ameliorates monocrotaline-induced pulmonary artery hypertension in rats. *Am J Respir Cell Mol Biol* **43:**740-749.

CHAPTER 2.

ENZYMATIC AND FREE RADICAL FORMATION OF *CIS*- AND *TRANS*-EPOXYEICOSATRIENOIC ACIDS *IN VITRO* AND *IN VIVO*

This chapter was published, in part, in *Free Radic. Biol. Med.*, 2017, 112, pp 131-140

2.1. INTRODUCTION

Polyunsaturated fatty acids (PUFAs) in general are highly susceptible to free radical oxidation also known as lipid peroxidation. A recent review on reactions involved in lipid peroxidation can be found in Yin et al. (Yin et al., 2011). Many diseases such as diabetes and cardiovascular disease are associated with an imbalance of reactive oxygen species (ROS), which leads to increased oxidative stress and eventually increased lipid peroxidation. Free radical oxidation associated with lipid peroxidation is initiated by the formation of a lipid radical followed by a lipid peroxyl radical after molecular oxygen addition. The propagation step involves the reaction of the peroxyl radical by either abstraction of a hydrogen atom from another lipid molecule or addition to a double bond (Figures 2.1 A and 2.1 B, respectively). The radical formed after the addition reaction tends to undergo intramolecular homolytic substitution (S_Hi) to give an epoxide and an alkoxyl radical to continue the chain reaction. The detailed mechanism of peroxyl radical addition reactions has been discussed by Xu et al. (Xu and Porter, 2015). Lipid peroxidation in vivo has been linked to the underlying pathophysiology of various disease states, including atherosclerosis, myocardial ischemia-reperfusion injury, diabetes, cancer, and neurodegenerative injury (Lucas and Szweda, 1998; Davì et al., 2005; Shao and Heinecke, 2009; Barrera, 2012; Abeti et al., 2015).

Arachidonic acid (AA) is an essential ω-6 PUFA found mainly esterified at the *sn*-2 position of phospholipids. Like other PUFAs, AA is highly susceptible to lipid peroxidation leading to several products including hydroperoxides and isoprostanes (Yin et al., 2011). Almost all products of AA autoxidation reported previously were derived from the hydrogen atom-transfer peroxidation mechanism due to the high reactivity of AA as a hydrogen atom donor at

the *bis*-allylic position. In contrast, there is limited data on the peroxyl radical addition pathway during AA autoxidation, which is the focus of this chapter.

Release of arachidonic acid (AA) from membranes is tightly regulated in vivo and is calcium-dependent. Upon activation of phospholipase A_2, AA is hydrolyzed from phospholipids and subject to oxidation through various pathways, including the CYP pathway (Figure 2.2). It is well established that AA can be metabolized by multiple CYP isoforms to all regioisomers of physiologically active *cis*- EETs among other oxidized metabolites (Oliw et al., 1982; Oliw, 1994). EETs play many crucial roles especially in the cardiovascular system, including, but not limited to, modulating vascular tone by activating calcium-sensitive potassium channels that in turn promotes hyperpolarization and relaxation of smooth muscle cells, attenuating the inflammatory process by inhibiting the pro-inflammatory transcription factor, nuclear factor-κB (NF-κB), and improving post-ischemic-reperfusion injury by enhancing ventricular repolarization recovery (Batchu et al., 2009; Yang et al., 2015).

Both *cis*- and *trans*-EETs detected in erythrocyte membranes and plasma are mostly esterified in phospholipid membranes (Jiang et al., 2004; Jiang et al., 2008; Jiang et al., 2011). In fact, red blood cell (RBC) membranes are proposed to be the reservoir for *cis*- and *trans*-EETs that can be formed through CYP oxidation, by hemoglobin, or by free radical oxidation (Nakamura et al., 1997; Jiang et al., 2008; Jiang et al., 2010). Like *cis*-EETs, *trans*-EETs are biologically active and have been shown to relax pre-constricted rat arcuate arteries (Jiang et al., 2011). They are also hydrolyzed to dihydroxy metabolites by soluble epoxide hydrolase at a faster rate than *cis*-EETs (Jiang et al., 2008). To date, the relative importance of *cis*- vs. *trans*-EETs in cardioprotection and their relative distribution in different biological samples from diseased patients have not been reported.

In chapter 2, we report the development of a sensitive UPLC-MS/MS method capable of separating *cis*- and *trans*- geometric isomers of all EET regioisomers. We also, determined the product distribution of EETs formed by free radical oxidation in benzene and in liposomes *in vitro*. Next, we measured the distribution *cis*- and *trans*-EETs in several tissues *in vivo*, including mouse heart tissue and RBC of young and old mice, as well as human heart tissue and RBC. A mechanism for non-enzymatic formation of *cis*- and *trans*-EETs is proposed to explain the product formation profile. Finally, *in vitro* CYP incubation conditions with AA were optimized using CYP2J2 as a model isozyme.

2.2. MATERIALS AND METHODS

2.2.1. REAGENTS

Stocks of AA, *cis*-EETs (14,15-, 11,12-, 8,9-, and 5,6-EETs), deuterated internal standards (14,15-EET-d_{11}, 8,9-EET-d_{11}, 5,6-EET-d_{11}, and 14,15-DHET-d_{11}) and 4-[[*trans*-4-[[(tricyclo[3.3.1.1^{3,7}]dec-1-ylamino)carbonyl]amino]cyclohexyl]oxy]-benzoic acid (*t*-AUCB) were purchased from Cayman Chemical (Ann Arbor, MI). 2,2′-azobis(4-methoxy-2,4-dimethylvaleronitrile) (MeOAMVN) and 2,2′-azobis(2-(2-imidazolin-2-yl) propane) dihydrochloride (AIPH) were obtained from Wako Chemicals USA, Inc (Richmond, VA). Pure AA stocks were purchased from Nu-Chek-Prep, Inc (Elysian, MN). Dulbecco's phosphate buffered saline (DPBS, 10 ×), Pierce bicinchoninic acid (BCA) protein assay kit, sodium chloride (NaCl), calcium chloride ($CaCl_2$), ACS-grade ethyl acetate, chloroform, optima-grade acetonitrile, water, and methanol were purchased from Fisher Scientific (Hampton, NH). Benzene, triphenylphosphine (TPP), butylated hydroxytoluene (BHT), Tris-hydrochloride (Tris-HCl), phospholipase A_2 from *Naja mossambica mossambica*, pyruvic acid, and

diethylenetriaminepentaacetic acid (DETAPAC) were obtained from Sigma-Aldrich (St. Louis, MO). 1,2-dilauryl-*sn*-glycero-3-phosphocholine (DLPC) and 1,2-dioleoyl-*sn*-glycero-3-phosphocholine (DOPC) were purchased from Avanti Polar Lipids, Inc (Alabaster, AL).

2.2.2. FREE RADICAL OXIDATION OF AA IN BENZENE

The total reaction volume was 200 μL. Pure AA was reconstituted in benzene that was filtered through neutral alumina. The stock solution of AA (164.2 mM) was diluted in benzene to obtain 1, 10, 25, and 50 mM solutions. The reaction was then initiated with addition of MeOAMVN (10 μL, 0.03 M) and incubated at 37°C in a sand bath for 1, 2, or 3 h. At the end of each time point, the reaction was terminated by adding BHT (50 μL, 0.2 M) and TPP (50 μL, 0.2 M) in benzene at room temperature. For the zero-time point, the reaction was immediately terminated after addition of AA. Samples were cooled to room temperature and a 10 μL aliquot was mixed with 10 μL of internal standard solution (a mixture of 14,15-, 8,9-, 5,6-EETs- d_{11} and 14,15-DHET- d_{11} in benzene, 3 μg/mL each). Samples were dried under nitrogen at 25°C followed by reconstitution in 1 mL of 50% of water and 50% of 80:20 acetonitrile:methanol. Samples were then analyzed on the same day by LC-MS as described below.

2.2.3. FREE RADICAL OXIDATION OF AA IN LIPOSOMES

Free radical oxidation of AA in liposomes was achieved following a procedure by Xu et al. (Xu et al., 2009). Briefly, chloroform solutions of DLPC (20 μL, 250 mM), of DOPC (mole fraction of oxidizable lipid, DOPC,n_{OA} , between 0 to 0.76), and of AA (mole fraction of AA, n_{AA}, between 0 to 0.76) were mixed together so that the concentration of total fatty acyl chains remain constant. The mixtures were dried under nitrogen at 25°C and kept under vacuum for 10

min. The dried samples were reconstituted in DPBS and sonicated for 20 sec. The suspension was incubated at 37°C for 10 min followed by another cycle of 20 second sonication. The free radical oxidation was initiated by addition of AIPH (10 μL, 20 mM). Addition of BHT (50 μL, 0.2 M) and TPP (50 μL, 0.2 M) terminated the reaction at room temperature. After 30 min, internal standards (10 μL, a mixture of 14,15-, 8,9-, 5,6-EETs- d_{11} and 14,15-DHET- d_{11} in 1× DPBS, 3 μg/mL each) were added. The EETs were then extracted twice using nitrogen-purged ethyl acetate containing 0.1 mM TPP. The ethyl acetate extracts were combined and dried under nitrogen at 25°C. The dried residue was reconstituted using 1 mL of a solution containing 50% of water and 50% of 80:20 acetonitrile:methanol. The samples were then analyzed on the same day by LC-MS.

2.2.4. MOUSE ERYTHROCYTE MEMBRANES AND HEART TISSUE

C57BL/6 mice (N=14, 10 females and 4 males) were purchased from Charles River Laboratories. These mice were separated into two groups based on their age. Mice that were approximately 4 month old were categorized into the young group, while mice that were between 18.3 to 22.5 months of age were categorized into the old group. Whole blood from mice was collected through cardiac puncture following treatment with CO_2. The collected blood was washed three-times with cold 1× DPBS and stored at -80°C until further processed. After removal of heart tissue from the chest cavity of the mouse, the tissue was immediately washed once with cold DPBS and flash frozen in liquid nitrogen. All animal experiments were performed in compliance with approved protocols by Institutional Animal Care and Use Committee of the University of Washington.

2.2.5. HUMAN ERYTHROCYTE MEMBRANES AND HEART TISSUE

Human erythrocyte membrane samples were prepared from a repository of sudden cardiac arrest cases and population-based controls. In this study, we used a random sample of 28 control samples that had been collected between October 1988 and September 2005 as part of a case-control study of erythrocyte fatty acids and incident sudden cardiac arrest (Siscovick et al., 1995). The University of Washington Human Subject Review Committee approved the study protocol. Discarded non-ischemic and ischemic human heart residual tissues were obtained from University of Washington Medical Center as surgical waste during cardiac transplants and other procedures. Ventricular tissues were immediately flash-frozen in liquid nitrogen and stored at -80°C until further processing.

2.2.6. EXTRACTION OF EETS FROM ERYTHROCYTE MEMBRANES

Prior to any EET extraction from erythrocyte membrane, each of the erythrocyte membranes sample was diluted 1:400 in 0.9% NaCl followed by determination of total protein content using Pierce BCA assay kit following manufacturer's protocol. Each erythrocyte membrane sample was then diluted using cold 1 × DPBS to 50 mg/mL for human samples or to 30 mg/mL for mouse samples.

Methods to extract RBC and cardiac tissue EETs were adapted from published protocols (Jiang et al., 2004; Goulitquer et al., 2008). Each tissue was extracted as duplicate samples. Briefly, for erythrocyte membranes, 498 μL of deionized water and 2 μL of internal standard (a mixture of 14,15-, 8,9-, 5,6-EETs- d_{11} and 14,15-DHET- d_{11}, 3 μg/mL each) were added to 0.5 mL of RBC membranes containing 50 mg/mL total protein for human and 30 mg/mL total protein for mouse. The samples were centrifuged at 3,500 rpm for 5 min at 4^{o}C. The RBC

samples were extracted using 4 mL of 2:1 chloroform:methanol containing 0.1 mM TPP, followed by rotary mixing for one hour at 4^{o}C. The mixture was then centrifuged at 3,500 rpm for 15 minutes at 4^{o}C to remove cellular debris. The chloroform layer was dried under nitrogen at 25^{o}C, followed by addition of 50 mM Tris-HCl, 100 mM NaCl, 1 mM $CaCl_2$ buffer, pH 9.2 containing 10 units of phospholipase A_2 from *Naja Mossambica Mossambica* (1 mL). The samples were incubated for 30 minutes at 37^{o}C to hydrolyze EETs from the membrane. The EETs were extracted twice with nitrogen-purged ethyl acetate containing 0.1 mM TPP (2 × 2mL), and the ethyl acetate fractions were pooled and evaporated to dryness under nitrogen at 25^{o}C. The lipid residue was reconstituted in 10 µL of DMSO to ensure complete dissolution of EETs and 40 µL of a solution containing 50% of water and 50% of 80:20 acetonitrile:methanol, respectively. The samples were then analyzed directly by LC-MS.

2.2.7. EXTRACTION OF EETS FROM CARDIAC TISSUE

EET extraction from cardiac tissue was initiated by homogenizing the cardiac tissue in 490 µL of cold 1× DPBS in the presence of 12.1 µM *t*-AUCB, a soluble epoxide hydrolase inhibitor, and six ceramic beads using Precellys24 (Bertin Instruments, Rockville, MD) at 6800 rpm for 6 × 30 seconds with 60 seconds delay between cycles. Prior to dividing the homogenized tissue into duplicate aliquots of 100 µL, 10 µL of internal standards (a mixture of 14,15-EET-d_{11}, 8,9-EET-d_{11}, 5,6-EET-d_{11}, and 14,15-DHET-d_{11}, 3 µg/mL each) were added to each sample of the homogenized tissue. The remainder of the EET extraction protocol from the cardiac tissue followed a similar procedure for EET extraction to that for RBC above. All extractions were performed in duplicate. After mass spectrometric analysis, mouse heart homogenates were

diluted 3:100 using 0.9% NaCl followed by total protein determination using Pierce BCA protein assay kit.

2.2.8. *IN VITRO* INCUBATION USING RECONSTITUTED CYP ENZYME SYSTEM

2.2.8.1. DILUTION OF AA

To determine if serial dilution of AA stock solution while keeping the percentage of organic solvent less than 0.1% is possible, an experiment in making dilutions to 50 μM of AA was undertaken. Three different dilutions were made. The first dilution was 50 μM of AA made directly by adding 821 mM AA stock into 100 mM potassium phosphate buffer, pH 7.4 containing 0.1 mM DETAPAC and 10 mM pyruvate. The second dilution was a two-step serial dilution in aqueous solution. Five mM of AA solution containing 10 mM pyruvate was made followed by 100-fold dilution of this stock solution into 100 mM potassium phosphate buffer, pH 7.4 containing 0.1 mM DETAPAC and 10 mM pyruvate. The third dilution was another two-step serial dilution in ethanol. A stock solution of AA (500 mM) containing 10 mM pyruvate was made in ethanol followed by 10,000-fold dilution into 100 mM potassium phosphate buffer, pH 7.4 containing 0.1 mM DETAPAC and 10 mM pyruvate. Two μL of each samples were injected by direct infusion in triplicate into a Waters Micromass/ Quattro PremierXE triple quadrupole mass spectrometer with negative electrospray ionization mode and single ion monitoring of m/z 303.2 with capillary voltage of 3.3 kV, cone voltage of 30 V, source and desolvation temperatures of 120^{o}C and 350^{o}C, respectively.

2.2.8.2. Optimization of percentage of organic solvents

Typical CYP incubations contain less than 0.1% organic solvent. Incubations using recombinantly expressed and purified CYP2J2 and 50 μM of AA containing 0.01%, 0.03%, and 0.06% ethanol were performed. The general incubation protocol is described in section 2.3.8.3. The internal standards used for these incubations were 1 μg/mL of 14,15-EET-d_{11} and 5,6-EET-d_{11}. Normalization of 14,15- and 11,12-EETs used 14,15-EET-d_{11} as their internal standards while 5,6-EET-d_{11} was used to normalize 8,9- and 5,6-EET.

2.2.8.3. Minimization of non-enzymatic formation of EETs and general incubation protocol

In vitro experiments were performed using recombinantly expressed and purified CYP2J2 (Evangelista et al., 2013). The experiments were performed in the dark while using polypropylene tubes. The reconstituted enzyme system consisted of purified CYP2J2 (25 pmol), cytochrome P450 reductase, and cytochrome b5 in a ratio of 1:2:1, respectively in 50 μg/mL of extruded DLPC (500 μL total incubation volume). The buffer was 100 mM potassium phosphate buffer, pH 7.4 containing 0.1 mM DETAPAC. Following addition of NADPH (1.0 mM), the samples were pre-equilibrated at 37^{o}C for 3 min after which the reaction was initiated with 50 μM AA containing 1 mM pyruvate. After 30 minutes, reactions were terminated with 2 mL of nitrogen-purged ethyl acetate containing 0.01% BHT to minimize non-enzymatic AA oxidation and a mixture of internal standards (1 μg/mL of 14,15-EET-d_{11}, 8,9-EET-d_{11}, and 5,6-EET-d_{11}, 3 μg/mL each) was added. The quenched reactions were vortexed rigorously for 10 minutes followed by centrifugation at 3500 rpm at 4^{o}C for 5 min. The ethyl acetate extraction was performed twice (2 × 2 mL), the organic layers were combined and evaporated to dryness under

a gentle stream of nitrogen at room temperature. The residue was reconstituted with 10 µL of DMSO and 40 µL of a solution containing 50% of water and 50% of 80:20 acetonitrile:methanol, respectively. Samples were analyzed using LC-MS-MS on the same day.

2.2.9. LIQUID CHROMATOGRAPHY AND MASS SPECTROMETRIC ASSAY TO QUANTIFY EETS

Quantification of cis- and trans-EETs was performed on a Waters Xevo TQ-S triple quadrupole mass spectrometer operated in negative ion mode electrospray coupled to a Waters UPLC. The EETs were separated on a Waters Acquity UPLC® BEH Shield RP C18 1.7 µm, 100 × 2.1 mm column. Several columns with various stationary and bonded phase using the UPLC system were compared. The Agilent Zorbax SBC18, Rapid resolution HT, 2.1 × 50 mm with 1.8 µicron particle size was used. This column had no end-capping with 10% carbon load, 80 Å pore size and 180 m^2/g surface area. The chromatographic resolution of individual EET was not satisfactory because there were not enough theoretical plates on this column. We switched to the current Waters Acquity UPLC® BEH Shield RP18, 2.1×100 mm with 1.7 µm particle size. The length of the column and a slight increase in the particle size of the column's stationary phase provided improved chromatographic resolution. The end-capping appeared to improve the chromatography.

The mobile phase consisted of water containing 0.05% acetic acid (solvent A) and 80:20 acetonitrile: methanol containing 0.05% acetic acid (solvent B). The various isomers of EETs were separated using the following gradient: solvent B was held at 62% from 0 to 5.5 min, then held at 55% from 5.5 to 6 min, followed by an increase to 58% from 6 to 18 min, and finally increased to 100% from 18.1 to 19.1 min. Solvent B was then held at 62% from 20 to 23 min to

re-equilibrate the column. Flow rate was constant at 0.3 mL/min throughout the run. For the first 2 min of runtime, 100% of the flow was diverted into waste. The MS conditions were the following: capillary voltage 2 kV, cone voltage 20 V, source temperature 150ºC, desolvation temperature 450ºC. The mass transitions that were monitored were 319.1 >219.1 (14,15-EET), 319.1>208 (11,12-EET), 319.1>166.7 (11,12-EET), 319.1>155.1 (8,9-EET), 319.1>191.2 (5,6-EET) and compared to their corresponding deuterated standards for quantitation. For 11,12-EET, 14,15-EET-d_{11} was used as the internal standard.

In the absence of authentic standards, *trans*-EETs were identified based on retention time, fragmentation pattern and comparison to previously published method (Nakamura et al., 1997). To further confirm the presence and identity of *trans*-EETs, a free radical oxidation sample that contained 50 mM AA and oxidized for 3 hours in liposomes was analyzed using High Resolution/High Mass Accuracy Thermo LTQ-OrbiTrap, which confirmed that peaks that were presumed to be *trans*-EETs came from the same parent ions and had the same fragmentation patterns as the corresponding *cis*-EET (Figure 2.3).

2.2.10. DATA ANALYSIS

Mass spectrometry data were analyzed using MassLynx 4.1. Data analysis was performed using Prism 5.04 (GraphPad, La Jolla, CA). For the free radical oxidation study, experiments were performed in triplicate and reported as the mean ± S.D. Mass transition 319.1>208 was used to obtain peak area ratio for 11,12-EET. Experiments measuring EETs from biological samples were reported as means ± standard deviations.

The integrated peak area of each analyte was normalized to the corresponding peak area of internal standard. In addition to analyte normalization to its internal standard, the normalized

peak areas of each analyte at the zero time point were subtracted from the corresponding peak areas of each sample.

To determine AA dilution, averages of absolute peak areas of three different dilutions were directly compared. To determine the tolerance of reconstituted CYP2J2 enzyme system to ethanol, each peak height was normalized to its internal standard. In order to calculate the percentage of autoxidation in the presence of different percentages of ethanol, normalized peak height ratio from incubations with no NADPH control was divided by normalized peak height ratio of the corresponding sample with addition of NADPH and then multiplied by 100%.

For optimization of *in vitro* incubations using reconstituted CYP enzyme system, experiments were performed in duplicate. In this subset of data, analyte peak height, instead of peak area, was used and further normalized to its corresponding internal standard. As mentioned above, two mass transitions were monitored for 11,12-EET; 319.1>166.7 and 319.1>208. The peak intensity of 11,12-EET at 319.1>166.7 was higher than 319.1>208 even though chromatographic separation between 11,12-EET and 8,9-EET at mass transition 319.1>166.7 was not at baseline level. The percentage of non-NADPH-dependent EETs was obtained by taking the ratio of the normalized peak height of no-NADPH control and the normalized peak height of corresponding sample that contained NADPH.

In the biological samples, integrated peak heights of each analyte were normalized to the corresponding peak heights of internal standard. In addition to analyte normalization to its internal standard, the peak heights ratios for each analyte were normalized to total protein content or tissue weight in the case of human heart tissue.

2.3. RESULTS

2.3.1. FREE RADICAL OXIDATION OF AA IN BENZENE OR LIPOSOMES LEADS TO FORMATION OF BOTH *CIS*- AND *TRANS*- EETS

Free radical oxidation of AA at various concentrations (ranging from 1 to 50 mM) was initiated by MeOAMVN at 37 °C and the formation of *cis*- and *trans*- EETs was monitored at different time points using UPLC-MS/MS. In addition to the major hydroxyl metabolites, both *cis*- and *trans*-EETs were formed under these conditions (Figure 2.4). Formation of *cis*- and *trans*- EETs was linear with time- and AA concentration for all regioisomers in benzene (Figure 2.5 A–D demonstrates this relationship for 14,15-EET and Figures. 2.6 and 2.7 show all other regioisomers). Furthermore, under all conditions, *trans*-EETs formation was favored over *cis*-EETs by approximately 1.5 to 6.2 fold (Figures 2.5 E, 2.8 A, and 2.9). The percentage of each isomer of EET (regio- or stereo- isomer) to total EETs formed remained relatively constant at different AA concentrations and various time points as summarized in Table 2.1.

To study radical formation of EETs in a more physiologically relevant system, oxidation of AA was performed in liposomes. The reaction contained a constant mole fraction of DLPC while varying the mole fractions of oxidizable phospholipid, DOPC, and AA, so that the total moles of fatty acyl chain remained constant in the incubation. Free radical oxidation was initiated with water-soluble radical initiator, AIPH, at 37 °C. Similar to radical reactions in benzene, *cis*- and *trans*-EETs formation was linear with time- and mole fraction of AA in liposomes for all regioisomers. The linear formation of 14,15-EET is shown as an example in Figure 2.10 A–D with other regioisomers shown in Figures 2.11 and 2.12. The ratio of each regioisomer of EET relative to total EETs remained unchanged for both *cis*- and *trans*-EETs at

various concentrations of AA and at various time points (Figures 2.10 E and 2.13). The formation of *trans*-EETs was also favored in liposomes by approximately 2.5 and 10.5 over *cis*-EETs formation (Figures 2.10 E, 2.8 B, and 2.13). Compared to free radical oxidation in solution (i.e. benzene), more variability was observed in liposome reactions. At 1 mM of AA (n_{AA} of 0.015), the levels of both *cis*- and *trans*-EETs were similar to those observed in benzene. However, the formation of EETs in the presence of liposomes at higher concentration of AA was more efficient than in benzene as seen in Figures 2.10 A-B, 2.11, and 2.12. Regardless of the difference in product distribution between benzene and liposome oxidations, the percentages of each regioisomer of EETs relative to total EETs was also unaltered across all conditions (concentration and time) in liposomes as seen in Table 2.1 (bottom half).

2.3.2. PRODUCT DISTRIBUTION OF *CIS*- AND *TRANS*- EETS IN BIOLOGICAL SAMPLES

Extraction of EETs from erythrocyte membranes of C57BL/6 mice and humans revealed the presence of both geometric isomers of all EET regioisomers (Figure 2.14). In contrast to the free radical oxidation reactions, *cis*-EETs were higher than *trans*-EETs in RBC membranes as evidenced by the larger normalized peak-height ratios in Tables 2.2 and 2.3. The ratios of *cis*-/*trans*-EETs for each regioisomer ranged from 0.9 to 2.2 for old mouse RBC membranes (N = 7), 1.3–4.0 for young mouse RBC membranes (N = 7), and 1.0–3.1 for human RBC membranes (N = 28). The ratios of *trans*-/*cis*-total EETs in old mouse RBCs were significantly higher than those in young mouse RBCs, suggesting increased contribution of the free radical mechanism to trans-EETs with aging (Figure 2.15). In general, for each EET pair, the *cis*-/*trans*- ratios in RBC membranes of both old mouse and human were similar. However, the *cis*-/*trans*- ratios of 8,9- and 5,6-EETs in young mouse RBC membranes were significantly larger than those in old mouse and human RBC membranes.

The ratios of *cis*-/*trans*-EETs for each regioisomer from mouse heart tissues ranged from 0.38 to 1.3 (N = 7), while the ratios from human heart tissues ranged from 0.80 to 2.8 (N = 12). In mouse heart tissues, the levels of *cis*-14,15- and *cis*-5,6-EETs were similar to their *trans*-EETs while the levels of *cis*-11,12- and *cis*-8,9-EETs were significantly lower than their *trans*-counterparts (Table 2.2). In diseased human heart tissues, the levels of all four *cis*-EETs were higher than their corresponding *trans*-EETs (Table 2.3).

2.3.3. *IN VITRO* ENZYMATIC AND NON-ENZYMATIC FORMATION OF *CIS*- AND *TRANS*-EETS

Part of the optimization of *in vitro* enzymatic incubation conditions was determining how to correctly dilute AA stock solutions in aqueous buffer and minimize the concentration of organic solvent that limits the non-enzymatic formation of EETs without compromising CYP activity. Based on resulst for the average absolute area of three different dilutions of AA, serial dilution of AA in aqueous solution was not possible. Serial dilution of AA in ethanol followed by aqueous solution seemed like a viable alternative, but there wass still approximately 43% of AA loss potentially due to adherence to various vials and syringes. Dilution of AA directly from the stock exhibited the least amount of AA loss as shown in the representative chromatogram in Figure 2.16. The presence of ethanol in the incubation appeared to slightly increase autoxidation, however, formation of non-enzymatic *cis*-EETs seemed minimal at 0.06% ethanol as shown in Figure 2.17.

CYP2J2 was chosen as a model CYP epoxygenase since it is capable of generating all four regioisomers of *cis*-EETs at approximately similar amounts (Kaspera and Totah, 2009). In a CYP2J2 reconstituted system including cytochrome P450 oxidoreductase and cytochrome b5,

both *cis*- and *trans*- regioisomers of EETs were observed in the presence and absence of NADPH (Figure 2.18), suggesting contribution from both enzymatic and autoxidation processes. We sought to establish conditions that would diminish, if not eliminate, the non-NADPH dependent formation of EETs during CYP incubations to facilitate accurate metabolite identification and kinetic studies of various fatty acids. Thus, we investigated the effect of an iron-chelating agent, DETAPAC, and a hydrogen peroxide scavenger, pyruvate, at various concentrations. Table 2.4 shows the percentage of remaining EETs that were formed in non-NADPH-dependent manner in the presence of each reagent. Spectrometric binding studies were conducted to confirm that neither pyruvate nor DETAPAC bind to the CYP2J2 active site and so had no effect on the iron spin state (Figure 2.19).

2.4. DISCUSSION

EETs have been implicated in many biological processes and play an important role in cardioprotection. We sought to determine the contribution of autoxidation to the formation of *cis*- and *trans*-EETs both in benzene and in liposomes, a more physiologically relevant system. The key finding is that EETs are readily formed from AA under free radical oxidation conditions. All regio- and geometric isomers were formed. The percentage of each *cis*- or *trans*-EET to total EETs did not change with increasing concentration of AA or with time, regardless whether reactions were carried out in benzene or liposomes. However, the percentages of both *cis*- and *trans*-14,15- and 5,6-EETs were significantly different between solution and liposome reactions. Formation of 14,15-EET appeared to be less favored in liposomes than in solution while the formation of 5,6-EET seemed to be more favored in liposomes. It is possible that the heterogeneous environment of liposomes contributes to 5,6-EET formation. The double bond at the C5 position is much closer to the carboxylic acid group than the double bond at the C14

position. In the presence of liposomes, AA would be more likely to bury its hydrophobic tail; therefore, access to the double bond at the C14 position would be slightly restricted by lipid peroxyl radicals and so oxidation would be expected to be more favorable at the 5,6-position. Similar regio-distribution of oxidation products of linoleic acid in liposomes has been reported previously, where formation of C9-isomers were preferred over C13-isomers (Xu et al., 2009).

The ratios of *cis*- to *trans*-EETs from free radical oxidation are, in general, higher in benzene than in liposomes as shown in Figures 2.5 and 2.10 E. Irrespective of the reaction medium, formation of *trans*-EETs was favored over *cis*-EETs. In contrast, levels of *cis*-EETs were, in general, either more favored or similar to *trans*-EETs depending on the specific regioisomer pairs in biological samples, such as human and mouse RBC membranes or human and mouse heart tissues. Of note, a considerably higher ratio of *cis*-/*trans*-8,9-EETs was observed in human heart tissues compared to both young and old mouse heart tissues (Tables 2.2 and 2.3). This may be due to the diseased nature of the human heart tissue available to us, compared to the mouse tissue. However, further studies using healthy human heart tissue will be necessary to confirm this observation.

In mouse erythrocyte membrane, both total *cis*- and *trans*-EETs increased in RBC of old mice as seen in Figure 2.15, but *trans*-EETs increased to a much larger extent. Aging is associated with progressive endothelial dysfunction (Celermajer et al., 1994; Weinsaft and Edelberg, 2001), defective vascular repair (Weinsaft and Edelberg, 2001), arterial thickening and stiffness (Lakatta and Levy, 2003), angiogenesis impairment (Rivard et al., 1999), an increased risk of developing atherosclerosis (Weingand et al., 1986), and an accumulation of senescent endothelial cells (Erusalimsky and Kurz, 2005). Yang et al. showed that the endothelial function was gradually reduced in 6-week, 20-week, and 80-week Sprague-Dawley rats and addition of

exogenous *cis*-14,15-EET improved endothelial function in aging mice as well as endothelial senescence in rat mesenteric arterial endothelial cells from 20-week-old rat through the mTORC2/Akt signaling pathway (Yang et al., 2014). 11,12-EET also attenuated inflammation by reducing phenylephrine-induced constriction and increased endothelial-dependent dilation of aortic rings from 22-month-ovariectomized Norway rats, while decreasing cytokine-stimulated upregulation of adhesion molecules on human aortic endothelial cells (Sun et al., 2016). However, in a 6-week 129 SvJ mouse model, 8,9- and 5,6-EETs had been shown to promote angiogenesis and *de novo* vascularization, while 14,15- and 11,12-EETs did not exhibit the same mitogenic properties (Pozzi et al., 2005). All aforementioned studies demonstrated that all EETs had protective properties, however, each regioisomer required different biological pathways to be activated to promote cell proliferation. In pulmonary murine microvascular endothelial cells, 8,9- or 11,12-EETs has been shown to be involved in activation of p38 MAPK, whereas mitogenic activity of 5,6- or 14,15-EETs has been reported to be mediated by PI3-kinase/Akt signaling (Pozzi et al., 2005). Because aging is a progressively complicated process, any negative effect of aging could compromise various downstream signaling pathways involved in cell proliferation. These compromised pathways could alter EETs levels, especially trans-EETs which are primarily formed via a free radical oxidation process, thereby warranting measurement of both the *cis*- and *trans*-isomers.

The presence of all four *cis*- regioisomers of EETs in human RBC membranes was shown by Nakamura et al., but these authors did not report the presence of both *cis* and *trans* isomers (Nakamura et al., 1997). In the analytical method developed in this study, both the *cis*- and *trans*-EETs present in RBC membranes were easily resolved (Figure 2.14), which enabled their detection for the first time. While we clearly demonstrated that both geometric isomers of EETs

are present in the RBC membranes of mouse and human, their origin is less certain. EETs, both *cis*- and *trans*-, could potentially result from various sources, including enzymatic CYP, hemoglobin oxidation of hydrolyzed AA or free radical oxidation of either free AA or AA esterified to phospholipids in the membrane.

CYP epoxygenases are known to only form *cis*-EETs (Figure 2.18 K–T), while autoxidation of AA leads to formation of both *cis*- and *trans*-EETs with preference for *trans*-regioisomers (Figure 2.18 A–E) (Oliw et al., 1982; Oliw, 1994). The most likely mechanism of *trans*-EETs formation is through a peroxyl radical addition mechanism (Yin et al., 2011; Xu and Porter, 2015). Peroxyl radical addition to any of the double bonds of AA leads to the formation of a carbon radical, which could directly undergo an S_Hi reaction to give the *cis*-EETs, or undergo S_Hi after rotation of the σ bond to give the *trans*-EETs, as proposed in Figure 2.20.

Another potential mechanism is the *cis*-*trans* isomerization of AA prior to free radical oxidation or enzyme catalysis. Roy et al. reported that certain *trans* double bonds of AA lead to formation of *trans*-EETs in CYP-catalyzed reactions (Roy et al., 2004). The process of *cis*- to *trans*- AA isomerization can be mediated by nitrogen dioxide, a free radical byproduct of nitric oxide and nitrite oxidation or thiyl radicals (Jiang et al., 1999; Ferreri et al., 2004). However, these mechanisms are unlikely to occur under *in vitro* reaction conditions. On the other hand, in CYP-mediated reactions, the iron-oxo species (or potentially the hydroperoxy species) catalyzes epoxide formation in a one-step concerted mechanism that does not allow for bond rotation and formation of *trans*-EETs (Vaz et al., 1998).

Owing to the fact that EETs are formed from autoxidation of AA, it is important to optimize *in vitro* CYP incubation conditions to minimize the contribution from autoxidation.

This will ensure that formation of *cis*-EETs observed in the presence of NADPH is mediated exclusively by CYP catalysis. Thus, we tested several approaches to minimize autoxidation without affecting enzymatic activity. In *in vitro* systems, non-NADPH-dependent EETs are potentially generated from Fenton chemistry. Indeed, we found that addition of iron-chelating agents, EDTA or DETAPAC, markedly inhibited the formation of EETs from autoxidation. Another major uncoupling product of CYP catalysis is hydrogen peroxide, which can initiate the P450 cycle via the peroxide shunt, and also lead to EETs formation. To circumvent this reaction, pyruvate was also added to scavenge hydrogen peroxide (Long and Halliwell, 2009). Combination of both an iron-chelating agent and pyruvate efficiently inhibited the majority of EET formation from autoxidation, as shown in Table 2.4. In addition, all experiments were performed in the dark to avoid photooxidation and all analyses by UPLC-MS/MS were performed immediately following extractions to minimize oxidation and degradation of metabolites.

2.5. CONCLUSION

Lipid peroxidation is involved in the pathophysiology of various human disorders including cardiovascular disease. Oxidative stress during these disease states leads to increased reactive oxygen species, which increases lipid peroxidation due to the susceptibility of unsaturated lipids to oxidation. Autoxidation of AA has been previously reported to form hydroperoxides, isoprostanes, and monohydroxylated metabolites. In this study, we report EETs as another important class of products readily formed from AA autoxidation. Non-enzymatic *trans*-EETs are formed more favorably via free radical oxidation mechanisms, while CYP epoxygenases are major contributors to the formation of *cis*-EETs. A number of studies have measured EETs in plasma of cardiovascular disease patients compared to healthy volunteers,

however, future efforts should focus on determining if one (or more) geometric isomer is more likely to vary during cardiovascular disease. In this way, the contribution of both free radical and enzymatic oxidation to the total circulating EET pool can be assessed, leading to a better understanding of the protective roles played by each regioisomer, and establishing whether certain regio- or geometric- isomers can serve as potential biomarkers for specific cardiovascular conditions.

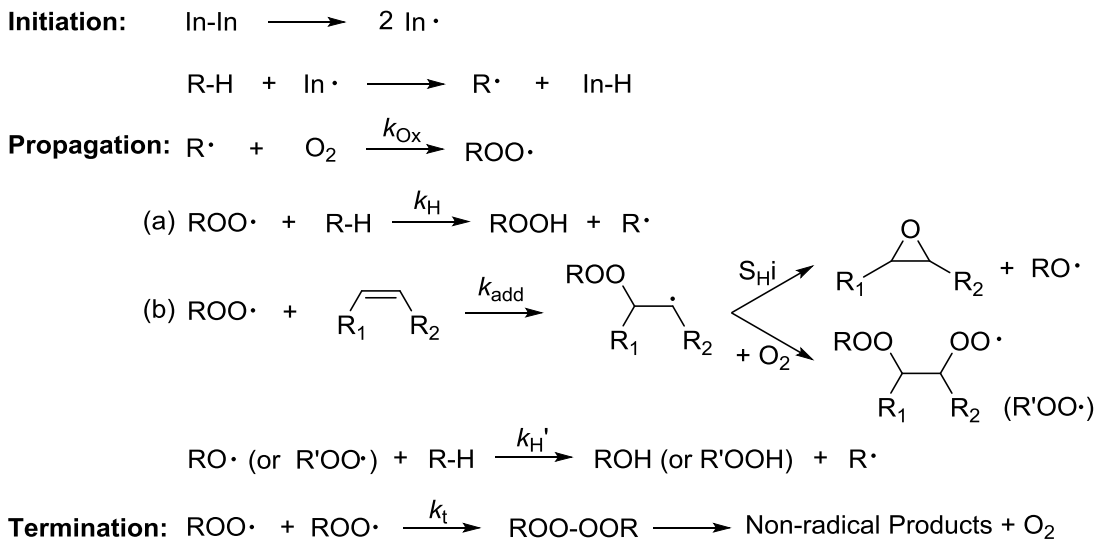

Figure 2.1. Free radical chain oxidation reaction and generation of epoxides by peroxyl radical addition.

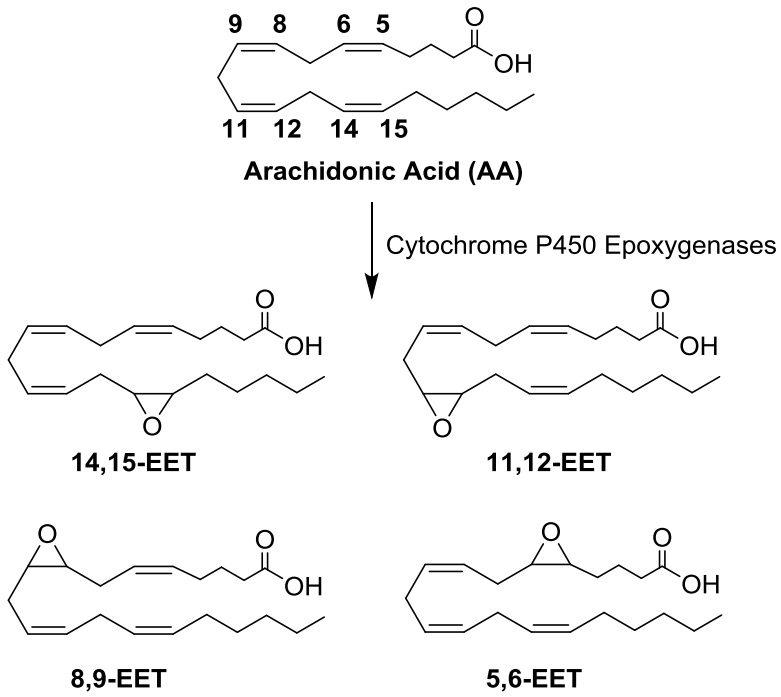

Figure 2.2. AA metabolic pathway mediated by CYP epoxygenases to form all regioisomers of *cis*-EETs.

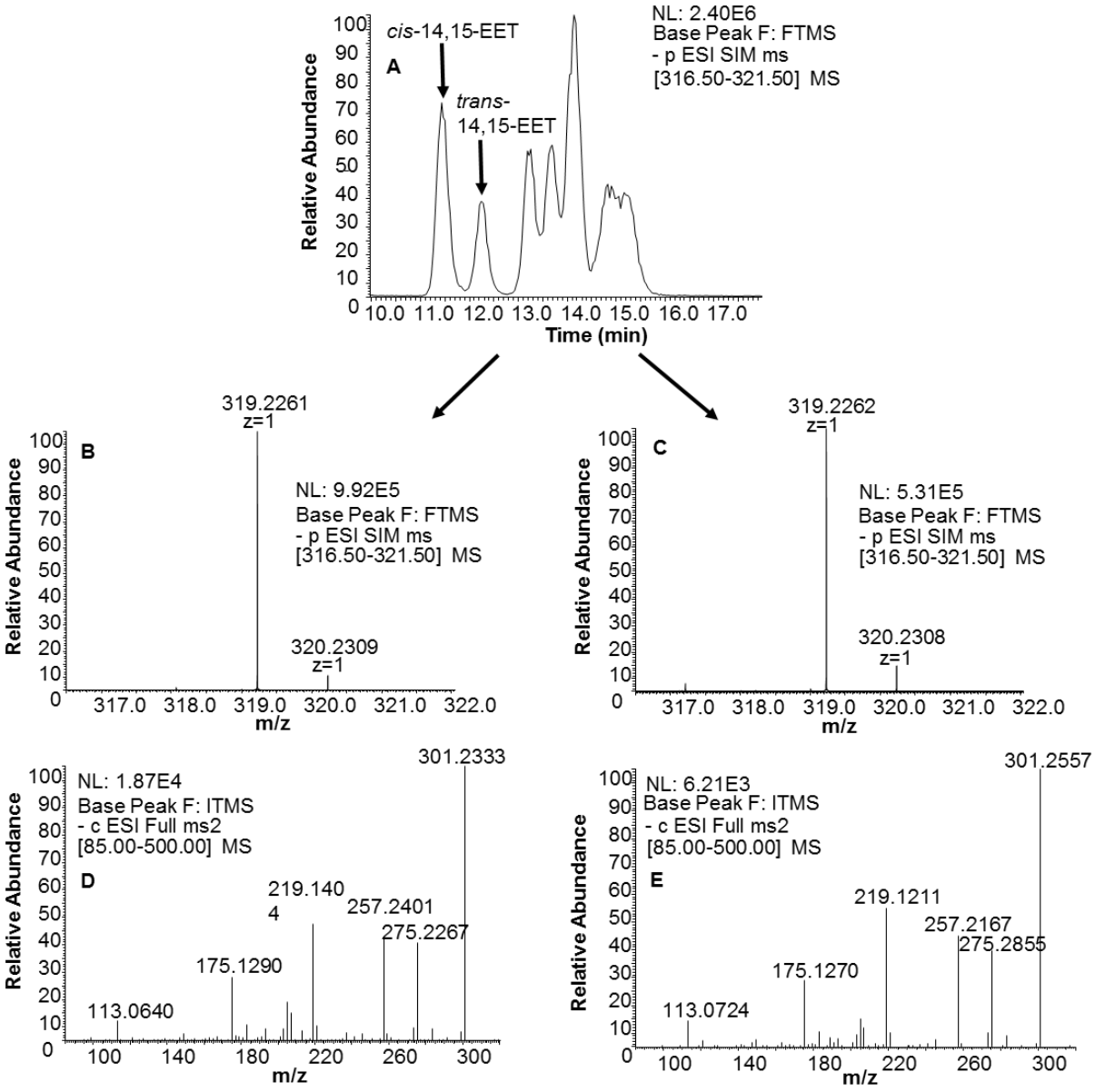

Figure 2.3. Confirmation of *trans*-EET presence in liposomes using High Resolution/High Mass Accuracy Thermo LTQ-OrbiTrap. (A) Total ion chromatogram showing all regio- and geometric isomers of EETs. The same parent ions for both (B) *cis*- and (C) *trans*-14,15-EETs were observed at m/z of 319.226 as well as very similar patterns of fragmentations for both (D) *cis*- and (E) *trans*-14,15-EET.

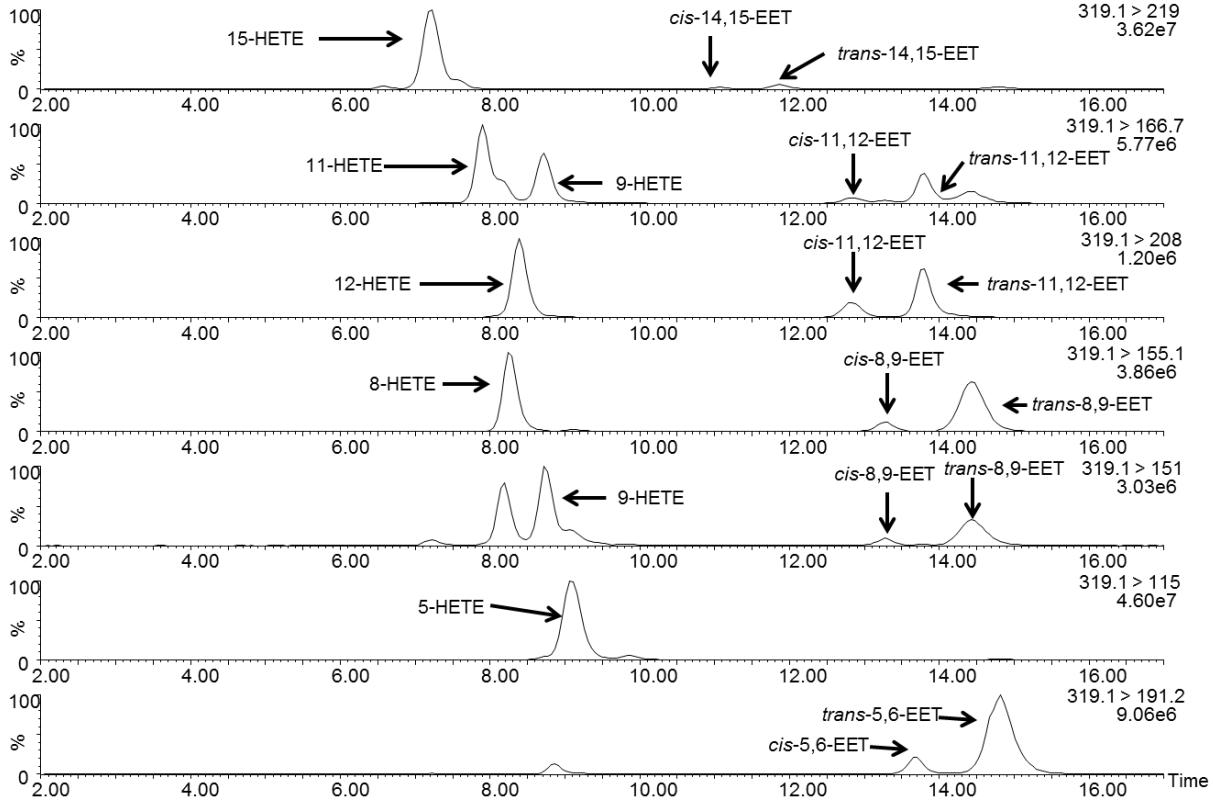

Figure 2.4. Extracted ion chromatogram showing the formation of non-enzymatic AA metabolites after three hours at n_{AA} of 0.15 in liposomes. One of the major autoxidation products of AA, hydroxyeicosatetraenoic acids (HETEs), were formed at higher levels than EETs through comparison of their peak area ratios.

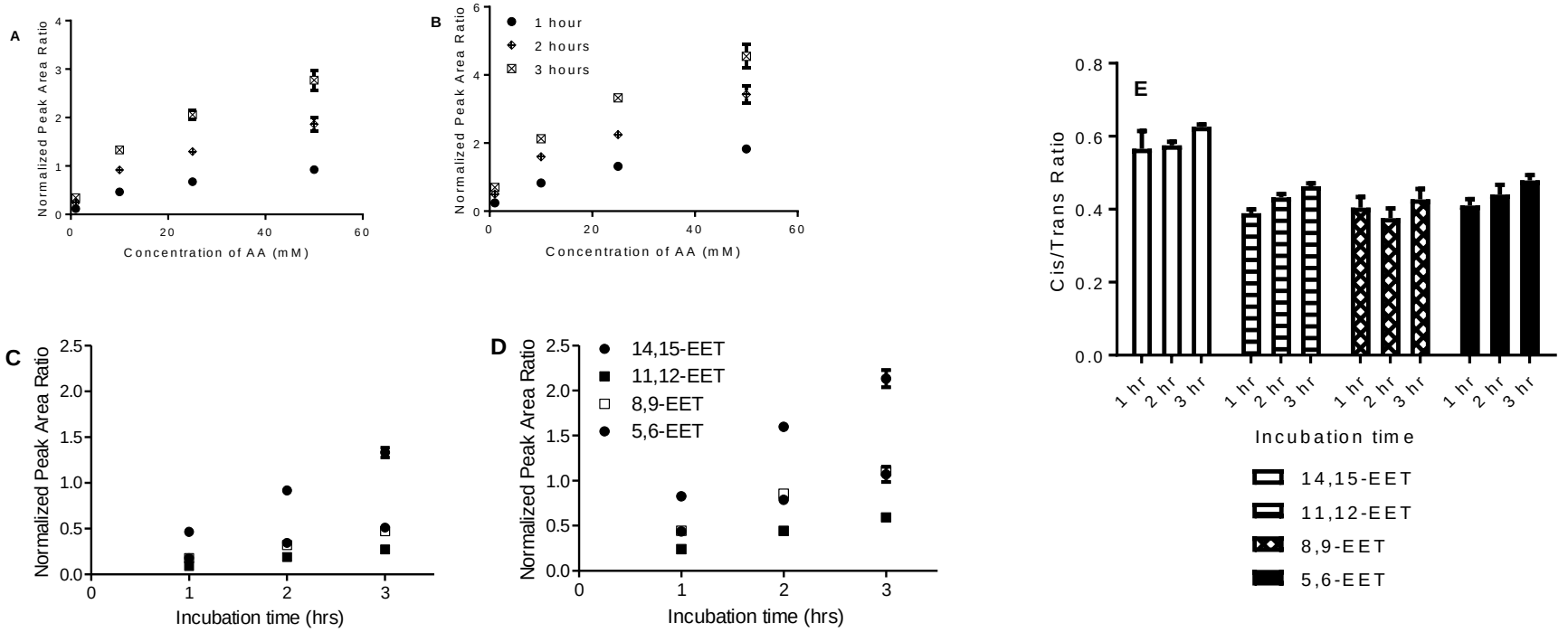

Figure 2.5. Concentration- and time-dependent formation of EETs and ratio of *cis-/trans*-EETs from AA in benzene. Concentration-dependent formation of free radical-generated (A) *cis*-14,15-EET, (B) *trans*-14,15-EET. Time-dependent formation of non-enzymatic (C) *cis*-EETs, (D) *trans*-EETs at 10 mM AA. (E) Ratios of *cis*- to *trans*-EETs in benzene in the presence of 10 mM AA at various incubation time points remained unaltered. For this subset of experiments, each time point reaction was performed in triplicate and normalized to its zero-time point. Each data point shows mean±S.D.

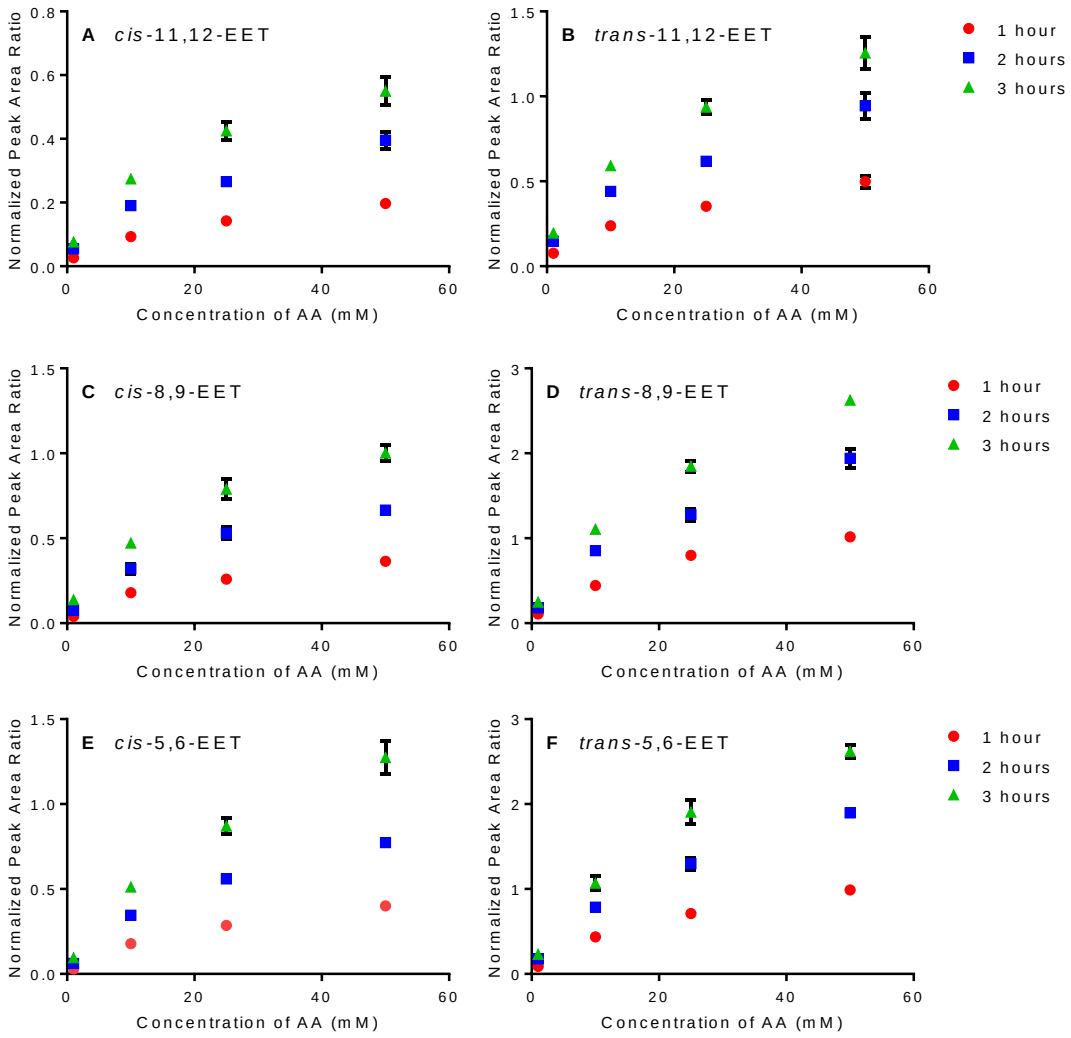

Figure 2.6. Concentration-dependent formation of non-enzymatic (A) *cis*-11,12-EET, (B) *trans*-11,12-EET, (C) *cis*-8,9-EET, (D) *trans*-8,9-EET, (E) *cis*-5,6-EET, and (F) *trans*-5,6-EET in benzene. Each time point reaction was performed in triplicate and normalized to its zero time point. Each data point shows mean ± S.D.

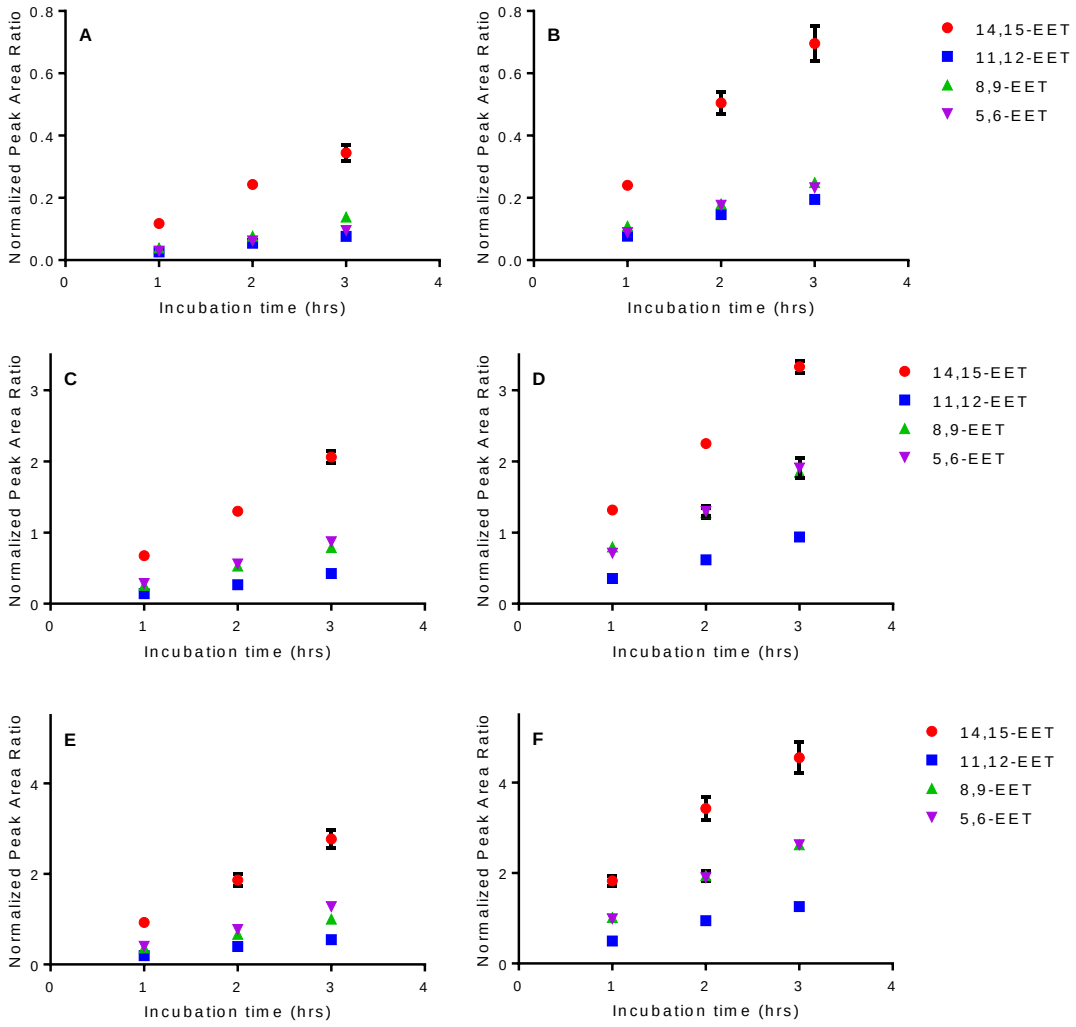

Figure 2.7. Time-dependent formation of non-enzymatic *cis*-EETs and *trans*-EETs at 1 mM (A and B), 25 mM (C and D), and 50 mM (E and F) in benzene. Each time point reaction was performed in triplicate and normalized to its zero time point. Each data point shows mean ± S.D.

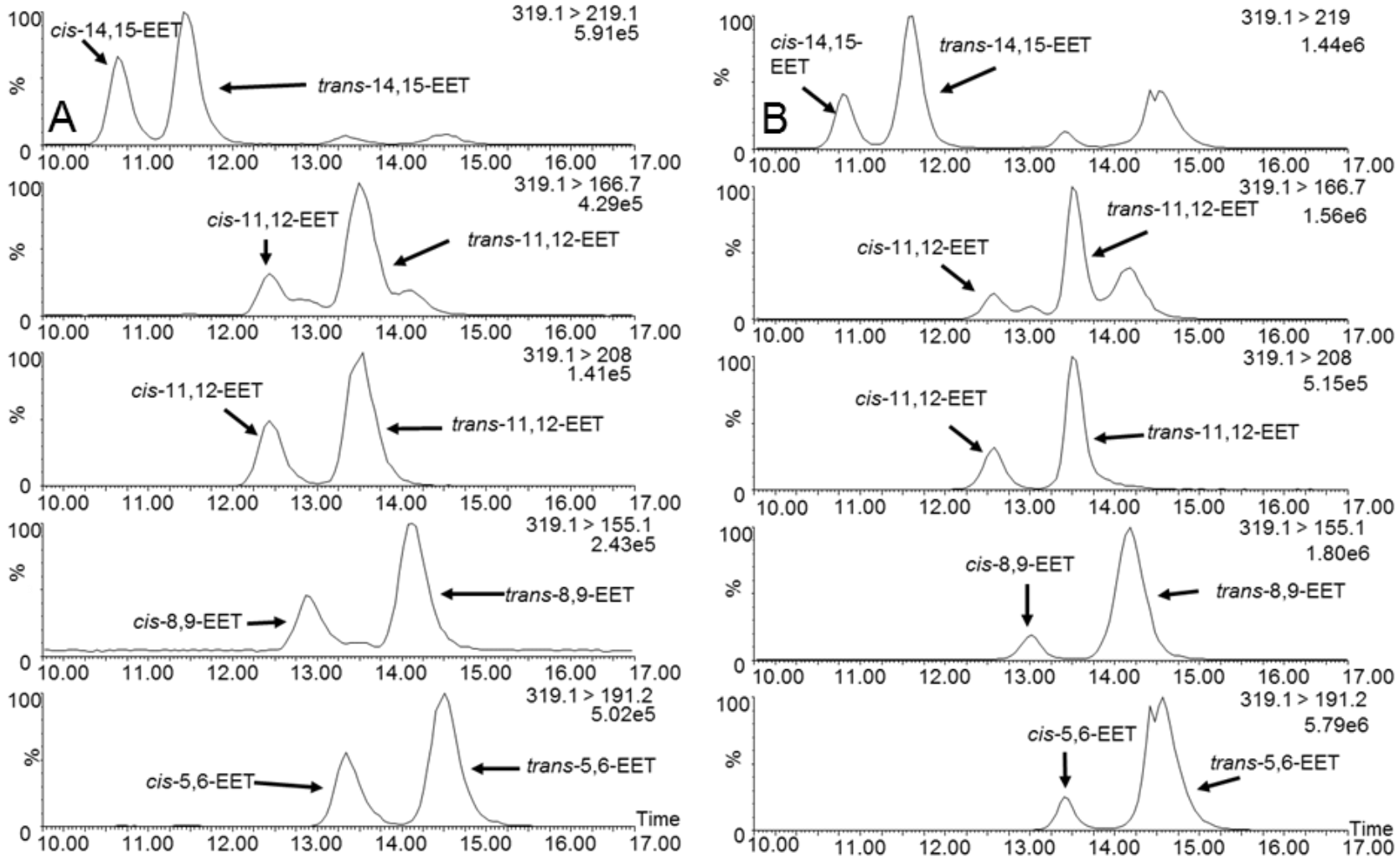

Figure 2.8. Extracted ion chromatograms of EETs formed during free radical oxidation in (A) benzene and (B) liposomes. Chromatograms demonstrate separation of *cis*- and *trans*-EETs.

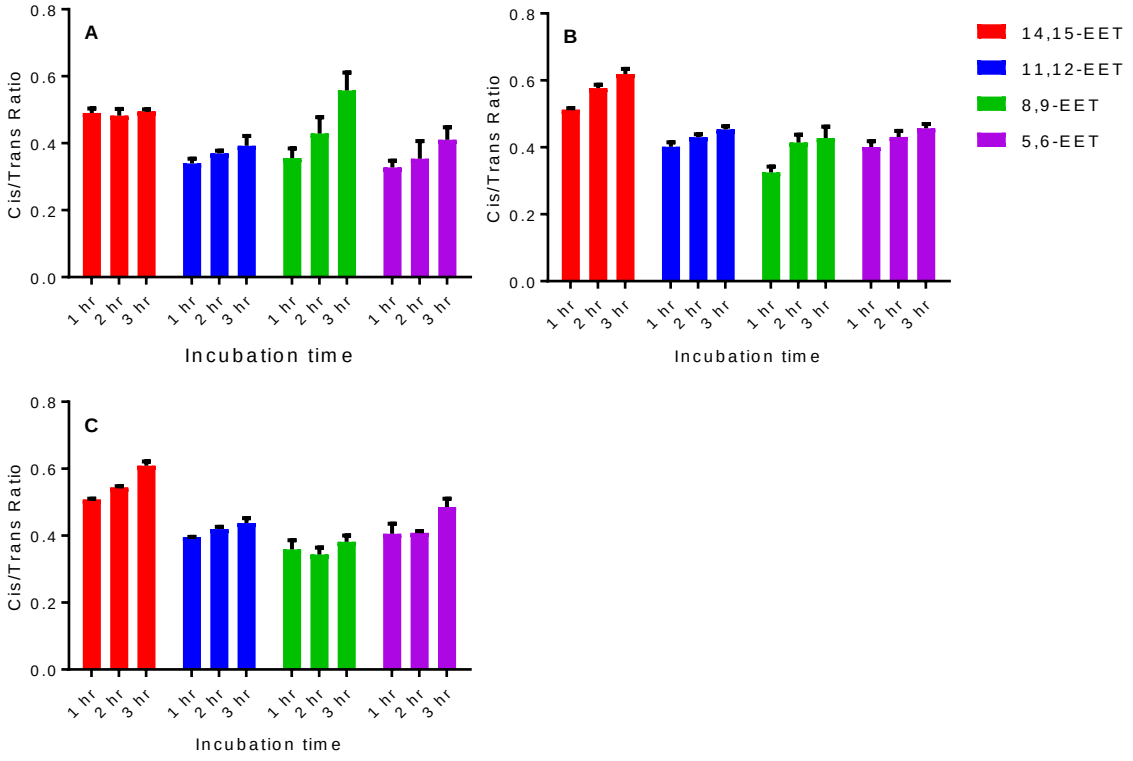

Figure 2.9. Ratios of *cis*- to *trans*-EETs in benzene in the presence of (A) 1 mM, (B) 25 mM, and (C) 50 mM of AA at various incubation time points. Each time point reaction was performed in triplicate and normalized to its zero time point. Each data point shows mean ± S.D.

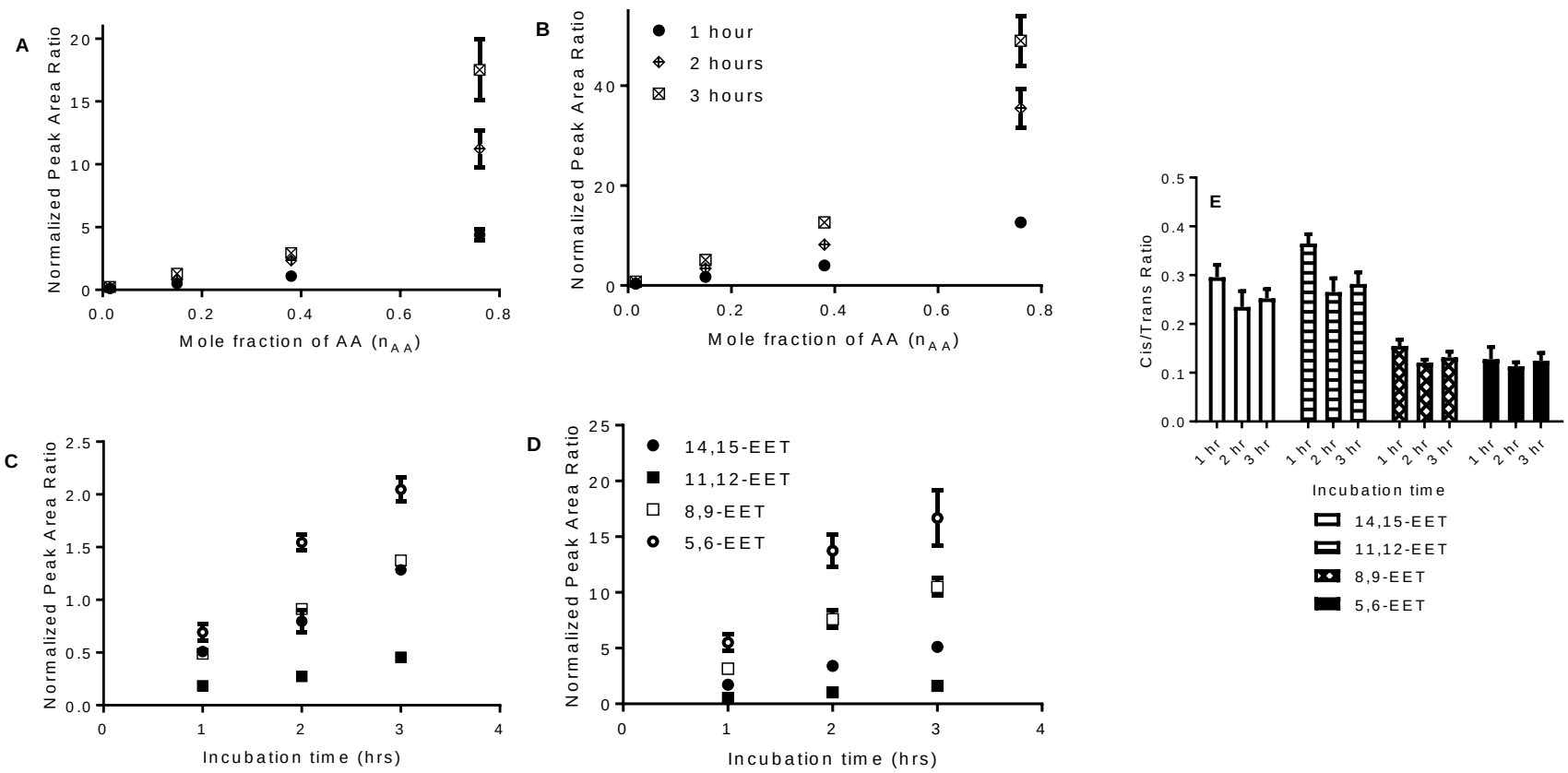

Figure 2.10. Mole fraction- and time-dependent formation of EETs and ratio of *cis-/trans*-EETs from AA in liposomes. Mole fraction-dependent formation of free radical (A) *cis*-14,15-EET, (B) *trans*-14,15-EET. Time-dependent formation of non-enzymatic (C) *cis*-EETs, (D) *trans*-EETs at n_{AA} of 0.15. (E) Ratios of *cis*- to *trans*-EETs in liposomes at various incubation time points and at n_{AA} of 0.15 did not change significantly. For this subset of experiments, each time point reaction was performed in triplicate and normalized to its zero time point. Each data point shows mean ± S.D.

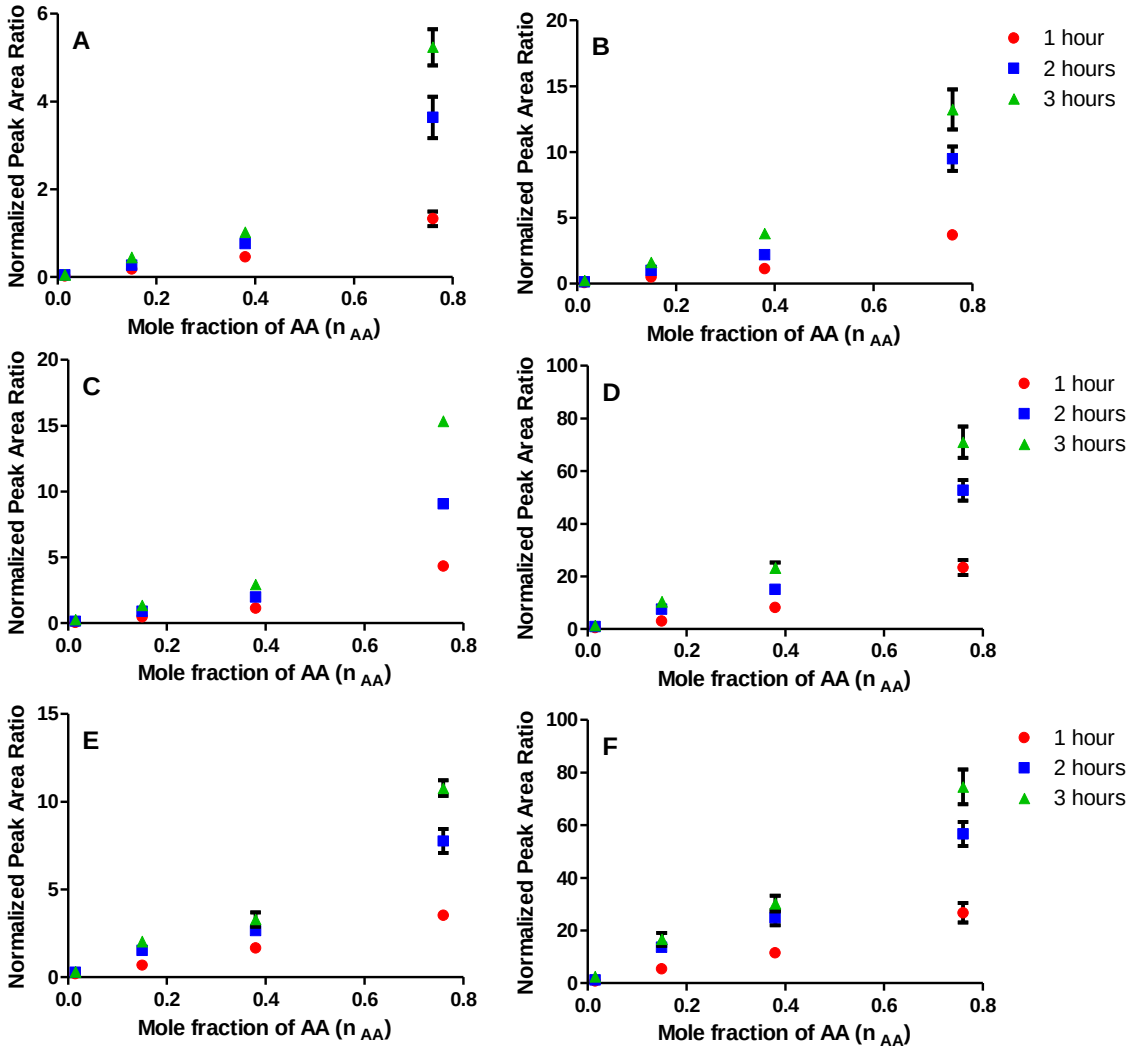

Figure 2.11. Mole fraction-dependent formation of non-enzymatic (A) *cis*-11,12-EET, (B) *trans*-11,12-EET, (C) *cis*-8,9-EET, (D) *trans*-8,9-EET, (E) *cis*-5,6-EET, and (D) *trans*-5,6-EET in liposomes. Each time point reaction was performed in triplicates and normalized to its zero time point. Each data point shows mean ± S.D.

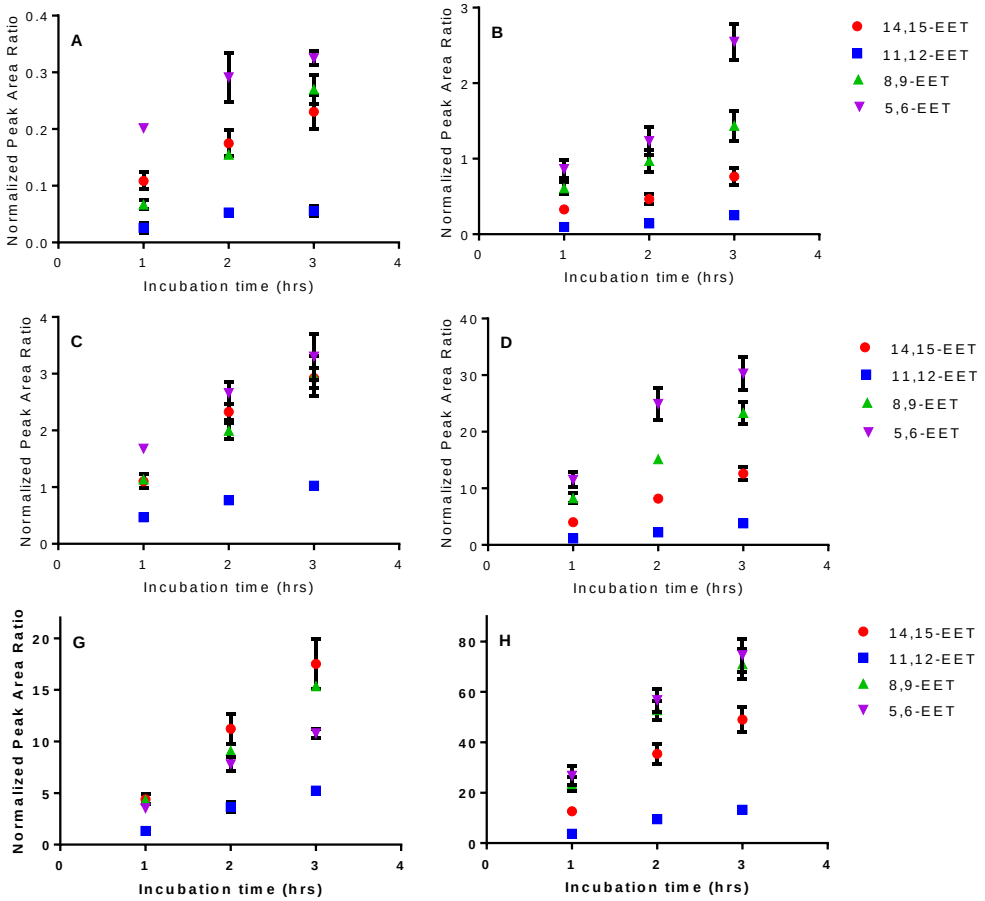

Figure 2.12. Time-dependent formation of non-enzymatic *cis*-EETs and *trans*-EETs at n_{AA} of 0.015 (A and B), n_{AA} of 0.38 (C and D), and n_{AA} of 0.76 (E and F) in liposomes. Each time point reaction was performed in triplicate and normalized to its zero time point. Each data point shows mean ± S.D.

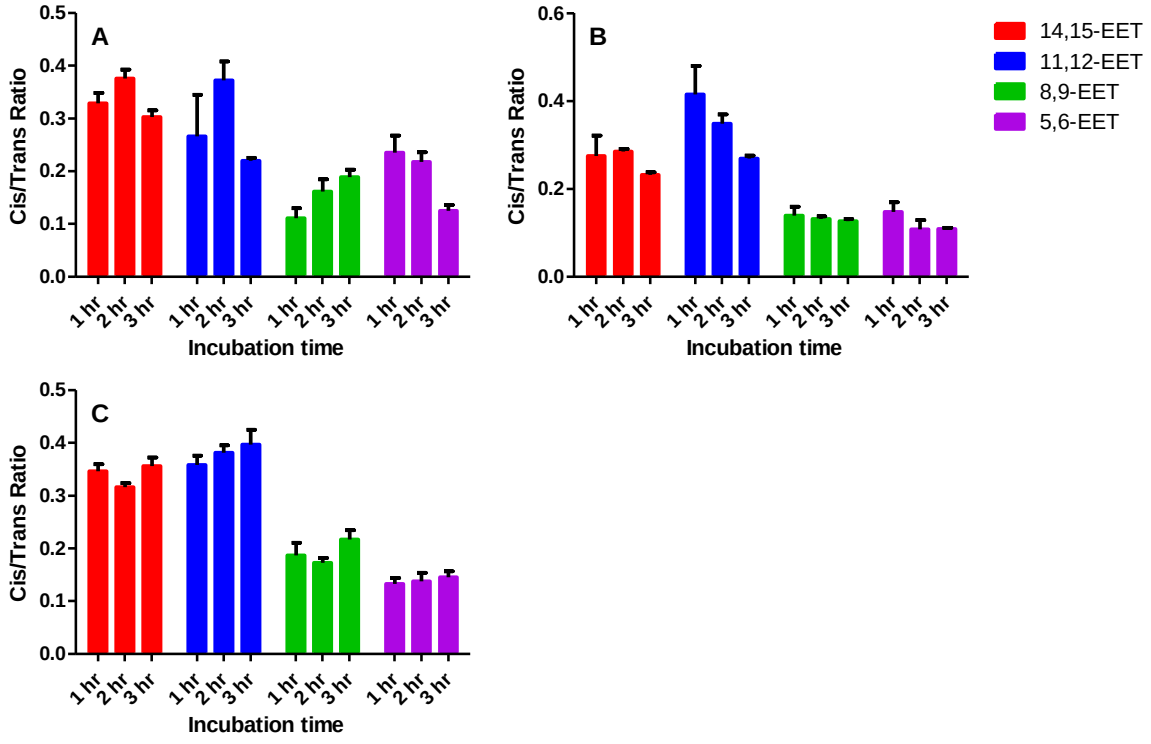

Figure 2.13. Ratios of *cis*- to *trans*-EETs in liposomes at n_{AA} of (A) 0.015, (B) 0.38, and (C) 0.76 at various incubation time points. Each time point reaction was performed in triplicate and normalized to its zero time point. Each data point shows mean ± S.D.

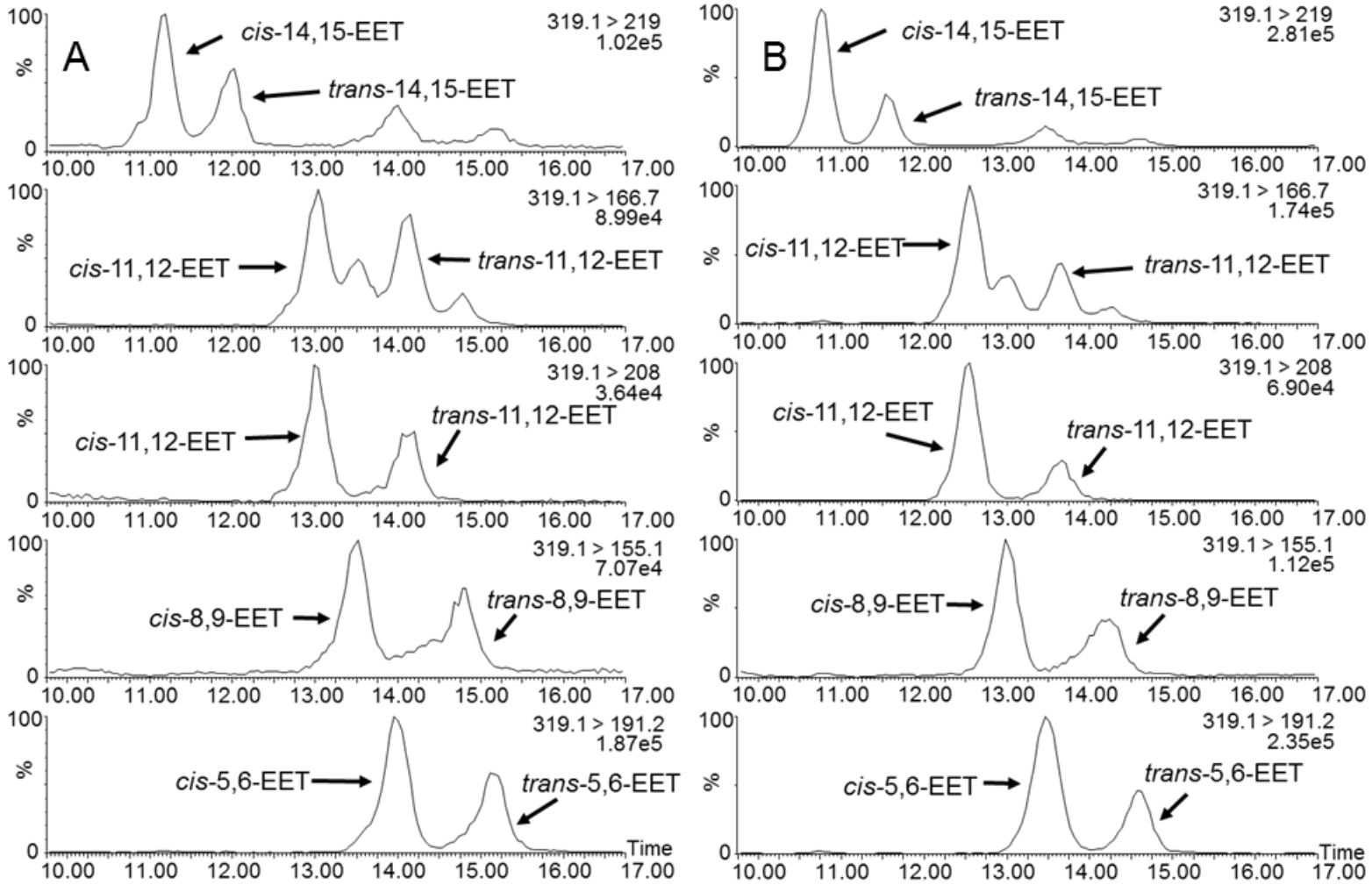

Figure 2.14. Extracted ion chromatograms of EETs obtained from erythrocyte membrane of (A) C57BL/6 mice and (B) human.

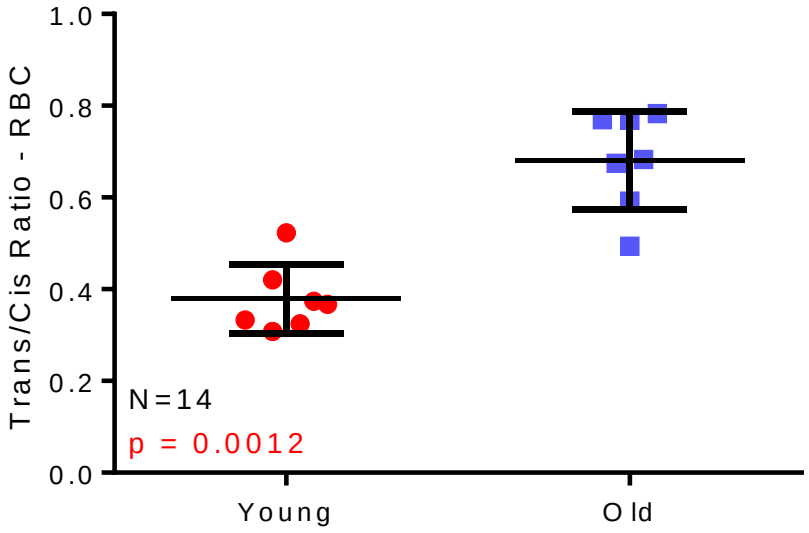

Figure 2.15. Comparison of total *trans*-/*cis*-EETs in RBC of young and old mice.

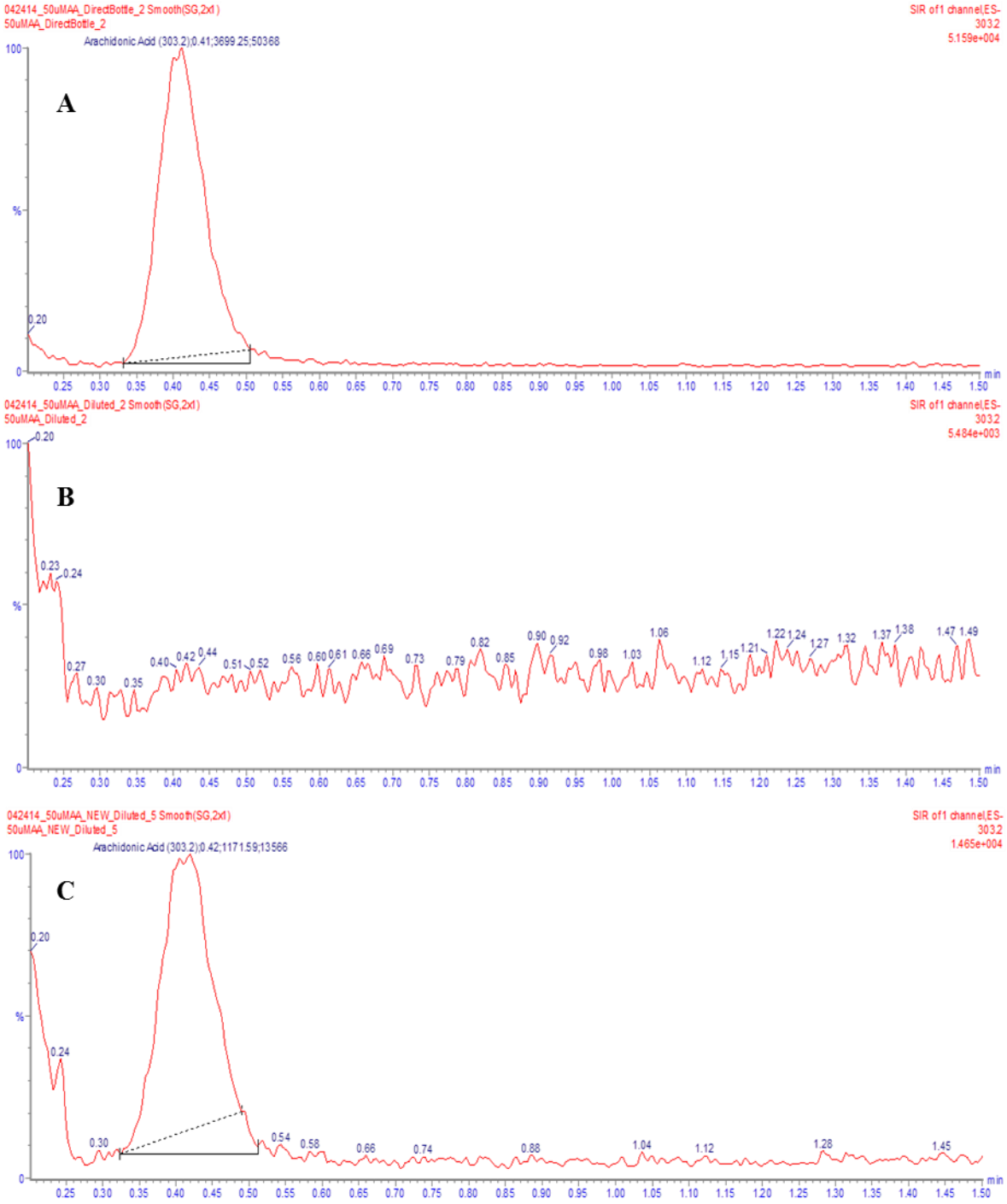

Figure 2.16. Total ion chromatograms from a direct infusion of 50 μM of AA (A) diluted directly from the stock bottle into an aqueous buffer, (B) serially diluted from an aqueous buffer into another aqueous buffer, and (C) serially diluted from ethanol into an aqueous buffer.

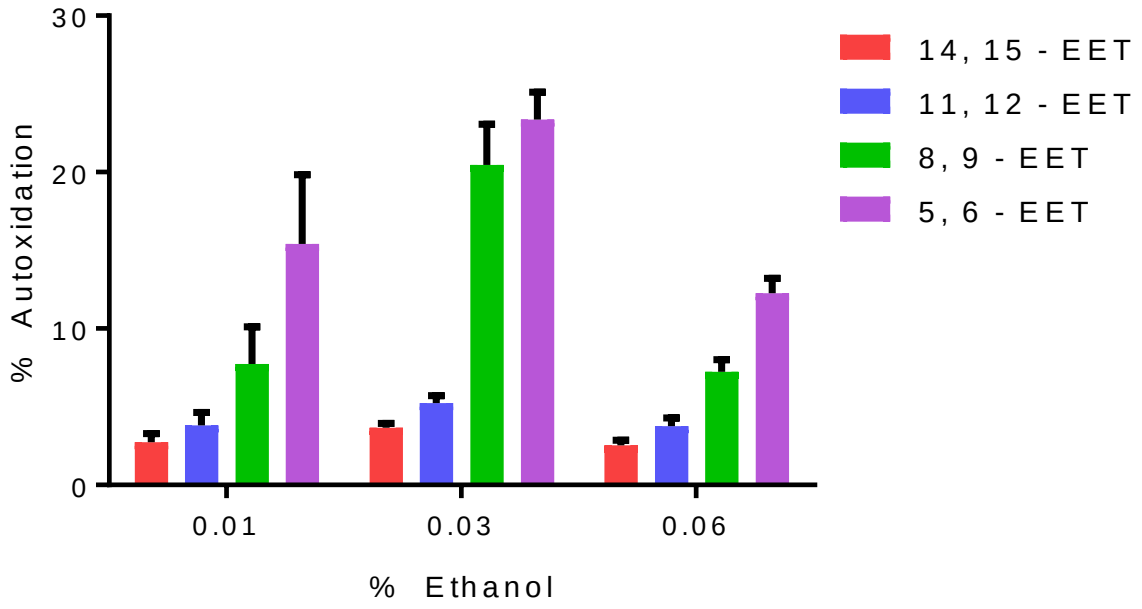

Figure 2.17. Effect of ethanol on autoxidation of AA demonstrated by non-enzymatic formation of individual regioisomer of *cis*-EETs. AA incubation was performed in reconstituted recombinant CYP2J2 enzyme systems. At 0.06% ethanol, formation of non-enzymatic *cis*-EETs is the minimum.

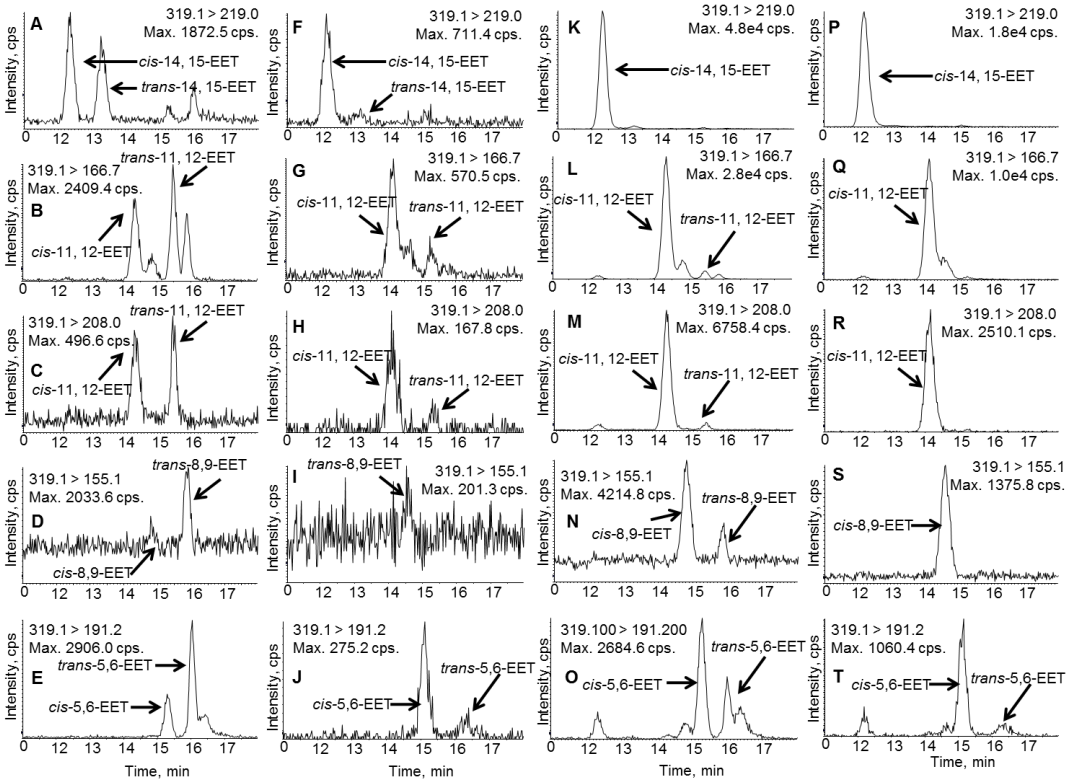

Components				
KPi	+	+	+	+
DETAPAC	-	+	-	+
Pyruvate	-	+	-	+
NADPH	-	-	+	+

Figure 2.18. Extracted ion chromatograms of reconstituted CYP enzyme incubation of AA in the absence and presence of NADPH, DETAPAC, and pyruvate. Formation of non- NADPH-dependent *cis*- and *trans*-EETs was observed at greater intensity in the no NADPH control in potassium phosphate (KPi) buffer (A-E), while addition of DETAPAC and pyruvate markedly reduced NADPH-independent formation of EETs (F–J). In the presence of NADPH and absence of both DETAPAC and pyruvate, *cis*-EETs were observed at a very high level, which confirmed that CYP exclusively make *cis*-EETs (K-O). In this sample, *trans*-EETs were still observed. Addition of DETAPAC and pyruvate markedly diminished the formation of non-NADPH-dependent EETs (P-T). Normalization of EETs formed in the incubation to its corresponding no NADPH control was still necessary for all samples.

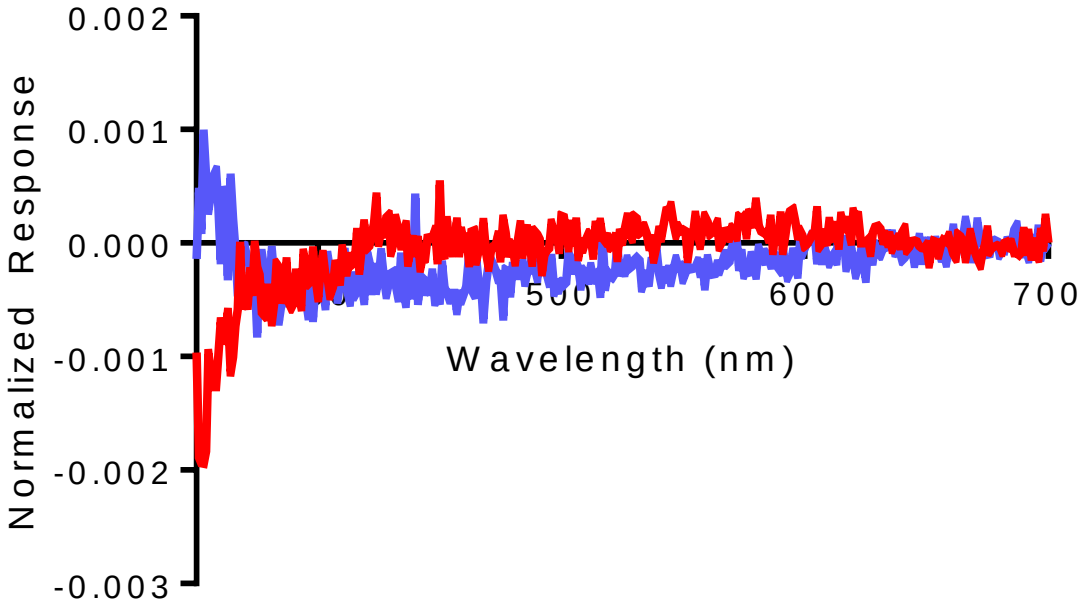

Figure 2.19. Soret spectrum of CYP2J2 in the presence of 1 mM pyruvate (red), and 1 mM pyruvate and 0.1 mM DETAPAC (blue).

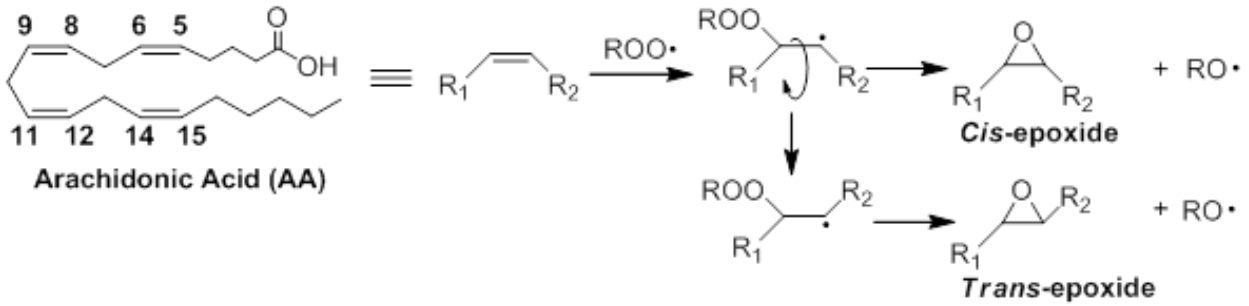

Figure 2.20. Proposed mechanism of *cis*- and *trans*-EET formation via free radical oxidation.

Table 2.1. Percentages of each *cis*- and *trans*-EET relative to total *cis*- or *trans*-EETs, respectively, in benzene and liposomes.

Reaction condition		**% 14,15-EET**	**% 11,12-EET**	**% 8,9-EET**	**% 5,6-EET**
Benzene	*cis*-	51 ± 2	11 ± 1	19 ± 1	19 ± 3
	trans-	43 ± 4	12 ± 1	22 ± 2	21 ± 3
Liposomes	*cis*-	28 ± 5	9.1 ± 2	27 ± 4	36 ± 9
	trans-	18 ± 3	5.1 ± 0.8	32 ± 3	45 ± 6

Each entry is an average of four concentrations and three time points. Experiments were performed in triplicates and data are presented as mean ± S.D.

Table 2.2. Normalized peak height ratios and ratios of each *cis*- and *trans*-EET in (A) old and (B) young mouse RBC membranes and hearts.

A	**Mouse RBC (N=7)**			**Mouse Heart (N=7)**		
	cis-	*trans*-	*cis*-/*trans*-	*cis*-	*trans*-	*cis*-/*trans*-
14,15-EET	68 ± 10	35 ± 6	2.0 ± 0.2	4.5 ± 0.08	3.8 ± 0.7	1.2 ± 0.1
11,12-EET	81 ± 20	65 ± 20	1.3 ± 0.4	4.6 ± 0.9	6.1 ± 1	0.77 ± 0.07
8,9-EET	27 ± 4	19 ± 6	1.6 ± 0.5	3.4 ± 0.6	8.0 ± 2	0.43 ± 0.05
5,6-EET	26 ± 6	21 ± 5	1.3 ± 0.3	2.5 ± 0.5	2.6 ± 0.5	1.0 ± 0.2

B	**Mouse RBC (N=7)**			**Mouse Heart (N=7)**		
	cis-	*trans*-	*cis*-/*trans*-	*cis*-	*trans*-	*cis*-/*trans*-
14,15-EET	7.9 ± 2	3.0 ± 0.7	2.6 ± 0.4	3.7 ± 0.9	3.3 ± 0.8	1.1 ± 0.2
11,12-EET	4.4 ± 1	2.9 ± 0.7	1.5 ± 0.2	2.8 ± 0.7	3.1 ± 0.8	0.9 ± 0.1
8,9-EET	19 ± 5	7.3 ± 2	2.6 ± 0.5	3.8 ± 0.9	9.3 ± 2	0.41 ± 0.06
5,6-EET	31 ± 9	9.5 ± 2	3.3 ± 0.7	6.6 ± 2.0	12 ± 4	0.60 ± 0.2

Mouse RBC membranes were normalized to 30 mg/mL of total protein while mouse heart tissues were normalized to weight. The data in the tables are presented as means ± S.D. For ease of comparison, the data in the table were multiplied by 1000.

Table 2.3. Normalized peak height ratios and ratios of each *cis*- and *trans*-EET in human RBC membranes and diseased hearts.

	Human RBC (N=28)			Human Heart (N = 12)		
	cis-	*trans*-	*cis*-/*trans*-	*cis*-	*trans*-	*cis*-/*trans*-
14,15-EET	0.017 ± 0.005	0.0094 ± 0.006	2.0 ± 0.6	0.0033 ± 0.0007	0.0019 ± 0.0007	1.9 ± 0.6
11,12-EET	0.013 ± 0.006	0.010 ± 0.007	1.5 ± 0.5	0.0057 ± 0.001	0.0056 ± 0.002	1.2 ± 0.4
8,9-EET	0.016 ± 0.005	0.010 ± 0.007	1.9 ± 0.6	0.011 ± 0.003	0.0050 ± 0.002	2.3 ± 0.5
5,6-EET	0.014 ± 0.009	0.0076 ± 0.007	2.2 ± 0.9	0.0091 ± 0.004	0.0056 ± 0.002	1.7 ± 0.6

Human RBC membranes were normalized to 50 mg/mL of total protein while heart tissues were normalized to tissue weight. The data in the table are presented as means ± S.D.

Table 2.4. Percent remaining of NADPH independent formation of EETs in reconstituted CYP enzyme system according to materials and methods.

Additives	14,15-EET	11,12-EET	8,9-EET	5,6-EET
EDTA	10.3%	14.2%	25.1%	56.3%
DETAPAC	6.5%	9.2%	15.9%	61.9%
EDTA + Pyruvate	4.8%	7.4%	12.2%	29.9%
DETAPAC + Pyruvate	3.2%	4.7%	6.9%	21.3%

Each condition was performed in duplicates.

REFERENCES

Abeti R, Uzun E, Renganathan I, Honda T, Pook MA, and Giunti P (2015) Targeting lipid peroxidation and mitochondrial imbalance in Friedreich's ataxia. *Pharmacol Res* **99:**344-350.

Barrera G (2012) Oxidative stress and lipid peroxidation products in cancer progression and therapy. *ISRN Oncol* **2012:**137289.

Batchu SN, Law E, Brocks DR, Falck JR, and Seubert JM (2009) Epoxyeicosatrienoic acid prevents postischemic electrocardiogram abnormalities in an isolated heart model. *J Mol Cell Cardiol* **46:**67-74.

Celermajer DS, Sorensen KE, Spiegelhalter DJ, Georgakopoulos D, Robinson J, and Deanfield JE (1994) Aging is associated with endothelial dysfunction in healthy men years before the age-related decline in women. *J Am Coll Cardiol* **24:**471-476.

Davì G, Falco A, and Patrono C (2005) Lipid peroxidation in diabetes mellitus. *Antioxid Redox Signal* **7:**256-268.

Erusalimsky JD and Kurz DJ (2005) Cellular senescence in vivo: its relevance in ageing and cardiovascular disease. *Exp Gerontol* **40:**634-642.

Evangelista EA, Kaspera R, Mokadam NA, Jones JP, and Totah RA (2013) Activity, inhibition, and induction of cytochrome P450 2J2 in adult human primary cardiomyocytes. *Drug Metab Dispos* **41:**2087-2094.

Ferreri C, Samadi A, Sassatelli F, Landi L, and Chatgilialoglu C (2004) Regioselective cis-trans isomerization of arachidonic double bonds by thiyl radicals: the influence of phospholipid supramolecular organization. *J Am Chem Soc* **126:**1063-1072.

Goulitquer S, Dréano Y, Berthou F, Corcos L, and Lucas D (2008) Determination of epoxyeicosatrienoic acids in human red blood cells and plasma by GC/MS in the NICI mode. *J Chromatogr B Analyt Technol Biomed Life Sci* **876:**83-88.

Jiang H, Anderson GD, and McGiff JC (2010) Red blood cells (RBCs), epoxyeicosatrienoic acids (EETs) and adenosine triphosphate (ATP). *Pharmacol Rep* **62:**468-474.

Jiang H, Kruger N, Lahiri DR, Wang D, Vatèle JM, and Balazy M (1999) Nitrogen dioxide induces cis-trans-isomerization of arachidonic acid within cellular phospholipids. Detection of trans-arachidonic acids in vivo. *J Biol Chem* **274:**16235-16241.

Jiang H, McGiff JC, Quilley J, Sacerdoti D, Reddy LM, Falck JR, Zhang F, Lerea KM, and Wong PY (2004) Identification of 5,6-trans-epoxyeicosatrienoic acid in the phospholipids of red blood cells. *J Biol Chem* **279:**36412-36418.

Jiang H, Quilley J, Doumad AB, Zhu AG, Falck JR, Hammock BD, Stier CT, and Carroll MA (2011) Increases in plasma trans-EETs and blood pressure reduction in spontaneously hypertensive rats. *Am J Physiol Heart Circ Physiol* **300:**H1990-1996.

Jiang H, Zhu AG, Mamczur M, Morisseau C, Hammock BD, Falck JR, and McGiff JC (2008) Hydrolysis of cis- and trans-epoxyeicosatrienoic acids by rat red blood cells. *J Pharmacol Exp Ther* **326:**330-337.

Kaspera R and Totah RA (2009) Epoxyeicosatrienoic acids: formation, metabolism and potential role in tissue physiology and pathophysiology. *Expert Opin Drug Metab Toxicol* **5:**757-771.

Lakatta EG and Levy D (2003) Arterial and cardiac aging: major shareholders in cardiovascular disease enterprises: Part I: aging arteries: a "set up" for vascular disease. *Circulation* **107:**139-146.

Long LH and Halliwell B (2009) Artefacts in cell culture: pyruvate as a scavenger of hydrogen peroxide generated by ascorbate or epigallocatechin gallate in cell culture media. *Biochem Biophys Res Commun* **388:**700-704.

Lucas DT and Szweda LI (1998) Cardiac reperfusion injury: aging, lipid peroxidation, and mitochondrial dysfunction. *Proc Natl Acad Sci U S A* **95:**510-514.

Nakamura T, Bratton DL, and Murphy RC (1997) Analysis of epoxyeicosatrienoic and monohydroxyeicosatetraenoic acids esterified to phospholipids in human red blood cells by electrospray tandem mass spectrometry. *J Mass Spectrom* **32:**888-896.

Oliw EH (1994) Oxygenation of polyunsaturated fatty acids by cytochrome P450 monooxygenases. *Prog Lipid Res* **33:**329-354.

Oliw EH, Guengerich FP, and Oates JA (1982) Oxygenation of arachidonic acid by hepatic monooxygenases. Isolation and metabolism of four epoxide intermediates. *J Biol Chem* **257:**3771-3781.

Pozzi A, Macias-Perez I, Abair T, Wei S, Su Y, Zent R, Falck JR, and Capdevila JH (2005) Characterization of 5,6- and 8,9-epoxyeicosatrienoic acids (5,6- and 8,9-EET) as potent in vivo angiogenic lipids. *J Biol Chem* **280:**27138-27146.

Rivard A, Fabre JE, Silver M, Chen D, Murohara T, Kearney M, Magner M, Asahara T, and Isner JM (1999) Age-dependent impairment of angiogenesis. *Circulation* **99:**111-120.

Roy U, Loreau O, and Balazy M (2004) Cytochrome P450/NADPH-dependent formation of trans epoxides from trans-arachidonic acids. *Bioorg Med Chem Lett* **14:**1019-1022.

Shao B and Heinecke JW (2009) HDL, lipid peroxidation, and atherosclerosis. *J Lipid Res* **50:**599-601.

Siscovick DS, Raghunathan TE, King I, Weinmann S, Wicklund KG, Albright J, Bovbjerg V, Arbogast P, Smith H, and Kushi LH (1995) Dietary intake and cell membrane levels of long-chain n-3 polyunsaturated fatty acids and the risk of primary cardiac arrest. *JAMA* **274:**1363-1367.

Sun C, Simon SI, Foster GA, Radecke CE, Hwang HV, Zhang X, Hammock BD, Chiamvimonvat N, and Knowlton AA (2016) 11,12-Epoxyecosatrienoic acids mitigate endothelial dysfunction associated with estrogen loss and aging: Role of membrane depolarization. *J Mol Cell Cardiol* **94:**180-188.

Vaz AD, McGinnity DF, and Coon MJ (1998) Epoxidation of olefins by cytochrome P450: evidence from site-specific mutagenesis for hydroperoxo-iron as an electrophilic oxidant. *Proc Natl Acad Sci U S A* **95:**3555-3560.

Weingand KW, Clarkson TB, Adams MR, and Bostrom AD (1986) Effects of age and/or puberty on coronary artery atherosclerosis in cynomolgus monkeys. *Atherosclerosis* **62:**137-144.

Weinsaft JW and Edelberg JM (2001) Aging-associated changes in vascular activity: a potential link to geriatric cardiovascular disease. *Am J Geriatr Cardiol* **10:**348-354.

Xu L, Davis TA, and Porter NA (2009) Rate constants for peroxidation of polyunsaturated fatty acids and sterols in solution and in liposomes. *J Am Chem Soc* **131:**13037-13044.

Xu L and Porter NA (2015) Free radical oxidation of cholesterol and its precursors: Implications in cholesterol biosynthesis disorders. *Free Radic Res* **49:**835-849.

Yang C, Pan S, Yan S, Li Z, Yang J, Wang Y, and Xiong Y (2014) Inhibitory effect of 14,15-EET on endothelial senescence through activation of mTOR complex 2/Akt signaling pathways. *Int J Biochem Cell Biol* **50:**93-100.

Yang L, Mäki-Petäjä K, Cheriyan J, McEniery C, and Wilkinson IB (2015) The role of epoxyeicosatrienoic acids in the cardiovascular system. *Br J Clin Pharmacol* **80:**28-44.

Yin H, Xu L, and Porter NA (2011) Free radical lipid peroxidation: mechanisms and analysis. *Chem Rev* **111:**5944-5972.

CHAPTER 3.

POTENTIAL ROLES OF EPOXYEICOSATRIENOIC ACIDS IN PROTECTING AGAINST ACUTE MI AND AS BIOMARKERS OF CARDIOVASCULAR DISEASE

3.1. INTRODUCTION

Arachidonic acid (AA) is an ω-6 polyunsaturated fatty acid (PUFA) that is mostly esterified at the *sn*-2 position in the phospholipid membrane. Upon activation of phospholipase A_2 (PLA_2), AA is released and metabolized through various pathways, including cyclooxygenase, lipoxygenase, and CYP pathways (Bellien et al., 2011). Through the CYP pathway and primarily by CYP2C and CYP2J subfamilies, AA is metabolized to four bioactive regioisomers of *cis*-epoxyeicosatrienoic acids (EETs)(Capdevila et al., 2000). These EETs are rapidly hydrolyzed to less biologically active dihydroxyeicosatrienoic acids (DHETs) by soluble epoxide hydrolase (sEH)(Yu et al., 2000). EETs can be re-esterified back into the phospholipid membrane via an acyl-coenzyme A-dependent mechanism and can also circulate in erythrocyte membranes, plasma lipoproteins, and fatty acid binding protein (FABP) (Karara et al., 1992; Weintraub et al., 1997; Jiang et al., 2005; Jiang et al., 2010). In two male adults, almost half of the EETs in circulating lipoprotein were bound to high density lipoprotein (HDL) (49%) followed by low density lipoprotein (LDL)(28%), and very low density lipoprotein (VLDL)(23%) (Karara et al., 1992).

EETs are signaling molecules, with numerous physiological functions, including anti-inflammatory, pro-angiogenesis and vasodilatory effects and can activate several ion channels (Lu et al., 2006; Webler et al., 2008; Behm et al., 2009; Kaspera and Totah, 2009; Shahabi et al., 2014). Extensive literature from animal studies, and emerging evidence in humans, suggest protective roles of EETs in cardiovascular events, especially during myocardial ischemia reperfusion injury. Two factors that influence EET levels in heart, and potentially circulating levels, are age and cardiovascular disease, both of which will be the focus of Chapter 3.

In a study we recently published, we found that *cis*-EET levels esterified in the erythrocyte membrane of C57/BL6 mice increase with age (Aliwarga et al., 2017). This observation may be due to chronic and low-grade inflammation associated with the aging process that could increase EET production (Franceschi and Campisi, 2014). Conversely, a study by Chaudhary and colleagues reported that young mice (2-3 months) carrying the human CYP2J2 transgene in their heart had overall improved heart function post-ischemia when compared to wild-type mice. However, the cardioprotective effect of CYP2J2 overexpression significantly declined in old transgenic mice (11-13 months) (Chaudhary et al., 2013). Unfortunately, the authors only measured *cis*-EET levels in aged mice in this study. It is unclear if reduction in the cardioprotective effect of CYP2J2 overexpression in aged mice was due to alterations in EET levels or if perhaps overexpression of CYP2J2 could not compensate for the stress-associated with ischemia and cellular dysfunction-associated with normal aging.

The effect of disease state on *cis*-EET levels has been demonstrated in coronary artery disease (CAD) patients. Higher plasma EET levels were observed in CAD patients compared to healthy volunteers, although, obesity within CAD patients led to lower plasma EET levels (Theken et al., 2012; Schuck et al., 2013). A follow up study from the same group showed opposite results where total EET levels in both non-obstructive and obstructive CAD patients were generally lower than their control group (no apparent CAD) (Oni-Orisan et al., 2016). Due to the functional importance of EETs in cardiovascular health, monitoring the levels of circulating EETs could conceivably serve as a reporter for cardiac events and a predictor of risk or injury prior to the occurrence of the cardiovascular disease or injury. Performing heart biopsies to determine cardiac EET levels is not a viable option and so other alternatives must be investigated, such as measuring circulating EETs. When we examine the percent distribution of

each individual regioisomer relative to total EETs measured in rat cardiac tissue or rat plasma published in separate studies by two different groups, we find that the ratio of EETs is similar in both compartments (Karara et al., 1992; Wu et al., 1997). Another study in humans showed a strong correlation (r = 95%) between plasma and red blood cell (RBC) membrane levels of EETs (Goulitquer et al., 2008). Collectively, these published data suggest that levels of EETs in RBC or plasma can potentially be used to report on EET concentrations in heart tissue, especially prior to a cardiac event.

Current methods to diagnose patients with acute coronary syndromes involve the utilization of multimarker tests, namely B-type Natriuretic Peptide (BNP) for hemodynamic stress, high sensitivity C-Reactive Protein (hsCRP) for inflammation, and cardiac troponin that measures both troponin T and troponin I for myocardial necrosis (Morrow and Braunwald, 2003). BNP is a 32-amino acid polypeptide secreted mainly by the cardiac ventricles in response to volume expansion and pressure overload. In dyspneic patients, BNP levels are typically used to determine if observed dyspnea is a result of Congestive Heart Failure (CHF). In addition to using BNP level as diagnostic marker for CHF, BNP is also a useful marker for prognosis, and risk stratification in patients who have had prior CHF (Maisel, 2002). CRP is an inflammatory marker whose transcription is primarily regulated by Interleukin-6 (IL-6). CRP was thought to be exclusively synthesized in the liver, however, several studies now suggest that CRP is produced in atherosclerotic lesion, kidney, neurons, and alveolar macrophages (Jialal et al., 2004). The hsCRP test is usually recommended for patients whose Framingham risk score is between 10%-20% because inflammation has been shown to be key in the pathogenic mechanism of atherosclerosis. HsCRP has been shown to be useful in predicting the reoccurrence of coronary events in patients with unstable angina, myocardial infarction, stroke, and peripheral arterial

disease. In addition, the hsCRP test is deemed to be beneficial in prognosis and risk stratification in patients with prior history of cardiovascular disease (Pearson et al., 2003). Troponin complex is located on the myofibrillar thin filament of striated muscle and consists of troponin C, troponin I, and troponin T. Only troponin I and troponin C isoforms are expressed in cardiac muscle. Troponin complex regulates the calcium-modulated interaction of actin and myosin in the heart. Cardiac troponin C regulates the activation of actin filament upon calcium binding, cardiac troponin I inhibits muscle contraction in the absence of calcium binding to cardiac troponin C, and cardiac troponin C attaches the troponin complex to tropomyosin and to the actin filaments (Korff et al., 2006). Myocardial necrosis due to prolonged ischemia can be observed by the appearance of circulating various proteins including myoglobin, cardiac troponin I, cardiac troponin T, creatine kinase, lactate dehydrogenase, and many others. Due to the localization of cardiac troponin I and T in the cardiac muscle, the cardiac troponin test remains the choice biomarker test for myocardial necrosis. Additionally, troponin release can be used as an indicator of how well patients will respond to anti-platelet and anti-thrombin therapy (Morrow and Braunwald, 2003). The common advantage for the existing marker tests for CVD is that they have relatively rapid analyses and turnaround times. However, these tests are advantageous only if the individual has developed CVD. For example, the BNP test is only effective in symptomatic patients who have had CHF and the cardiac troponin test is useful for evaluating the extent of myocardial damage and how well patients would respond to therapy. In the case of the hsCRP test, several factors including lifestyle, diet, cigarette smoking, alcohol consumption, metabolic syndrome, birth control use, cholesterol lowering medications, and many others conditions, can alter CRP levels and complicate test results. Therefore, measuring EET levels as an indicator of cardiovascular health and function as well as surrogate marker for any cardiac event prior to

development of severe cardiovascular injury could be beneficial. Given the intrinsic instability of EETs, the proper blood collection, handling and separation of plasma and RBC components is crucial. In addition, the turnaround time for analysis of EETs from blood samples is not quite high-throughput. Yet, despite these limitations, EETs (either collectively or individually) could be a useful marker to report on cardiovascular health pre- and post-cardiac events.

CYP2J2 is the only CYP2J subfamily member that is expressed in humans (Wu et al., 1996). Because we are using a mouse model that overexpresses cardiomyocyte-specific CYP2J2, it is important to understand the distribution and function of endogenous mouse cyp2j isoforms. Seven mouse cyp2j genes and three cyp2j pseudogenes have been identified to date. Most mouse cyp2j isoforms are expressed extrahepatically. Evidence for both transcript and protein expression of cyp2j5 were found in the kidney and liver (Ma et al., 1999). *Cyp2j6* transcript was found in high levels in small intestine and to a much lesser extent in the heart, while its unstable protein *in vitro* caused inconclusive Western blot results (Ma et al., 2002). *Cyp2j8* transcript was found in kidney, brain, and small intestine, but the protein could only be detected in the brain and kidney (Graves et al., 2013). *Cyp2j9* transcripts and protein were found predominantly in the brain but not in the heart (Qu et al., 2001). *Cyp2j11* transcript was found in the kidney and heart, while the protein was expressed prominently in proximal convoluted tubules of kidney, liver, and to a lesser extent in cardiomyocytes (heart) (Graves et al., 2013). *Cyp2j12* and *cyp*2j13 transcripts were found prominently in brain and kidney, respectively, however, antibodies for cyp2j12 and cyp2j13 in the study cross-reacted with other cyp2j isozymes (Graves et al., 2013). Based on a comparison of turnover rates of AA and linoleic acid, cyp2j11 appeared to slightly prefer linoleic acid compared to AA and performed slightly more hydroxylation reactions than epoxygenation (Graves et al., 2013). However, the limitation of this study was that the authors

did not account for non-enzymatic formation of EETs and the monohydroxylated metabolites of AA. Perhaps enzymatic characterization of mouse cyp2j isozymes, and the fatty acid metabolite profiles need to be re-determined using specific antibodies or quantitative proteomics to assess protein expression in various tissues.

In this Chapter, we demonstrate the potential of using erythrocyte membrane EETs as surrogate markers for cardiac events in a mouse model that specifically overexpress human CYP2J2 in the cardiomyocytes and not endothelial cells. This is the most suitable model available due to difficulties in obtaining matched cardiac and blood samples from the same subject. We report on the effect of age and disease in altering both *cis*- and *trans*-EET levels in cardiac tissue and RBC membranes in these mice. We also show that in the disease model of acute MI, there is clear evidence of protection in the transgenic (Tr) mice compared to wild-type (WT). The overexpression of CYP2J2 is also associated with increasing EET levels esterified to the membrane in the heart. Finally, in order to provide further evidence that our observations in the mouse model can be translated to humans, levels of *cis*- and *trans*-EETs extracted from erythrocyte membrane of controls and sudden cardiac arrest (SCA) cases were measured.

3.2. MATERIALS AND METHODS

3.2.1. REAGENTS

Stocks of AA, *cis*-EETs (14,15-, 11,12-, 8,9-, and 5,6-EETs), deuterated internal standards (14,15-EET-d_{11}, 8,9-EET-d_{11}, 5,6-EET-d_{11}, and 14,15-DHET-d_{11}) and 4-[[*trans*-4-[[(tricyclo[3.3.1.1^{3,7}]dec-1-ylamino)carbonyl]amino]cyclohexyl]oxy]-benzoic acid (*t*-AUCB) were purchased from Cayman Chemicals (Ann Arbor, MI). CM-H2DCFDA (general oxidative

stress indicator) was obtained from Thermo Fisher Scientific (Waltham, MA). Dulbecco's phosphate buffered saline (DPBS, 10 ×), ACS-grade ethyl acetate, chloroform, optima-grade acetonitrile, water, and methanol were purchased from Fisher Scientific (Hampton, NH) and used without further purification. Triphenylphosphine (TPP), phospholipase A_2 from *Naja mossambica mossambica*, TMR Red *in situ* cell death detection kit was obtained from Sigma-Aldrich (St. Louis, MO).

3.2.2. CALIBRATION CURVE OPTIMIZATION

The calibration curves were prepared either in erythrocyte membranes as a biological matrix or in 1× DPBS to compare the matrix effect on the EETs standard levels. Quantitation of volunteer 1's EET levels were determined and compared using either a calibration curve made in 1 ×DPBS or in expired RBC membranes. We extracted blood from volunteer 1 in every extraction performed to serve as an external quality control. The calibration curve ranged from 0 to 75 ng/mL for each regioisomer of *cis*-EET always made fresh on the day of extraction.

For both erythrocyte membranes and cardiac tissue samples, final concentrations of each regioisomer of *cis*-EET were 0, 5, 10, 25, 50, 75, 100, 250, and 500 ng/mL. Two quality control samples were used at 10 and 100 ng/mL of *cis*-EETs. Quality controls were diluted and prepared from original stocks separately to the calibration curve standards. Calibration curve samples were treated and extracted in the same way as the biological samples. The only exception was during the phospholipase A_2 hydrolysis step. In this step, the dried calibration curve extracts were dissolved in 1× PLA_2 buffer followed by addition of nitrogen-purged ethyl acetate instead of the enzyme. The rest of the extraction procedure followed the same steps in section 2.3.6 or 2.3.7 for the different tissues.

3.2.3. ANIMAL MODEL

Mice with cardiomyocyte-specific overexpressing CYP2J2 driven by the α-myosin heavy chain promoter (α-MHC) were described previously (Seubert et al., 2004). These mice were obtained from Dr. Darryl Zeldin's lab at NIEHS. They were created on the background of wild-type (WT) mice. C57BL/6 WT female mice were purchased from Charles River Laboratories (Wilmington, MA) and bred with Tr male mice to produce a heterozygote offspring expressing CYP2J2. Mice were bred in-house and managed by the University of Washington Department of Comparative Medicine. Pups were weaned at 21 days at which time a tail biopsy was obtained. Genotyping and assignment of a Tr or WT genotype was performed following procedures previously published (Lee et al., 2010).

In general, whole blood was collected through cardiac puncture following asphyxiation with CO_2. The collected RBC were washed three-times with cold 1 × DPBS and stored at -80°C until further processing. After removal of the heart from the mouse chest cavity, the tissue was immediately washed with cold 1 × DPBS and flash frozen in liquid nitrogen. All animal experiments were performed in compliance with approved protocols by Institutional Animal Care and Use Committee of the University of Washington.

Young and aged mice of both genotypes and genders were used for studies correlating heart vs. RBC membrane EET levels. Mice were considered young if they were an average of 4.1 months old for both genotypes. The age ranged between 10.1 to 22.5 months old for the aged WT mice and between 12 to 20 months old for aged Tr mice. To study the effect of age, the mice were separated into groups based on genotype and age. To study the effect of disease, the mice

were separated into 4 groups. Within each group, there were 4 male and 4 female mice that were between 3-4 months old. The groups were WT sham, Tr sham, WT- MI and Tr-MI.

3.2.4. ECHOCARDIOGRAPHY AND MYOCARDIAL INFARCTION SURGERY

These procedures were performed by Dr. Xiaoyun Guo from University of Washington, Department of Physiology and Biophysics. Mice were anesthetized with 1.5% isoflurane prior to echocardiography. Echocardiographic imaging was performed with a VisualSonics Vevo 2100 imaging system as described previously (Li et al., 2016). Briefly, M-mode ventricular dimensions were measured and averaged from 3-5 cycles. Fractional shortening (FS) was calculated using the following equation:

$$FS = \left[\frac{(LVED - LVES)}{LVED}\right] \times 100\%$$

LVES is left ventricular dimension at the end of systole, whereas, LVED is dimension of left ventricle at the end of diastole. Echocardiography was performed prior to surgery, a week post-surgery, and two weeks post-surgery prior to tissue harvesting. The surgical procedure for MI in the mouse with permanent ligation of the left anterior descending artery has been described previously (Guo et al., 2017). A similar procedure without ligation was performed on sham mice.

3.2.5. HISTOLOGICAL ANALYSIS, CELL SURFACE AREA MEASUREMENT, AND TERMINAL DEOXYNUCLEOTIDYL TRANSFERASE DUTP NICK END LABELLING (TUNEL)

Histological analysis of fibrosis, and cell surface area measurements were described previously (Guo et al., 2017). Briefly, mouse hearts (N= 4-5) were fixed in 10% formalin/PBS

and dehydrated for paraffin embedding. The dehydrated, paraffin-embedded fixed hearts were then cut into 5-μm sections for Masson's trichrome staining. The percentage of myocardial fibrosis was determined using the ratio of the total interstitial fibrosis area to longitudinal sectional area of a left ventricle section using MetaMorph 6.1 software as described previously (Guo et al., 2017). Using a section of dehydrated, paraffin-embedded fixed hearts, TUNEL was performed using TMR Red *in situ* cell death detection kit following manufacturer's instructions.

3.2.6. DETECTION OF REACTIVE OXYGEN SPECIES (ROS)

Using frozen cardiac sections, cellular production of ROS was detected using CM-H2DCFDA staining following manufacturer's instruction. The percentage of ROS generated was calculated as ratio of the total fluorescent area to the whole area using ImageJ software (National Institutes of Health, Bethesda, MD). The values reported for % ROS was an average from 4~5 images.

3.2.7. FRACTIONATED HUMAN PLASMA

Fractionated human plasma was obtained from Dr. Tomas Vaisar's laboratory following a previously published protocol (Reardon et al., 2001). Briefly, human plasma (150-200 μL per injection, total plasma 2 mL) was injected into tandem Superose 6 fast protein liquid chromatography in 200 mM sodium phosphate, pH 7.4, 50 mM sodium chloride, 0.03% EDTA, and 0.02% sodium azide. For each plasma injection, 500 μL fractions were collected for each lipoprotein. Prior to EET extraction, the fractions of the same lipoprotein were pooled and concentrated using EMD Millipore^{TM} Centriprep^{TM} centrifugal filter unit with molecular weight cut-off of 10 kDa.

3.2.8. HUMAN ERYTHROCYTE MEMBRANES

Human erythrocyte membrane samples were obtained from the same repository of SCA cases and population-based controls used previously in Chapter 2. For every EET extraction from erythrocyte membrane, RBC from healthy volunteer 1 was used as external control and to account for inter- and intra-day variability. In this study, we used a random sample of 25 controls and 27 case samples that had been collected between October 1988 and September 2005 as part of a case-control study of erythrocyte fatty acids and incident SCA. The University of Washington Human Subject Review Committee approved the study protocol.

3.2.9. EXTRACTION OF EETS FROM ERYTHROCYTE MEMBRANE AND HEART TISSUE

The extraction of EETs from both erythrocyte membranes and heart tissue followed a procedure detailed in sections 2.2.6 and 2.2.7 of Chapter 2 of this dissertation. The only difference was in the reconstitution of the samples prior to mass spectrometric analysis. EETs extracted from both erythrocyte membrane and cardiac tissue of mice subjected to MI or sham surgery were reconstituted in 50 µL of a solution containing 50% of water and 50% of 80:20 acetonitrile:methanol prior to MS analysis.

3.2.10. LIQUID CHROMATOGRAPHY AND MASS SPECTROMETRIC ASSAY TO QUANTIFY EETS

Quantification of *cis*- and *trans*-EETs was performed following methods in section 2.2.9 as published previously (Aliwarga et al., 2017).

3.2.11. DATA ANALYSIS

Mass spectrometry data were analyzed using MassLynx 4.1. Data analysis was performed using Prism 7.04 (GraphPad, La Jolla, CA). Correlation analyses were performed using non-parametric Spearman correlation as denoted by R_s values. The remaining statistical analyses performed using Prism were analyzed using non-parametric t-tests. The percent difference between EETs from calibration curves prepared in DPBS vs. RBC was calculated by taking the average difference in amount of each *cis*-EET in duplicate samples and dividing it by the average amount of the corresponding *cis*-EET in 1× DPBS and multiplying by 100%.

In the biological samples, integrated peak height of each analyte was normalized to the corresponding peak height of internal standard. Levels of each regioisomer of *cis*-EETs were quantified using calibration curve, while levels of *trans*-EETs were determined using normalized peak height ratios. In addition to analyte normalization to its internal standard, the amount or ratios of peak heights for each analyte were normalized to total protein contents for both erythrocyte membrane and cardiac tissue. Because only 1/5 of the heart homogenates were used for each sample replicate, the amount or ratios of peak heights of each analyte were multiplied by 5 to account for the whole cardiac tissue.

3.3. RESULTS

3.3.1. CALIBRATION CURVE OPTIMIZATION

Because one of our matrices was erythrocyte membranes, spiking expired erythrocyte membranes for our calibration curve to mimic the matrix of our samples was ideal. However, the challenge was that the presence of residual free EETs in the erythrocyte membrane could skew

our quantitation. As shown in Table 3.1, quantitation of *cis*-14,15- and *cis*-8,9-EETs using RBC-spiked calibration curve led to about 26% and 19% higher EETs compared to a DPBS-spiked calibration curve. The percent difference for both *cis*-11,12- and *cis*-5,6-EETs was less than 10%, which was considered acceptable. For *cis*-EET quantitation, the calibration curve was prepared fresh in cold 1 × DPBS prior to any extraction.

3.3.2. EET LEVELS IN ERYTHROCYTE MEMBRANE AND CARDIAC TISSUE OF WT AND CARDIOMYOCYTE-SPECIFIC OVEREXPRESSING CYP2J2 TR MICE AND CORRELATION BETWEEN EET LEVELS FROM THE TWO TISSUE COMPARTMENTS

Total EETs extracted from both young and old mice are shown in Figure 3.1. There is no significant difference in total EETs extracted from erythrocyte membranes of WT and Tr mice (Figure 3.1 A). However, a significantly higher level of total *cis*-EETs (and each individual regioisomers) extracted from cardiac tissue was observed in Tr compared to WT mice (Figure 3.1 B).

The correlation between EET levels in erythrocyte membrane and cardiac tissue was also examined. No correlation was observed between EET levels in erythrocyte membranes and cardiac tissue of WT mice, except for *cis*-5,6-EET ($R_s = 0.4769$, $p = 0.0159$; Figures 3.2 and 3.3). However, both geometric isomers of 14,15- ($R_s = 0.615$, $p = 0.0009$) and 11,12-EET ($R_s = 0.7062$, $p < 0.0001$) and total EET levels ($R_s = 0.4392$, $p = 0.0280$) in erythrocyte membranes and cardiac tissue of Tr mice were significantly and positively correlated, as seen in Figures 3.4 and 3.5.

3.3.3. EFFECT OF AGE ON LEVELS OF *CIS*- AND *TRANS*-EETS

When the mice were separated by age, there were significant positive correlations between age and levels of *cis*-14,15-, *cis*-11,12-, *cis*-8,9-, and total *cis*-EETs from erythrocyte membranes of both WT and Tr mice (Figures 3.6 and 3.7). The same trend was observed in the corresponding *trans*-EETs (Figures 3.8 and 3.9). However, the correlations seem to be regioisomer-specific in the cardiac tissue. In WT mice, there were significant positive correlations between age and levels of *cis*-14,15- and *cis*-11,12 and a negative correlation between age and level of *cis*-5,6-EET (Figure 3.10). While a significant positive correlation was only observed between age and level of *cis*-11,12-EET in cardiac tissue of Tr mice (Figure 3.11). The trends in *trans*-EETs extracted from cardiac tissue of WT mice were similar to their corresponding *cis*-EETs, with the exception that no significant correlation between age and *trans*-14,15-EET was observed (Figure 3.12). In Tr mice, the only correlation between age and *trans*-EET level was observed with *trans*-5,6-EET (Figure 3.13).

In addition to examining the effect of age on EET levels, ratios of each regioisomer of EETs relative to total EETs in different tissues and genotypes were analyzed. Mouse genotype did not appear to change the ratio of an individual EET regioisomers relative to the corresponding total EETs. Ratio of EET regioisomers for both geometric isomers within the same age group and same tissue compartments were generally very similar, as summarized in Table 3.2. (Figures 3.14 and 3.15) However, as the mice aged, ratios of some regioisomers of *cis*- and *trans*-EETs were altered (Figure 3.15). It is interesting to note that the ratio of *cis*-EETs in cardiac tissue approached 1:1:1:1 with increasing age (Figures 3.14 C-D and 3.15 C-D).

3.3.4. EFFECT OF MI ON *CIS*- AND *TRANS*-EETS LEVELS AND CARDIAC TISSUE MORPHOLOGY AND OVERALL FUNCTION

In this study, mice, WT and Tr, aged 3 to 4 months old were used for surgery. *cis*-EET levels extracted from erythrocyte membranes of WT mice subjected to either sham surgery or MI were similar and not affected by MI. On the other hand, MI appeared to significantly increase *cis*-EET levels in erythrocyte membrane of Tr mice with the exception of *cis*-5,6-EET (Figure 3.16). MI significantly decreased both *trans*-5,6-EET and total *trans*-EET levels extracted from erythrocyte membrane of WT mice, while MI significantly increased levels of all regioisomers of *trans*-EETs in Tr mice (Figure 3.17). Comparing total *cis*-EETs and *trans*-EETs levels in erythrocyte membrane within WT-sham, Tr-sham, WT-MI, and Tr-MI groups showed that total *cis*-EETs were generally higher than total *trans*-EETs (Figure 3.18).

In cardiac tissue, MI generally led to significantly elevated levels of both *cis*- and *trans*-EETs for both WT and Tr mice as seen in Figures 3.19 and 3.20. However, in contrast to what was observed in erythrocyte membrane, total *trans*-EETs in cardiac tissue were higher than total *cis*-EETs (Figure 3.21). Change in *trans*-EET levels due to MI was generally not observed in the erythrocyte membrane of WT mice with the exception of declining in *trans*-5,6-EET. In contrast, MI significantly increased *trans*-EETs in cardiac tissue of WT mice. Following the event of MI, *cis*-EET levels in erythrocyte membrane of WT mice were not affected while some *cis*-EET levels in cardiac tissue were significantly increased. In Tr mice, levels of EETs were generally increased in both erythrocyte membrane and cardiac tissue.

To demonstrate the protective effect of cardiac-specific CYP2J2 overexpression, which is associated with higher EET levels in cardiac tissue, echocardiographic and histological data,

measurements of infarction ratio and fibrosis ratio, and extent of apoptosis were compared in Tr vs WT mice subjected to MI. MI in both groups reduced cardiac contractility as represented by lower % fractional shortening, however, Tr mice subjected to MI significantly retained better cardiac contractility compared to WT mice (Figure 3.22 A). While the ratio of heart weight to body weight did not change, the ratio of lung weight to body weight significantly increased in WT mice subjected to MI. This increase in lung weight indicates some edema associated with MI (Figure 3.22 C).

From the Masson's Trichrome stained cardiac section, Tr mice appeared to be more protected against MI (Figures 3.23 A and C). Masson's Trichrome stains red to display cytoplasm and muscle fibers and blue to show collagen, which is present at a higher level in fibrotic tissue. Upon examining the entire cardiac slice (Figure 3.23 A), and infarct zones (Figure 3.23 C), cardiac-specific overexpressing CYP2J2 Tr mice exhibited less myocardial fibrosis associated with MI injury. Infarction ratio is measured by comparing the infarcted area of the left ventricle relative to the total area of left ventricle, while the fibrosis ratio is an indicator of the extent of fibrosis in the left ventricle. It is evident, that Tr mice subjected to MI had significantly less infarcted area and less myocardial fibrosis compared to their WT counterparts (Figures 3.23 B and D).

The extent of apoptosis observed due to MI was determined using a TUNEL assay. Tr mice subjected to MI had less cells that underwent apoptosis relative to their WT counterparts (Figures 3.23 E and F). Furthermore, MI injury is associated with an increased production of ROS. Here again, Tr-MI mice which generally had significantly higher *cis*-EETs, produced significantly less ROS than WT-MI mice (Figure 3.24). In all tests to measure effect of MI on cardiac tissue, transgenic mice performed better than WT.

3.3.5. DISTRIBUTION OF *CIS*-EETS IN FRACTIONATED HUMAN PLASMA

As previously reported, *cis*-EETs can circulate by binding to fatty acid binding protein and lipoproteins. We received fractionated human plasma from Dr. Tomas Vaisar. The highest levels of *cis*-EETs were found in LDL followed by HDL and VLDL (Table 3.4).

3.3.6. COMPARISON OF *CIS*- AND *TRANS*-EET LEVELS IN CONTROL AND SCA PATIENTS

Levels of both *cis*- and *trans*-EETs in the control group are generally higher than in SCA cases (Figure 3.25). In both control and SCA cases, it appears that levels of *cis*-EETs are generally higher than their corresponding *trans*-EETs (Figures 3.26 and 3.27), which is consistent with observed trends in both WT and Tr mouse erythrocyte membranes.

3.4. DISCUSSION

Currently available biomarkers for CVD are mostly useful after the patient has already developed a disease and has some level of cardiac dysfunction. Part of this study aimed to establish CYP2J2-mediated formation of *cis*-EETs as surrogate cardiac markers prior to development of CVD. Cardiomyocyte-specific overexpressing CYP2J2 Tr mice were used as the model system to measure EETs in cardiac tissue and erythrocyte membranes from the same animal. This transgenic murine model exhibited significantly higher *cis*- and *trans*-EETs in cardiac tissue, while levels of both EETs in erythrocyte membranes were not elevated compared to WT (Figure 3.1). There was no correlation between *trans*-EETs extracted from erythrocyte membrane and cardiac tissue of WT and Tr mice with the exception of *trans*-14,15- and *trans*-11,12-EETs in Tr mice. Erythrocyte membrane and cardiac tissue *cis*-EETs extracted from WT mice also did not exhibit any correlation. However, a significant and positive correlation was

observed between erythrocyte membrane and cardiac tissue *cis*-EETs extracted from Tr mice. These data suggest that CYP2J2-mediated *cis*-EETs, but not trans-EETs, in erythrocyte membrane could potentially report on cardiac *cis*-EETs. To validate this model, it would be ideal to administer a specific *in vivo* CYP2J2 inhibitor to both WT and transgenic mice that could show decreases both in cardiac tissue and in erythrocyte membrane EETs of transgenic mice, but not WT. Unfortunately, to date, a CYP2J2 specific inhibitor useful for *in vivo* studies does not exist.

We then examined age as a potential factor that could alter EET levels. Aging is associated with chronic and low-grade inflammation (Franceschi and Campisi, 2014). An elevated level of tumor necrosis factor-α (TNF-α), an inflammatory cytokine produced by macrophages during acute inflammation, was shown to induce expression of CYP2J2 in the human first trimester trophoblast-derived cell line (Herse et al., 2012). We expected that both *cis*- and *trans*-EET levels would increase with aging, but for distinctive reasons. An increased level of *cis*-EETs in response to aging was anticipated as our physiological response to attenuate inflammation associated with aging process. Furthermore, *trans*-EET levels would also be expected to be elevated. When discussing cardiac aging, we have to focus on mitochondrial aging because mitochondria constitute about 20-40% of cardiac tissue cellular volume (Marin-Garcia et al., 2001). Although there are some conflicting reports, the majority found that mitochondrial aging is associated with increased ROS production and reduced mitochondrial respiratory capacity, as indicated by a reduced phosphocreatine recovery time (Sun et al., 2016). In our study, both geometric isomers of 14,15-, 11,12-, and 8,9-EETs along with total EETs extracted from erythrocyte membrane of both WT and Tr mice exhibited a significant positive

correlation with age (Figures 3.6 - 3.9). The observations in erythrocyte membranes agree with our expectation that both *cis*- and *trans*-EETs would increase with age.

In cardiac tissue of WT mice, levels of *cis*-14,15- and 11,12-EETs increased with age, while levels of *cis*-5,6-EET decreased (Figure 3.10). In cardiac tissue of Tr mice, only *cis*-11,12-EET level increased with age (Figure 3.11). The cardiac level of *trans*-11,12-EET in WT mice appeared to be increasing with age (Figure 3.12), while levels of *trans*-5,6-EET in both WT and Tr mice seemed to be decreasing with age (Figure 3.13). Increasing levels of 14,15- and 11,12-EETs with age in cardiac tissue agreed with our expectation on how age would affect EET levels, however, the declining levels of 5,6-EET in cardiac tissue with age was somewhat unexpected. It is, however, plausible that decreasing levels of 5,6-EET with age are due to an increase in the clearance of this regioisomers through the thromboxane pathways that seem to be specific to this regioisomer. It is also plausible that endogenous murine sEH, the enzyme that hydrolyzes EETs to DHETs, has preference for a specific regioisomer. In normotensive Wistar Kyoto rats, sEH preferred 14,15-EET over 11,12- or 8,9-EETs based on their urinary DHET formations (Yu et al., 2000). However, it remains unknown specificity of sEH towards 5,6-EET and whether aging affects the selectivity of sEH towards various regioisomers. Interestingly, a decrease in the level of *cis*-5,6-EET caused the ratio of individual *cis*-EETs to their total EETs to approach 1:1:1:1 (Table 3.2). Furthermore, it is interesting to note that alteration in EET levels in cardiac tissue due to age appeared to be regioisomer-specific which lend support to changes in the clearance pathways due to aging. These alterations, however, did not seem to change the ratios among the regioisomers within the same tissue compartment and appear to be independent of the mouse genotype (Figures 3.14 and 3.15). The effect of aging on the clearance pathways of EETs in humans remains to be determined.

Like most studies, our study has several limitations. The age range in our older mouse population was not ideal and relatively narrow. It would have been preferable to have analyzed mice with multiple mice and a wider age range. The absence of EET levels extracted from mice between 5 to about 10 month of age confines the analysis and shows that the younger mice drive the correlation. Additionally, we did not assess cardiac functions or collect other vital signs such as blood pressure and blood glucose levels in the young and old mice, which would have been very helpful in understanding if older mice suffered cardiac dysfunction that affects EET levels. In addition, the effect of age on EET level in human cardiac tissue and erythrocyte membranes may not necessarily follow similar trends with mice and remains to be determined.

In order to elucidate the cardioprotective effects of CYP2J2-mediated EETs, we subjected our murine model to acute MI for two weeks. There have been two conflicting reports on how CAD affects EET levels. A study by Theken et al. reported that CAD patients had higher plasma EET levels than healthy volunteers, while a follow up study by Oni-Orisan et al. (from the same group) reported that total plasma EET levels in obstructive CAD patients were significantly lower than their control group (no apparent CAD) (Theken et al., 2012; Oni-Orisan et al., 2016). CAD patients in those earlier studies had experienced a chronic disease progression, while the mice in our study were exposed to acute MI. The conflicting reports and different exposure to the disease made it challenging to predict how EET levels would be altered *a priori*. In response to MI-induced stress, levels of almost all regioisomers of *cis*-EETs and total *cis*-EETs were significantly higher in both erythrocyte membranes and cardiac tissue of Tr-MI mice compared to their sham counterparts (Figures 3.16 and 3.19). Similarly, *trans*-EETs in both erythrocyte membranes and cardiac tissue of these Tr-MI mice also increased with MI (Figures 3.17 and 3.20). These observations support our hypothesis that higher EET levels protect against

ischemia-associated cardiac event. This finding was further corroborated by echocardiographic data that demonstrated cardiac contractility of Tr-MI, indicated by % FS, was significantly better than WT-MI (Figure 3.22 A). WT-MI also had significantly higher pulmonary fluid retention compared to Tr-MI (Figure 3.22 C). Furthermore, Tr-MI mice exhibited significantly less infarction and fibrosis and had significantly less apoptotic cells and ROS production (Figures 3.23 and 3.24). These data provide convincing evidence that cardiac-specific overexpression of CYP2J2 is protective against acute MI in all the tests we used to measure cardiac function. We also demonstrate that cardiac-specific overexpression of CYP2J2 in these Tr mice was associated with significantly higher *cis*- and *trans*-EETs (Figure 3.1 B). All the data collected from our mouse model that was subjected to sham or MI support our hypothesis that higher EET levels confer a protective effect against ischemia-associated cardiac events, i.e. acute MI.

Two puzzling results from our MI study remain unsolved. The first was the higher levels of cardiac *trans*-EETs in both WT and Tr mice compared to their *cis*-EETs counterparts (Figure 3.21). Formation of *trans*-EETs *in vivo* is most likely due to free radical oxidation processes (Aliwarga et al., 2017). In healthy heart tissue, ROS is always present as byproducts from mitochondrial electron transport chain. Mitochondria constitute about 20-40% of cardiac tissue cellular volume (Marin-Garcia et al., 2001). In addition, production of ROS was increased in non-infarcted left ventricular myocardium following MI in CD-1 mouse model (Kinugawa et al., 2000). As shown in Figures 3.22 C and D, cardiac tissue of Tr-MI mouse exhibited myocardial fibrosis even though it was at a lesser extent than WT-MI. A potential explanation is that the excess mitochondrial ROS production due to MI led to formation of more *trans*-EETs than *cis*-EETs in cardiac tissue of MI mice.

The second unexpected finding was again the higher levels of cardiac *trans*-EETs in Tr-MI mice compared to WT-MI mice, even though ROS ratio formed in Tr-MI was significantly lower than in WT-MI. The magnitude of EET increase due to MI in WT and Tr mice were similar as reflected by the observation that *trans*- to *cis*- ratios of each regioisomer of EET extracted from cardiac tissue did not change dramatically (Table 3.3). Levels of cardiac *trans*-EETs of untreated Tr mice at baseline were significantly higher compared to that of WT mice (Figure 3.1 B). Basal contractile function and cardiac anatomy of these Tr mice were shown to be normal (Seubert et al., 2004). However, the impact of insertion of CYP2J2 transgene on the expression and regulation of other enzymes and pathways remains unknown. Perhaps activity of endogenous murine sEH was more active in WT than Tr mice or clearance pathways of *cis*- vs. *trans*-EETs are altered with age.

In a human SCA disease model, levels of individual regioisomers of *cis*-EETs extracted from erythrocyte membrane of control group were significantly higher than SCA case group. However, total erythrocyte membrane levels of both *cis*- and *trans*-EETs were significantly higher in control than in the SCA case group (Figure 3.25). This finding also supports our hypothesis that higher circulating EET levels are protective against ischemia-associated cardiac event, i.e. SCA. In agreement with the data observed in mouse erythrocyte membranes, levels of *cis*-EETs in erythrocyte membrane of control subjects were significantly higher than levels of *trans*-EETs in SCA case groups (Figures 3.26 and 3.27).

3.5. CONCLUSION

Current clinical biomarkers for CVD are very sensitive and quite useful in detecting severity of damage associated with CVD. Establishing a new surrogate marker for CVD prior to

full manifestation of the disease in order to predict which patients are at higher risk of CVD will be useful. *Cis*-EETs have been shown to be cardioprotective in many studies using a cardiomyocyte-specific overexpressing CYP2J2 mouse model. In this study, we reported that *cis*-EETs could potentially be used as a marker to report CVD events, although a validation study using a specific CYP2J2 inhibitor is still needed. Despite the limitations of the study, age appeared to alter EET levels. Acute MI seems to elevate EET levels. However, exposure to disease acutely or chronically altered EET levels. Incorporating a CYP2J2 transgene in cardiomyocyte of the mouse model demonstrated full protective effects of having higher levels of EETs as supported by echocardiographic, cellular, and histological data. Lastly, given that the levels of each regioisomer of EETs change differently with age and disease, it will be useful to investigate the function of each regioisomer of EETs in a larger human subject study of SCA cases and controls. A study examining if inflammation markers that increase with age could induce CYP2J2 and increase EET production to combat age dependent inflammation will be necessary. When examining the effect of age and disease state, it is interesting to note that the alterations in *cis*-EET levels were mimicked by the *trans*-EETs. Therefore, function and regulation and clearance of *trans*-EETs *in vivo* and how *trans*-EETs are altered in the presence of stress need to be explored in more detail.

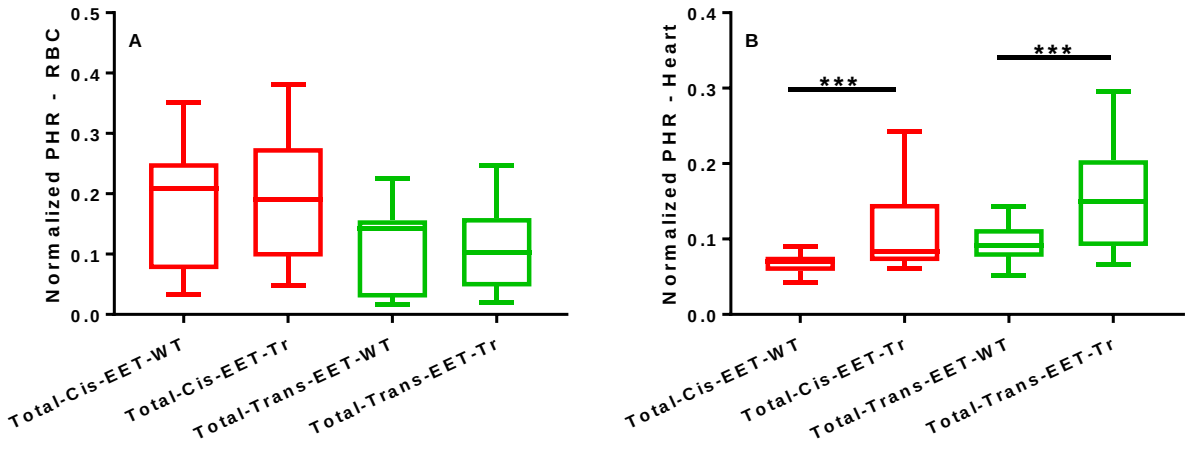

Figure 3.1. Total *cis*- and *trans*-EETs extracted from (A) erythrocyte membrane and (B) cardiac tissue of WT (N=25, 18 female and 7 male mice) and cardiomyocyte-specific overexpressing CYP2J2 Tr (N=25, 16 female and 9 male mice) mice.

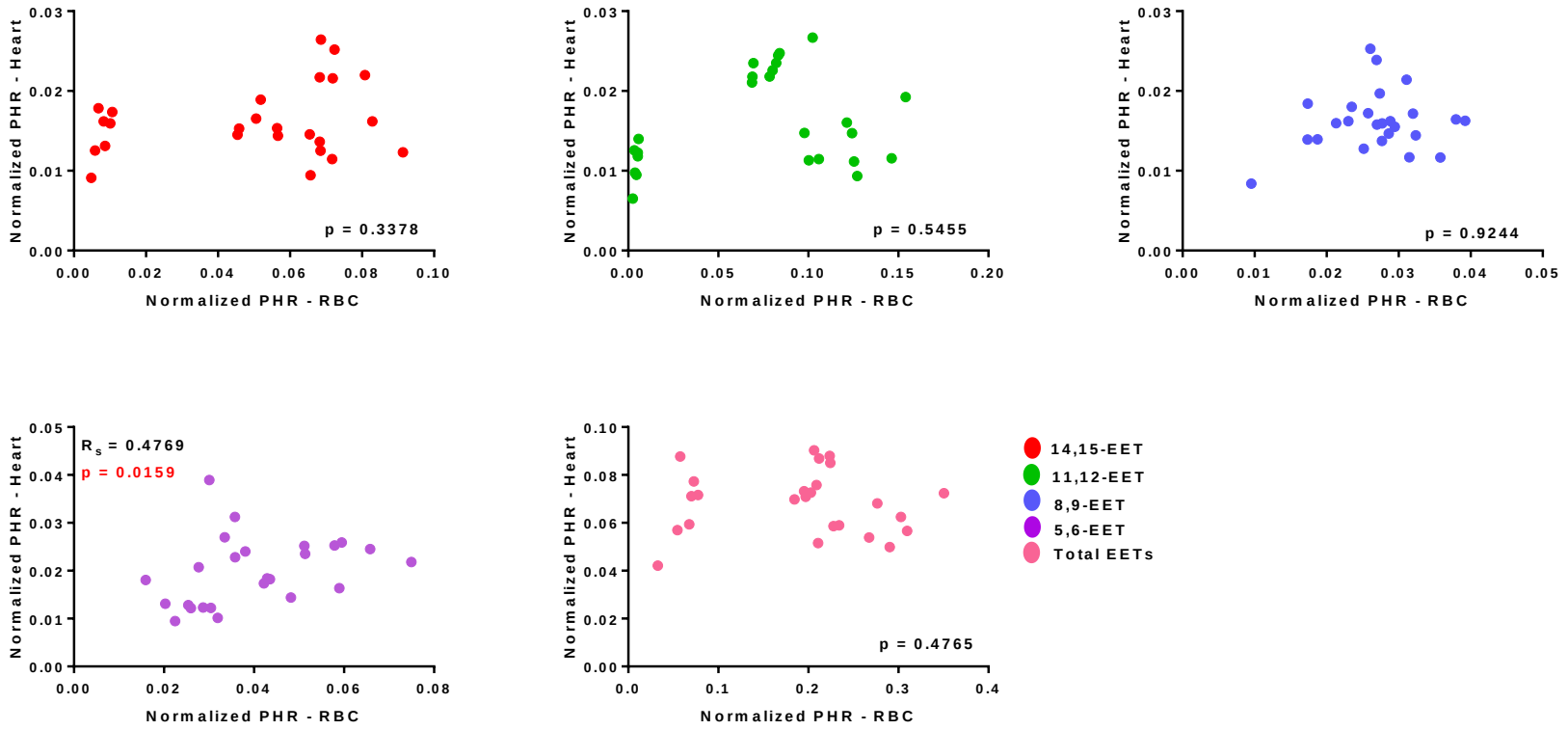

Figure 3.2. Correlation of each regioisomer of *cis*-EET and total *cis*-EETs in erythrocyte membrane and cardiac tissue of WT mice. A significant positive correlation was only observed in *cis*-5,6-EET levels which was not observed in total *cis*-EETs.

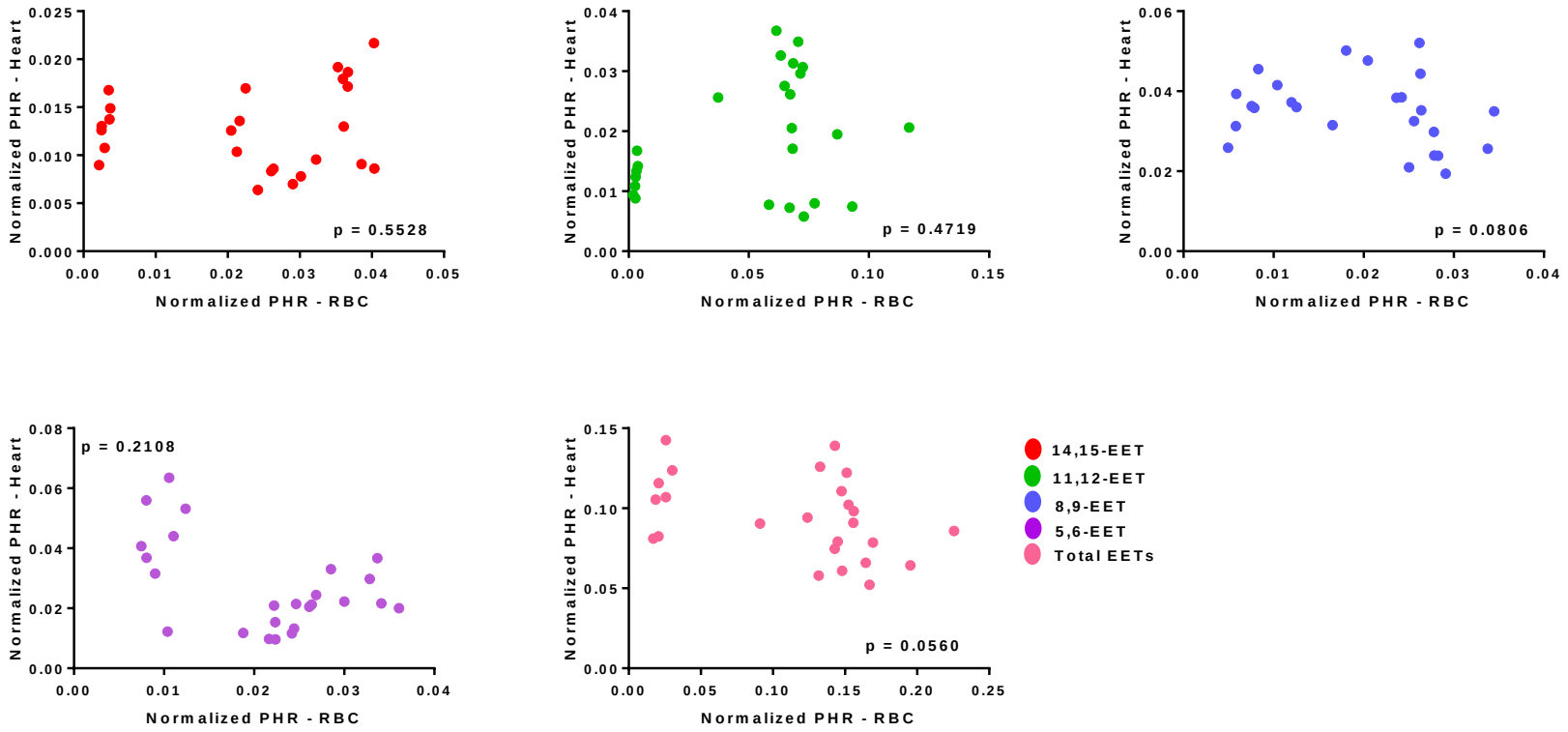

Figure 3.3. Correlation of each regioisomer of *trans*-EET and total *trans*-EETs in erythrocyte membrane and cardiac tissue of WT mice. There was no significant correlation observed in any of the *trans*-EETs in erythrocyte membrane and cardiac tissue.

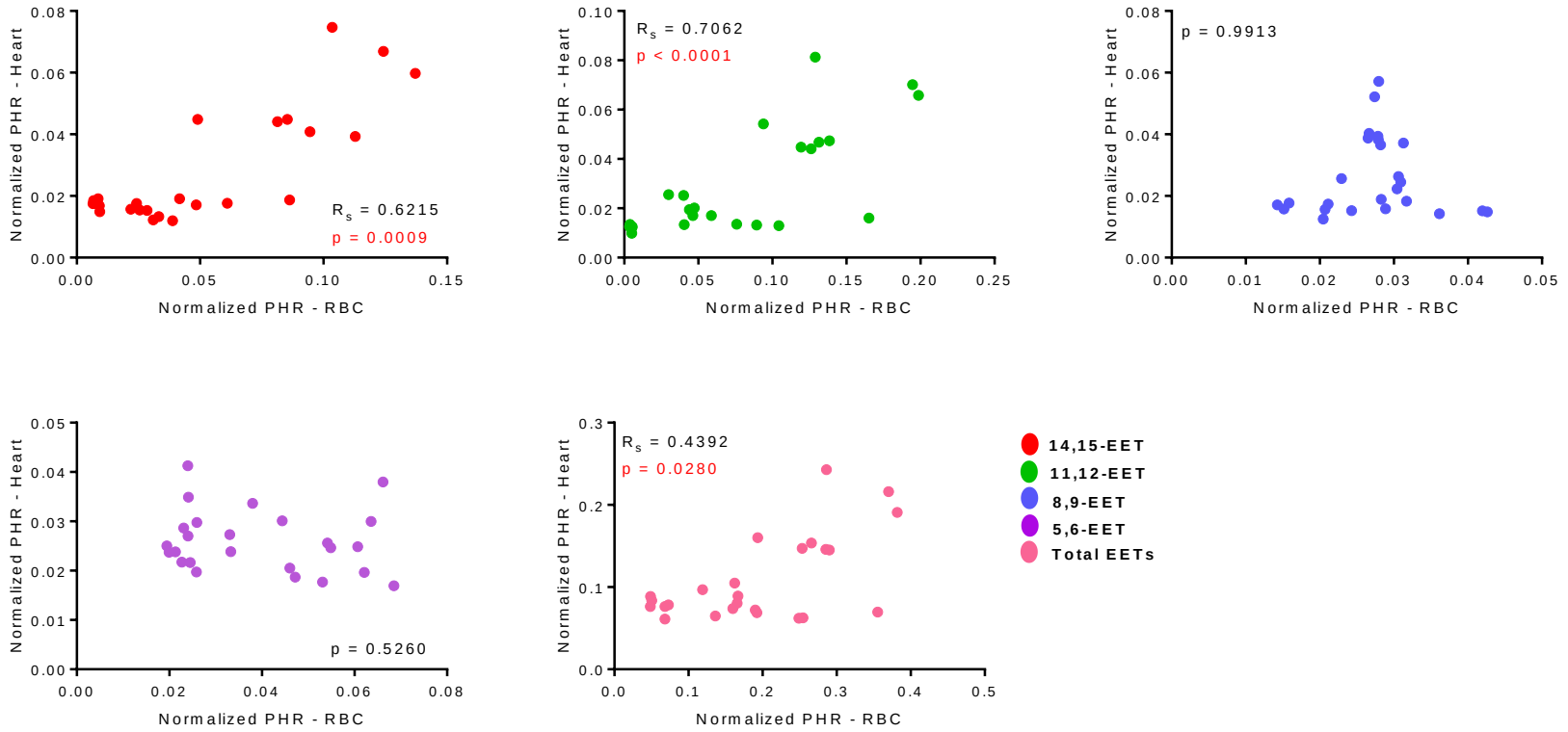

Figure 3.4. Correlation of each regioisomer of *cis*-EET and total *cis*-EETs in erythrocyte membrane and cardiac tissue of CYP2J2 Tr mice. Significant positive correlations were observed in *cis*-14,15-, *cis*-11,12-EET levels, and total *cis*-EETs.

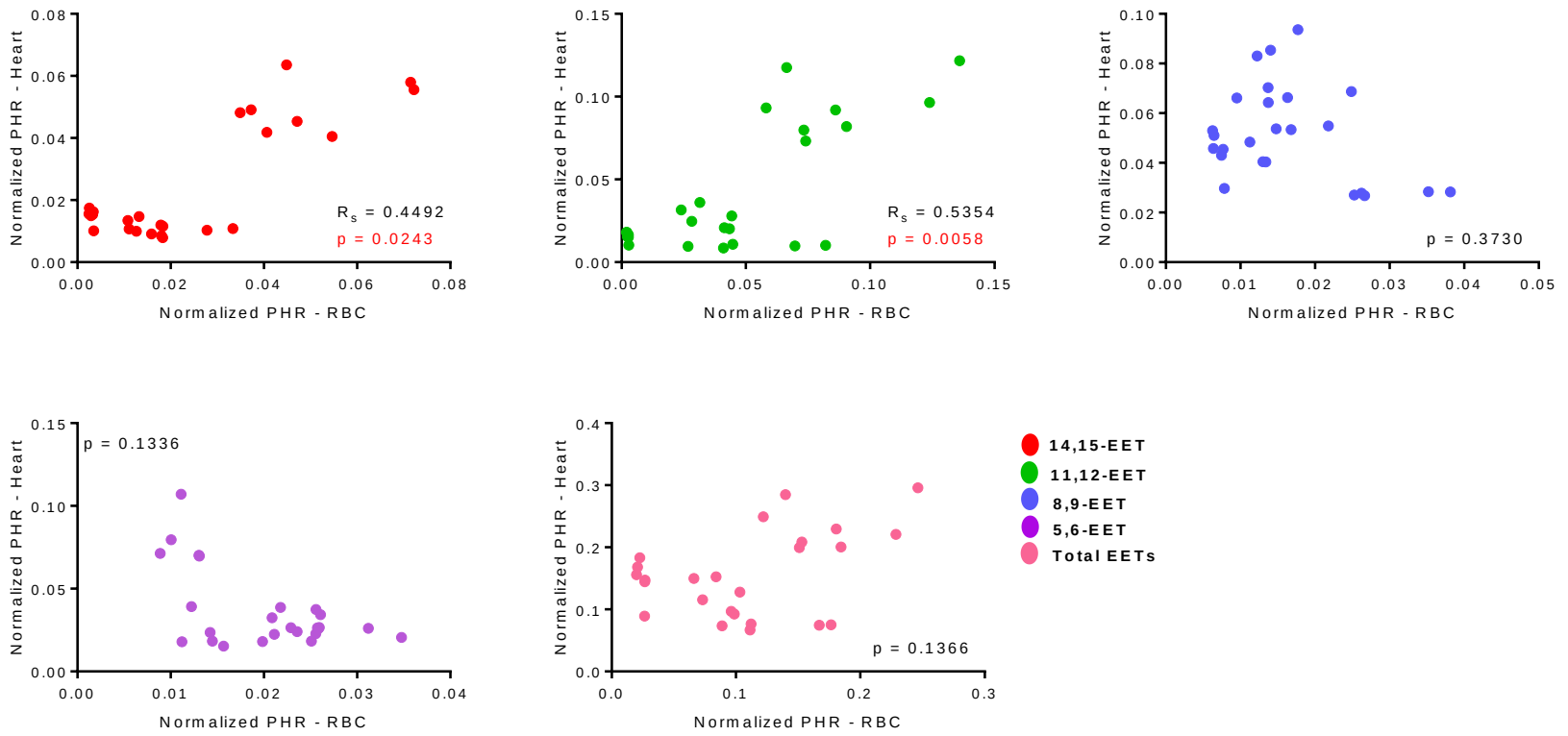

Figure 3.5. Correlation of each regioisomer of *trans*-EET and total *trans*-EETs in erythrocyte membrane and cardiac tissue of Tr mice. Significant positive correlations were observed in *trans*-14,15-, *trans*-11,12-EET levels, and total *trans*-EETs.

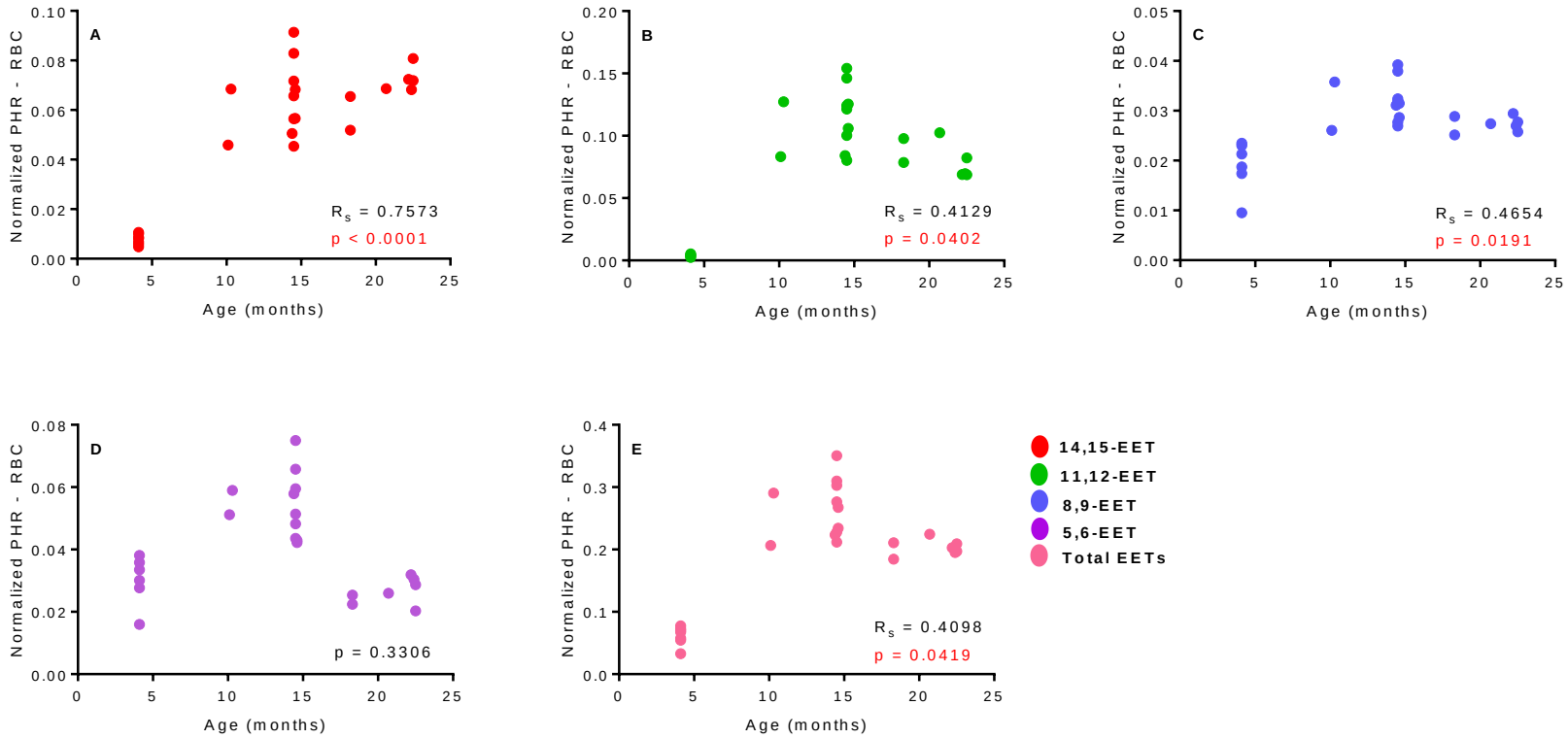

Figure 3.6. Effect of age on *cis*-EETs extracted from erythrocyte membrane of WT mice. Levels of (A) *cis*-14,15-EET, (B) *cis*-11,12-EET, (C) *cis*-8,9-EET, (D) *cis*-5,6-EET, and (E) total *cis*-EETs were positively correlated with age with the exception of *cis*-5,6-EET.

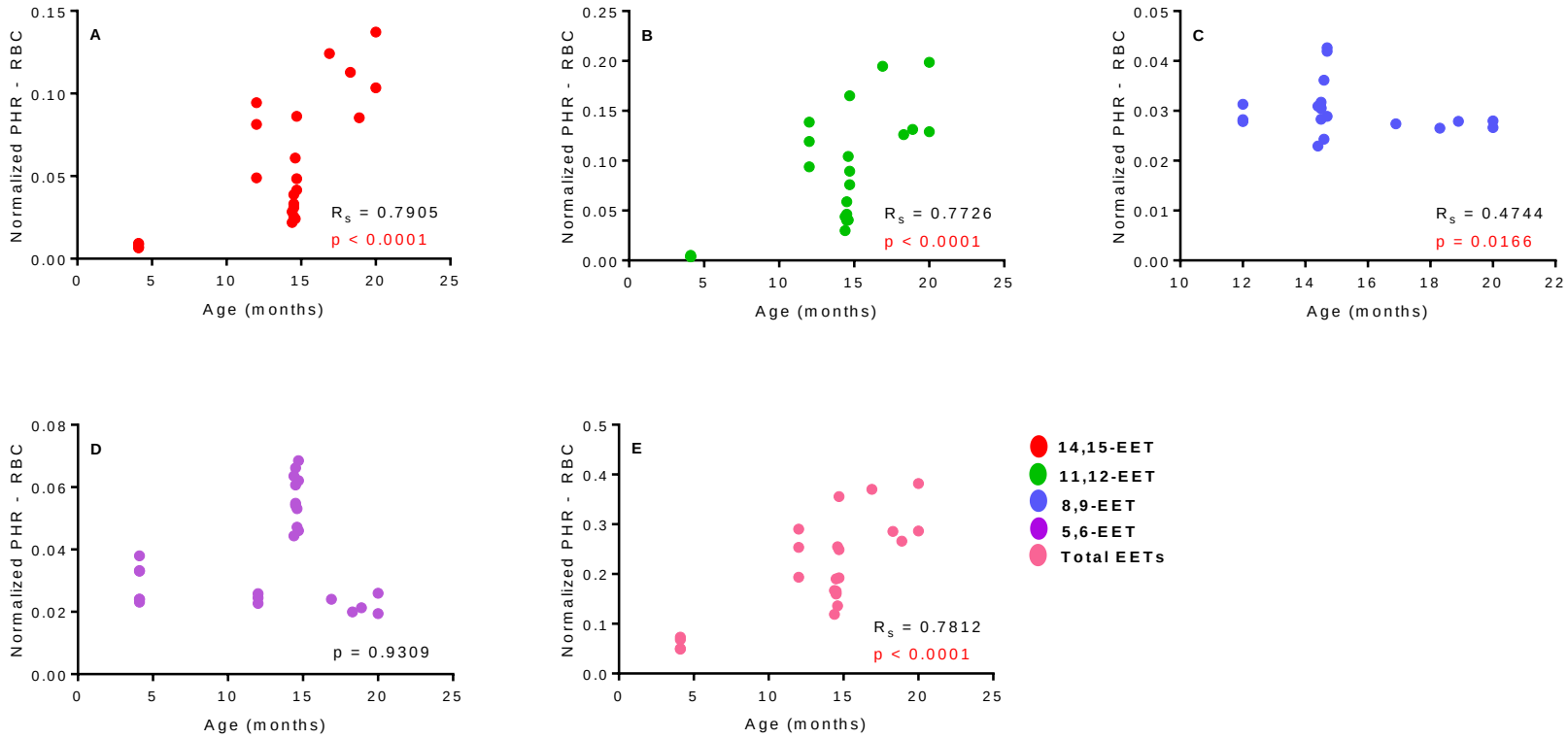

Figure 3.7. Effect of age on *cis*-EETs extracted from erythrocyte membrane of Tr mice. Levels of (A) *cis*-14,15-EET, (B) *cis*-11,12-EET, (C) *cis*-8,9-EET, (D) *cis*-5,6-EET, and (E) total *cis*-EETs were positively correlated with age with the exception of *cis*-5,6-EET.

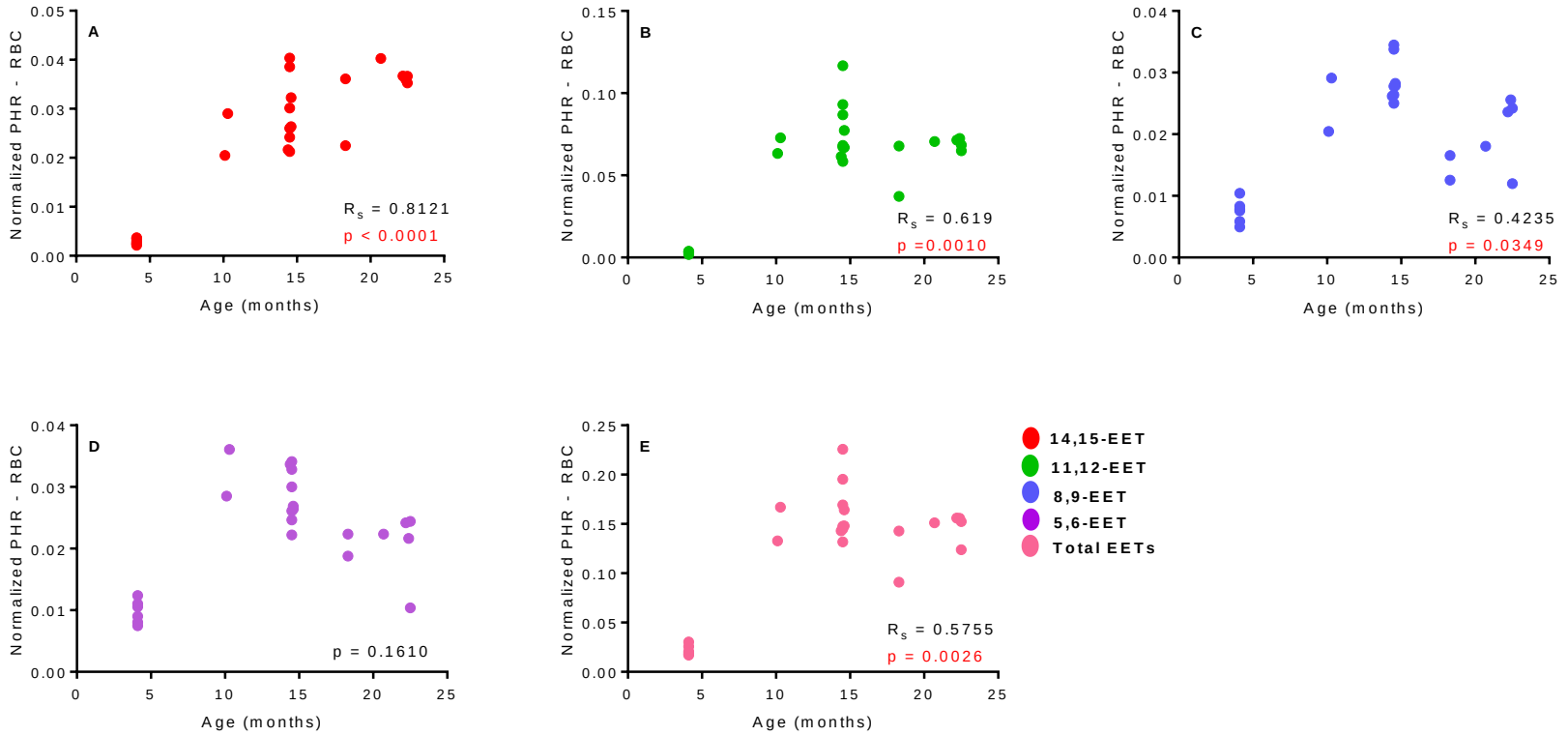

Figure 3.8. Effect of age on *trans*-EETs extracted from erythrocyte membrane of WT mice. Levels of (A) *trans*-14,15-EET, (B) *trans*-11,12-EET, (C) *trans*-8,9-EET, (D) *trans*-5,6-EET, and (E) total *trans*-EETs were positively correlated with age with the exception of *trans*-5,6-EET.

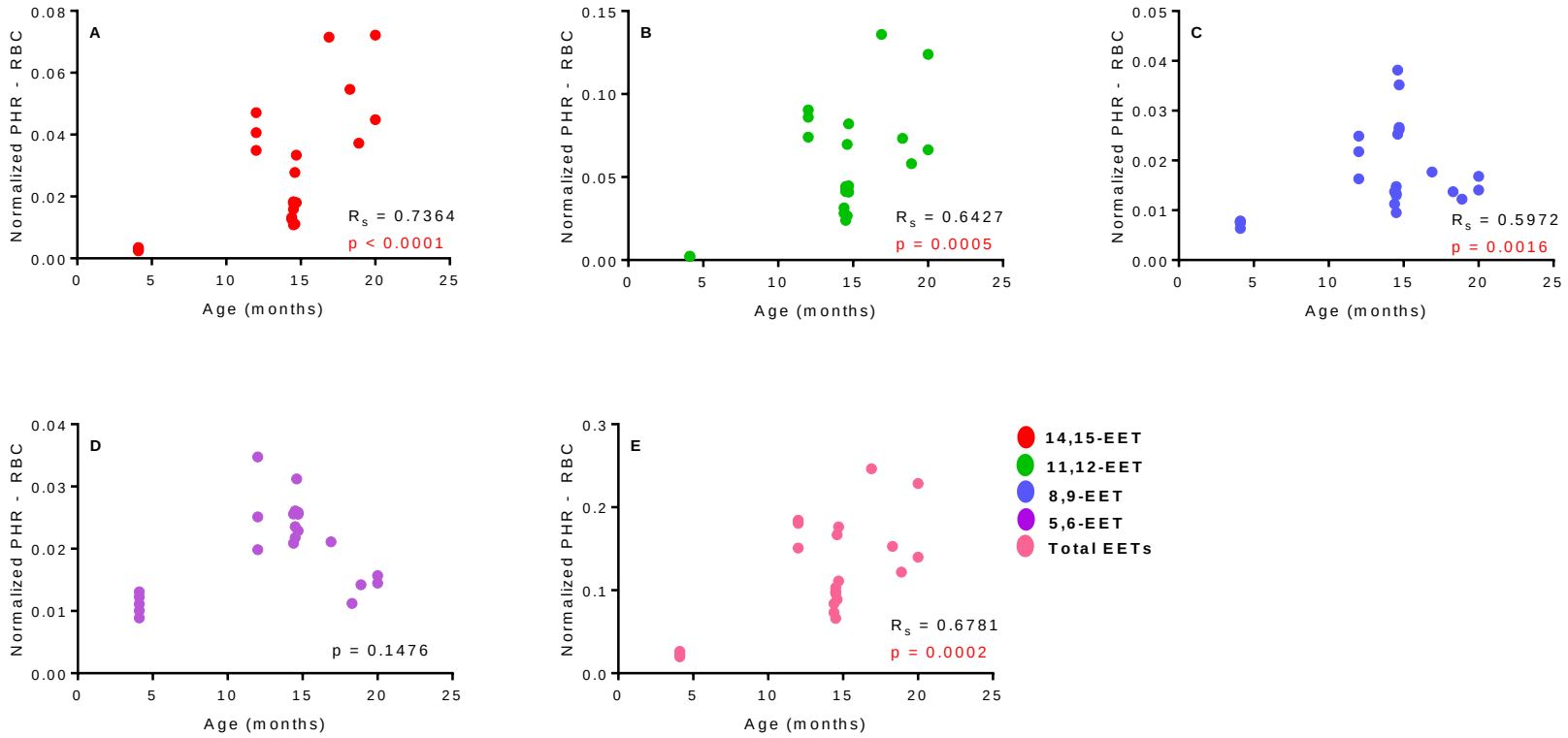

Figure 3.9. Effect of age on *trans*-EETs extracted from erythrocyte membrane of Tr mice. Levels of (A) *trans*-14,15-EET, (B) *trans*-11,12-EET, (C) *trans*-8,9-EET, (D) *trans*-5,6-EET, and (E) total *trans*-EETs were positively correlated with age with the exception of *trans*-5,6-EET.

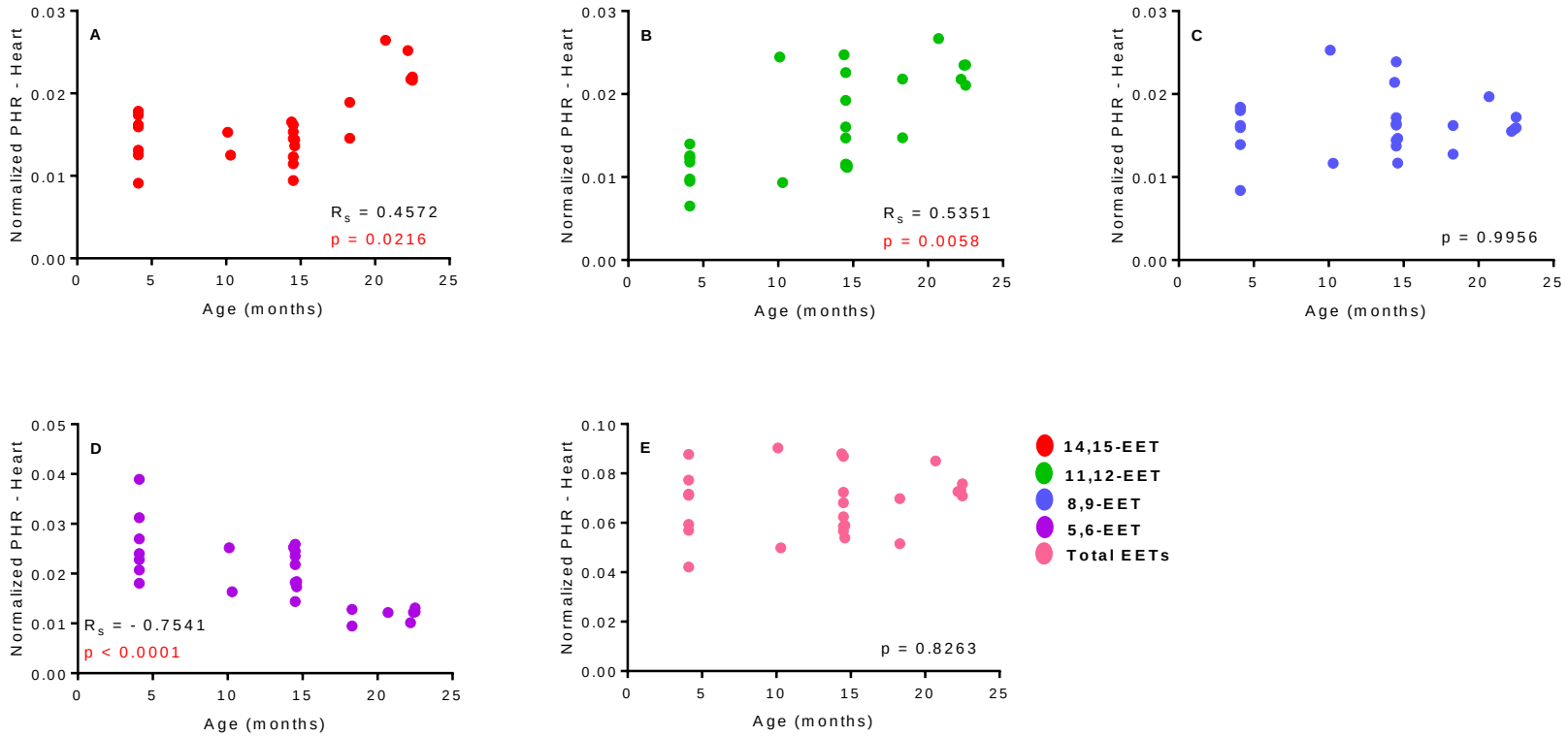

Figure 3.10. Effect of age on *cis*-EETs extracted from cardiac tissue of WT mice. Levels of (A) *cis*-14,15- and (B) *cis*-11,12-EETs were positively correlated with age while level of (C) *cis*-8,9-EET remained unchanged with age and level of (D) *cis*-5,6-EET had a negative correlation with age. The opposite correlation trend observed in *cis*-EETs extracted from cardiac tissue seems to cancel out the effect of age in (E) the total *cis*-EETs.

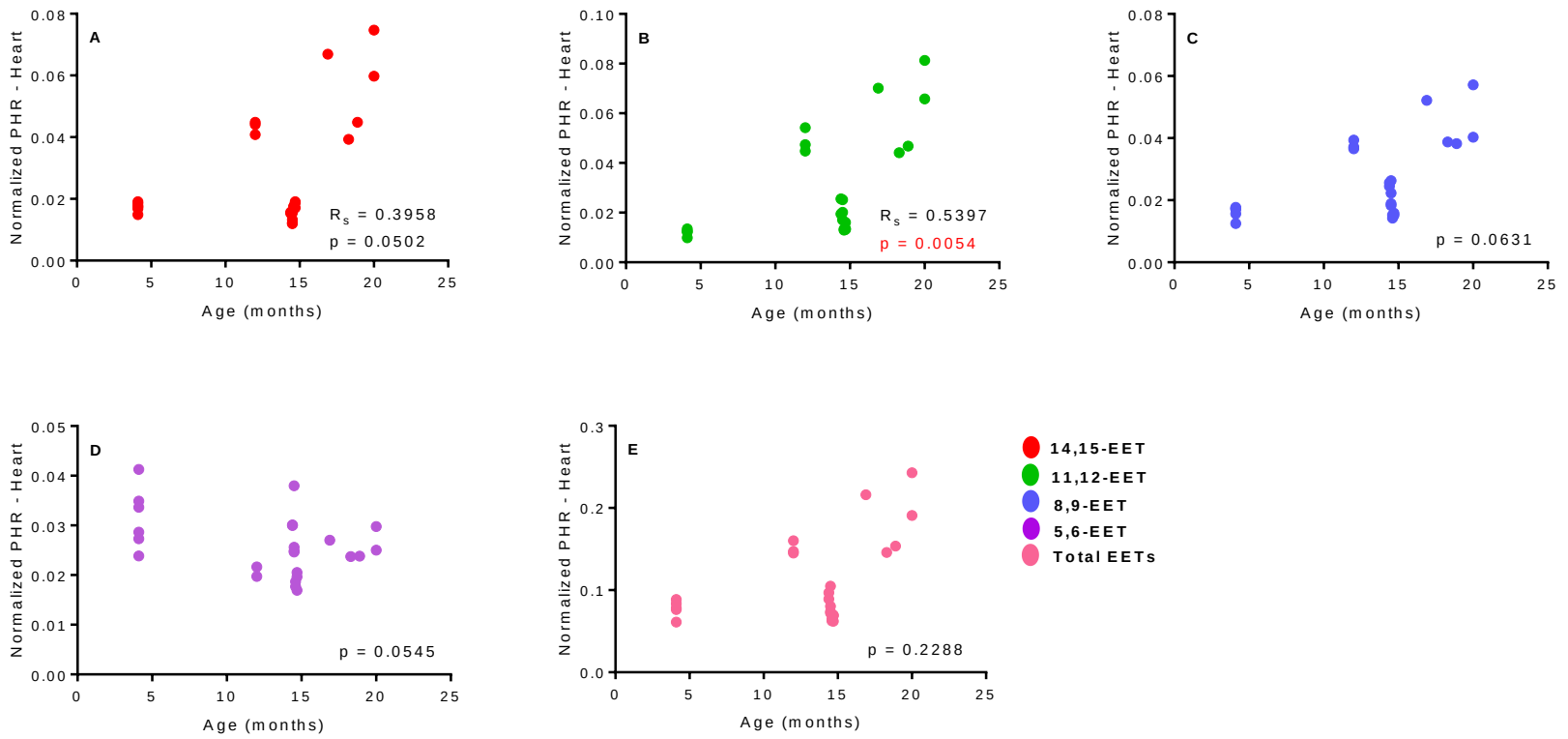

Figure 3.11. Effect of age on *cis*-EETs extracted from cardiac tissue of Tr mice. There were no significant correlation between age and levels of (A) *cis*-14,15-EET, (C) *cis*-8,9-EET, (D) *cis*-5,6-EET, and (E) total *cis*-EETs . However, a positive correlation between age and level of *cis*-EETs was observed in (B) *cis*-11,12-EET.

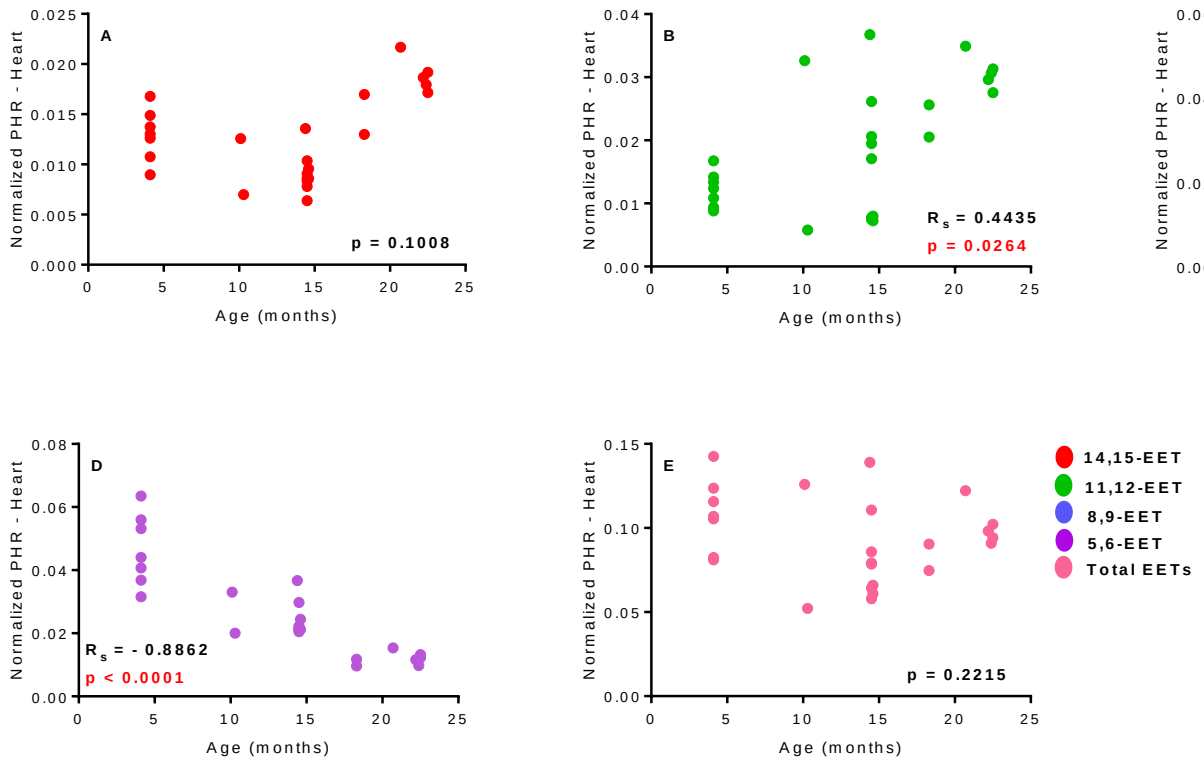

Figure 3.12. Effect of age on *trans*-EET extracted from cardiac tissue of WT mice. Significant correlations between age and levels of (A) *trans*-14,15-EET, (C) *trans*-8,9-EET, and (E) total *trans*-EETs were not observed. However, levels of (B) *trans*-11,12-EETs were positively correlated with age while levels of (D) *trans*-5,6-EET had a negative correlation with age. The opposite correlation trend between *trans*-11,12- and *trans*-5,6-EETs extracted from cardiac tissue seems to cancel out the effect of age in the total *trans*-EETs.

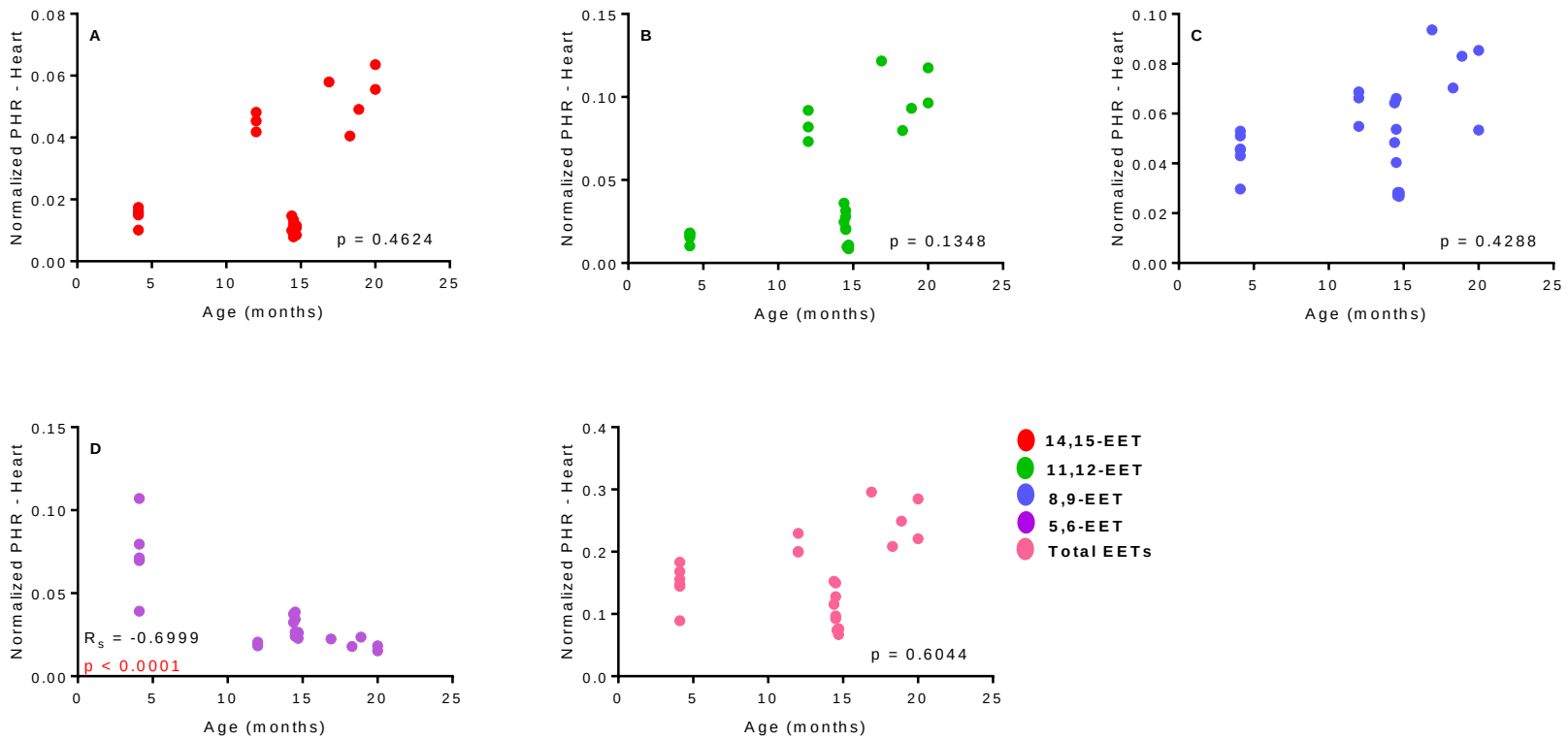

Figure 3.13. Effect of age on *trans*-EETs extracted from cardiac tissue of Tr mice. There were no significant correlations between age and levels of (A) *trans*-14,15-EET, (B) *trans*-11,12-EET, (C) *trans*-8,9-EET, and (E) total *trans*-EETs. However, level of (D) *trans*-5,6-EET had a negative correlation with age. The significant correlation observed in *trans*-5,6-EETs extracted from cardiac tissue was not enough to drive the correlation between age and total cardiac tissue of *trans*-EETs.

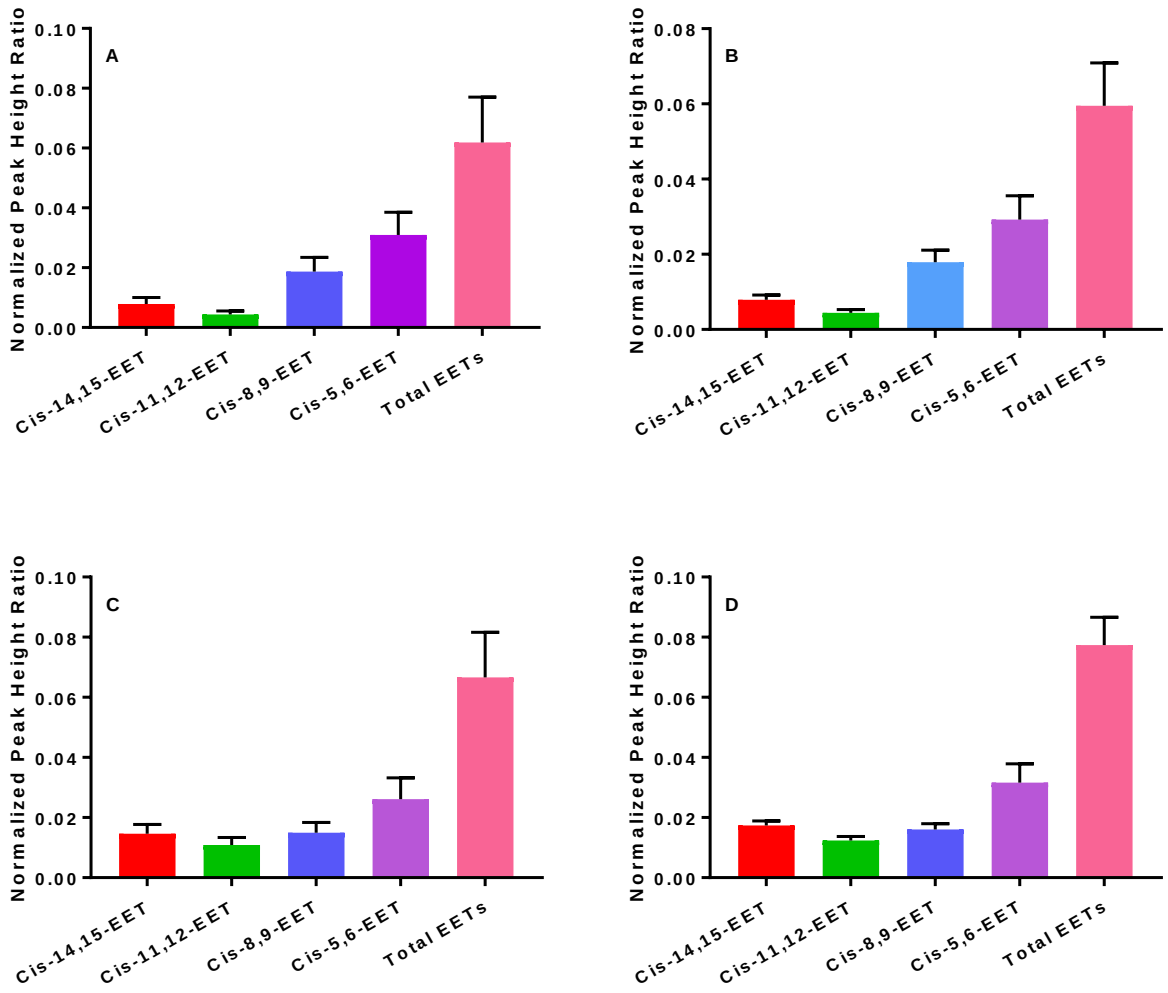

Figure 3.14. Normalized peak height ratios of *cis*-EETs extracted from erythrocyte membrane of young mice. The ratios were normalized to internal standards and total protein content of 30 mg/mL. The erythrocyte membrane samples came from young (A) WT (N=7, 6 female and 1 male mice) and (B) Tr (N=6, 4 female and 2 male mice) mice and from cardiac tissue of (C) WT and (D) Tr mice. Ratios of *cis*-EET in erythrocyte membrane of old WT and Tr mice are approximately 2:1:4:7. Interestingly, ratios of *cis*-EET in cardiac tissue of old WT and Tr mice are about 1:1:1:2.6.

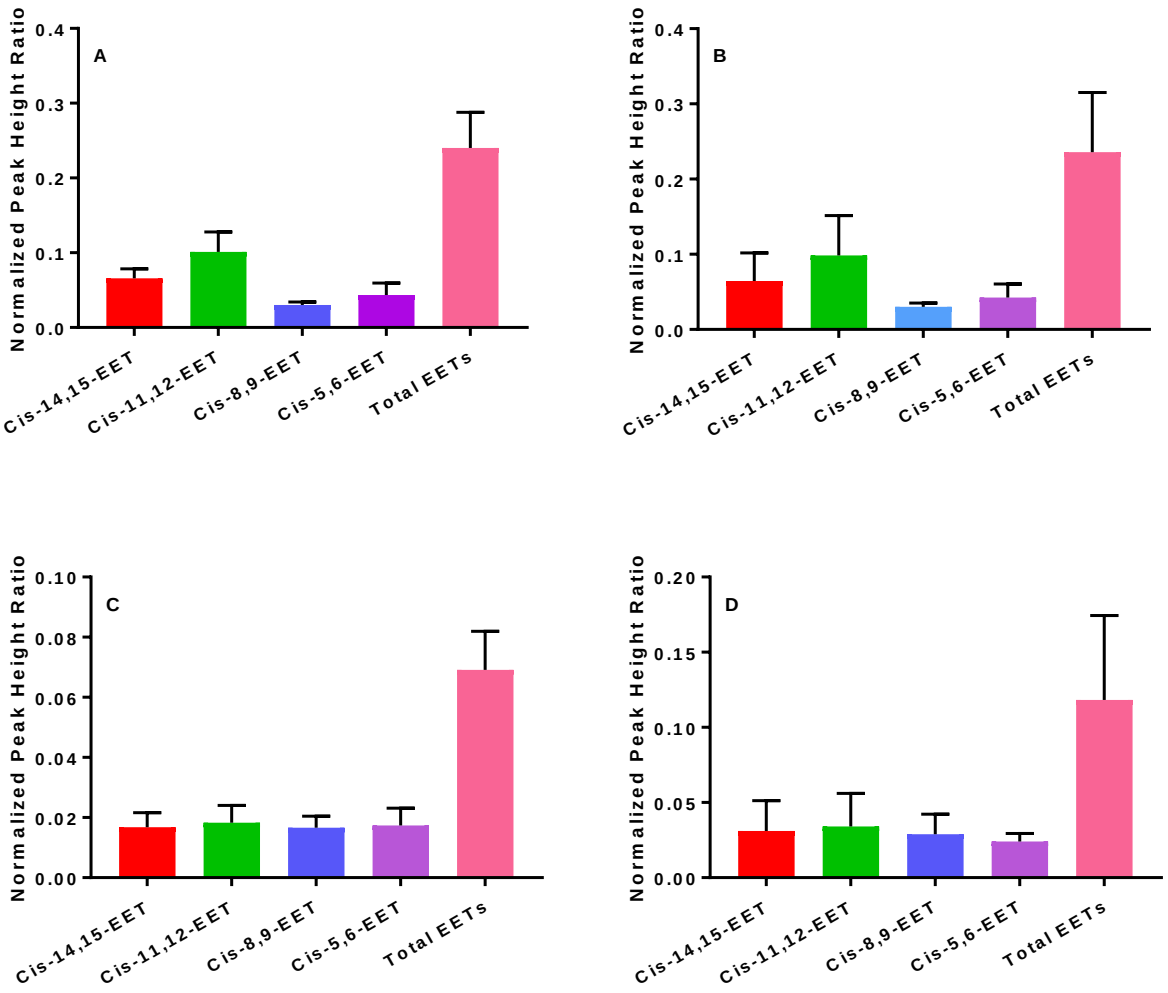

Figure 3.15. Normalized peak height ratio of *cis*-EETs extracted from erythrocyte membrane of old mice. The ratios were normalized to internal standards and total protein content of 30 mg/mL. The erythrocyte membrane samples came from old (A) WT (N=18, 12 female and 6 male mice) and (B) Tr (N=19, 12 female and 7 male mice) mice and from cardiac tissue of (C) WT and (D) Tr mice. Ratios of *cis*-EETs in the erythrocyte membrane of old WT and Tr mice are approximately 2:3:1:1. Interestingly, ratios of *cis*-EET in cardiac tissue of old WT and Tr mice are about 1:1:1:1.

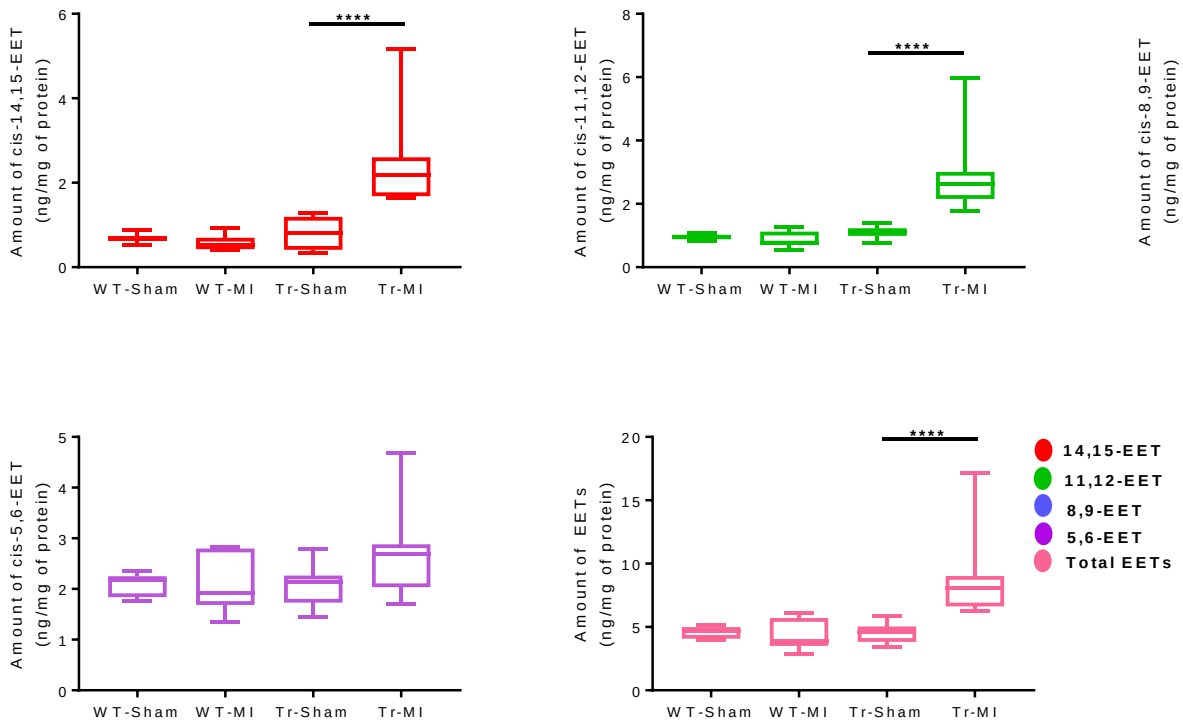

Figure 3.16. Levels of each regioisomer of *cis*-EETs and total *cis*-EET extracted from erythrocyte membrane of WT and Tr mice subjected to sham or MI surgery. There were 8 WT mice (4 female and 4 male mice) and 9 Tr mice (5 female and 4 male mice) subjected to sham surgery and 9 WT mice (4 female and 5 male mice) and 9 Tr mice (4 female and 5 male mice) subjected to MI surgery. There were not any significant differences in *cis*-EET levels between sham and MI-operated WT mice. However, significantly higher *cis*-EET levels, with the exception of *cis*-5,6-EET, were observed in Tr-MI-operated mice relative to Tr-sham mice. **** indicates $p \leq 0.0001$ and * indicates $p \leq 0.05$.

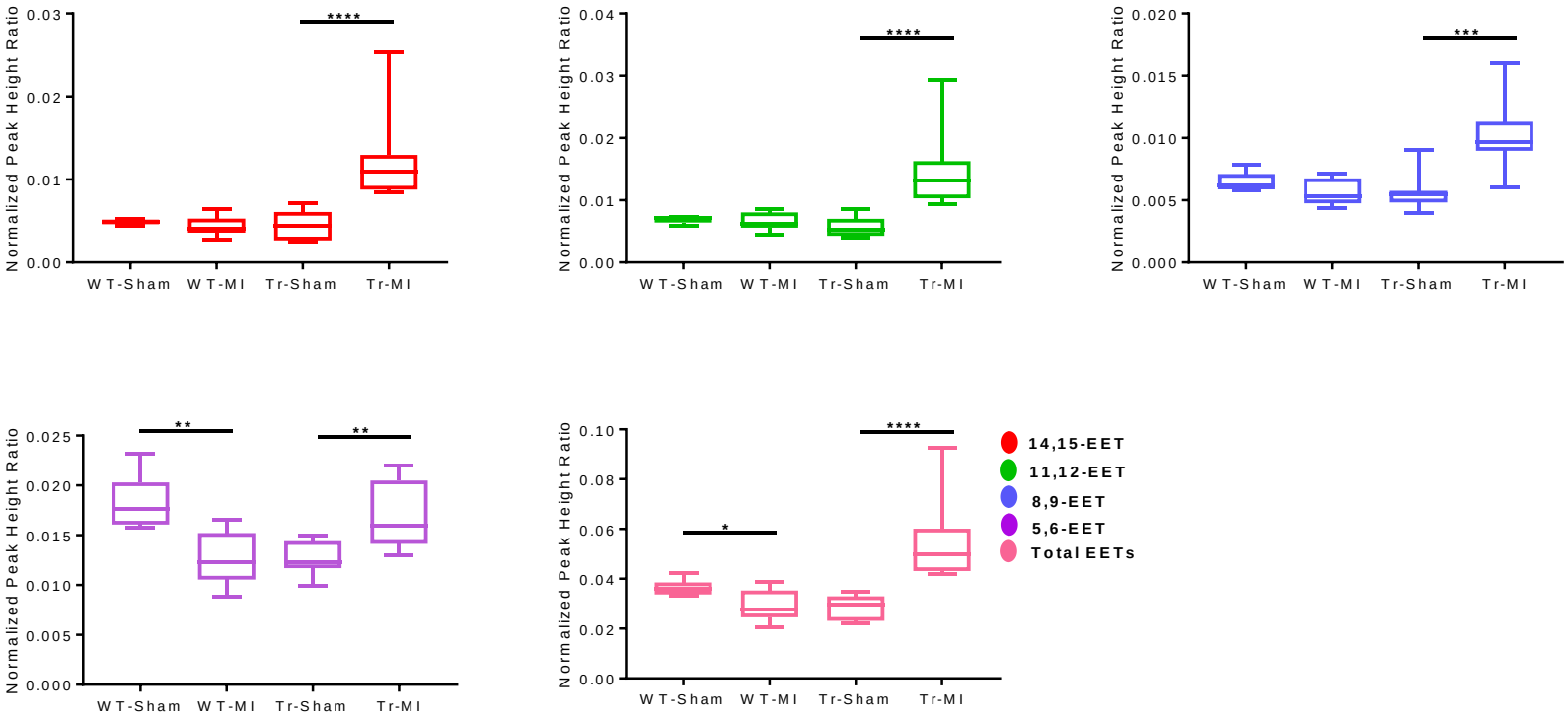

Figure 3.17. Levels of each regioisomer of *trans*-EETs and total *trans*-EET extracted from erythrocyte membrane of WT and Tr mice subjected to sham or MI surgery. There were significantly less *trans*-5,6-EET in WT-sham mice compared to WT-MI mice which carried through to the total *trans*-EETs. In addition, significantly higher levels of *trans*-EET were observed in MI-operated Tr mice compared to Tr-sham mice. **** indicates $p \leq 0.0001$, ** indicates $p \leq 0.01$, and * indicates $p \leq 0.05$.

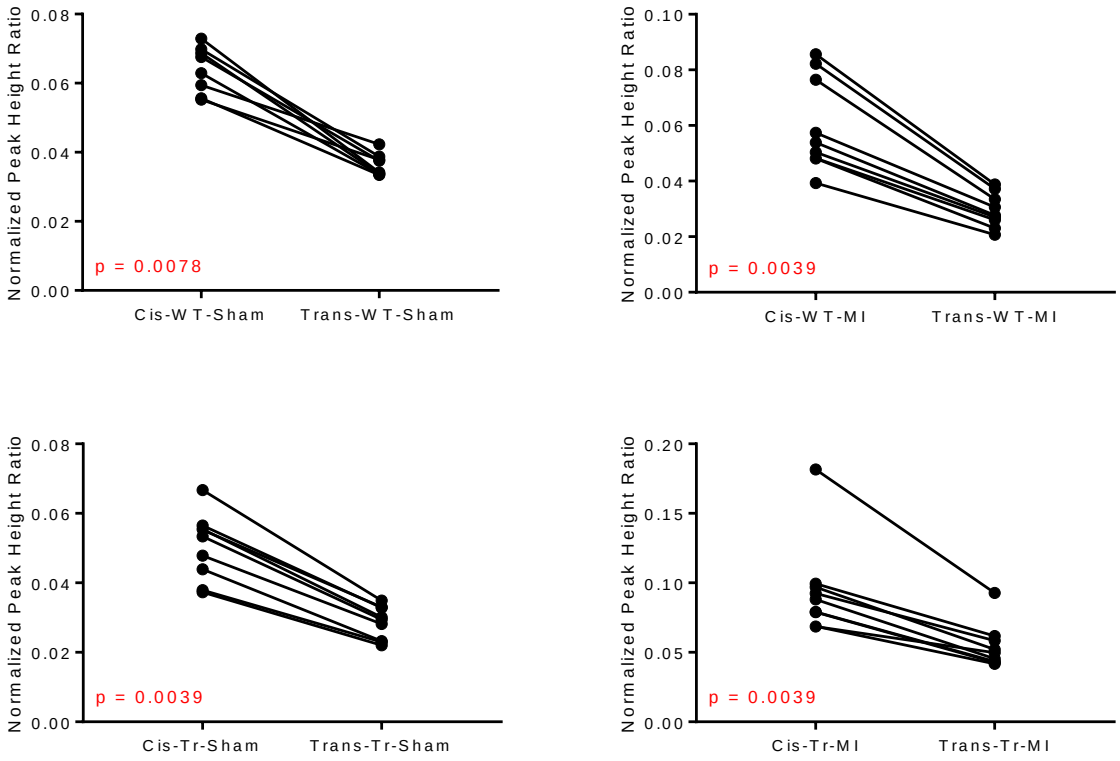

Figure 3.18. Comparison between total *cis*- and *trans*-EETs levels extracted from erythrocyte membrane of WT and Tr mice. Total *cis*-EETs levels in both WT and Tr mice are higher than total *trans*-EETs levels. Whether or not the mice subjected to sham or MI surgery, the lower total *trans*-EET levels was observed across all paired groups.

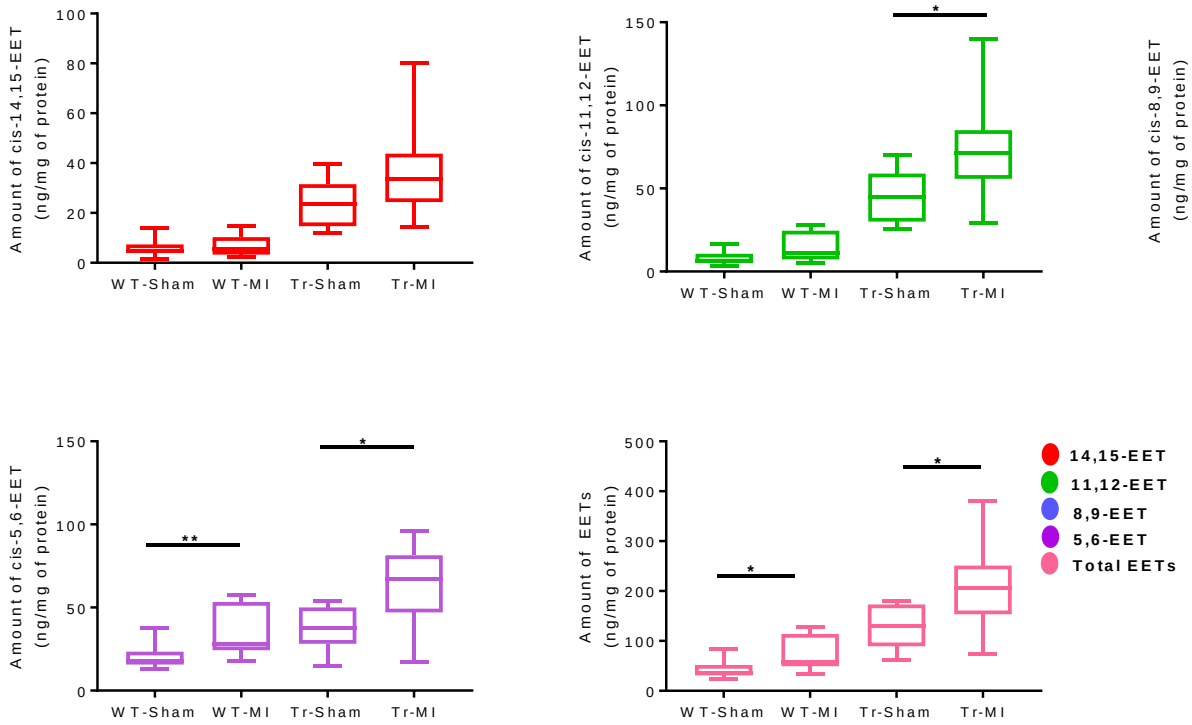

Figure 3.19. Levels of each regioisomer of *cis*-EETs and total *cis*-EETs extracted from cardiac tissue of WT and Tr mice subjected to sham or MI surgery. There were 8 WT mice (4 female and 4 male mice) and 9 Tr mice (5 female and 4 male mice) subjected to sham surgery and 9 WT mice (4 female and 5 male mice) and 9 Tr mice (4 female and 5 male mice) subjected to MI surgery. There were significant differences in *cis*-8,9- and *cis*-5,6-EET levels between sham and MI-operated WT mice which carried through to the total *cis*-EETs. In addition, significant differences in *cis*-EET levels, with the exception of *cis*-14,15-EET, were observed between sham and MI-operated Tr mice. ** indicates $p \leq 0.01$, and * indicates $p \leq 0.05$.

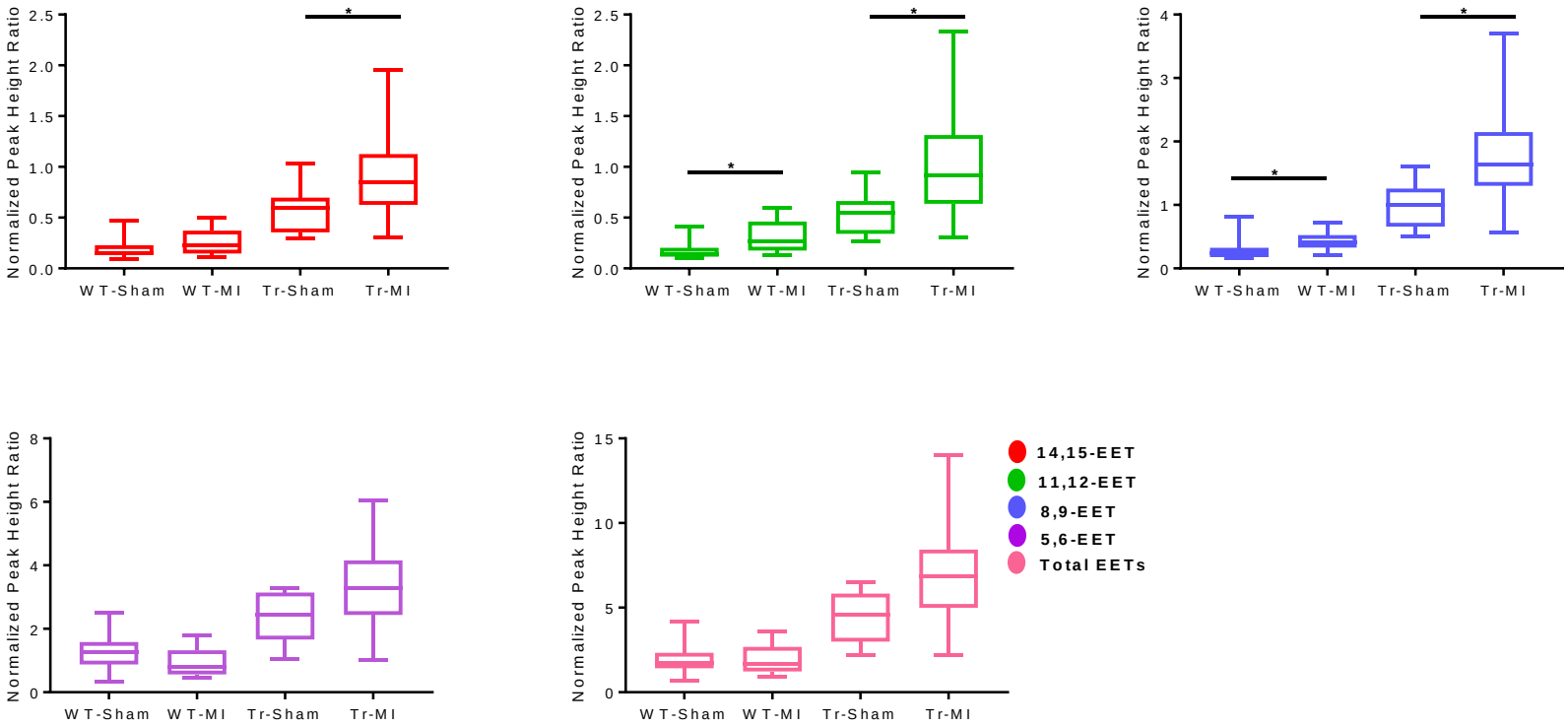

Figure 3.20. Levels of each regioisomer of *trans*-EETs and total *trans*-EETs extracted from cardiac tissue of WT and Tr mice subjected to sham or MI surgery. There were significantly higher *trans*-11,12- and *trans*-8,9-EETs in WT-MI mice. In addition, significantly higher levels of *trans*-14,15-, *trans*-11,12-, and *trans*-8,9-EETs were observed in MI-operated Tr mice compared to Tr-sham. * indicates $p \leq 0.05$.

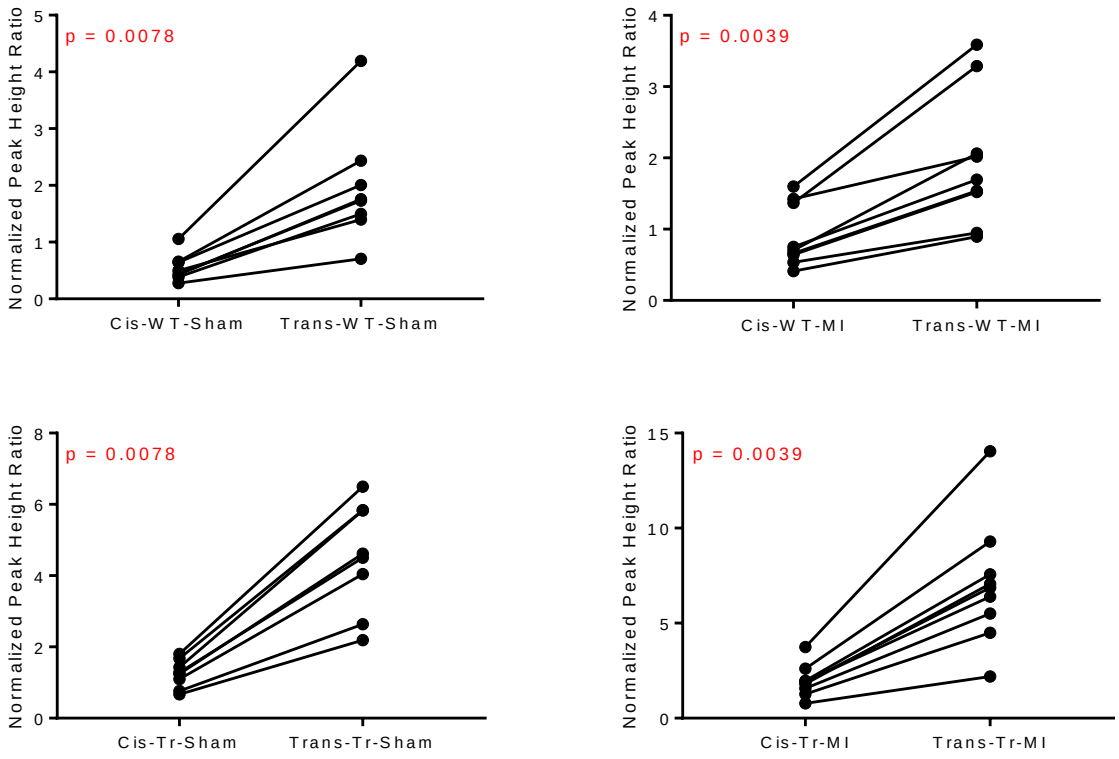

Figure 3.21. Comparison between total *cis*- and *trans*-EETs levels extracted from cardiac tissue of WT and Tr mice. Total *trans*-EETs levels in both WT and Tr mice are higher than total *cis*-EETs levels regardless of the mice surgery status. Interestingly, the trends observed in cardiac tissue are the opposite of what was observed in erythrocyte membrane.

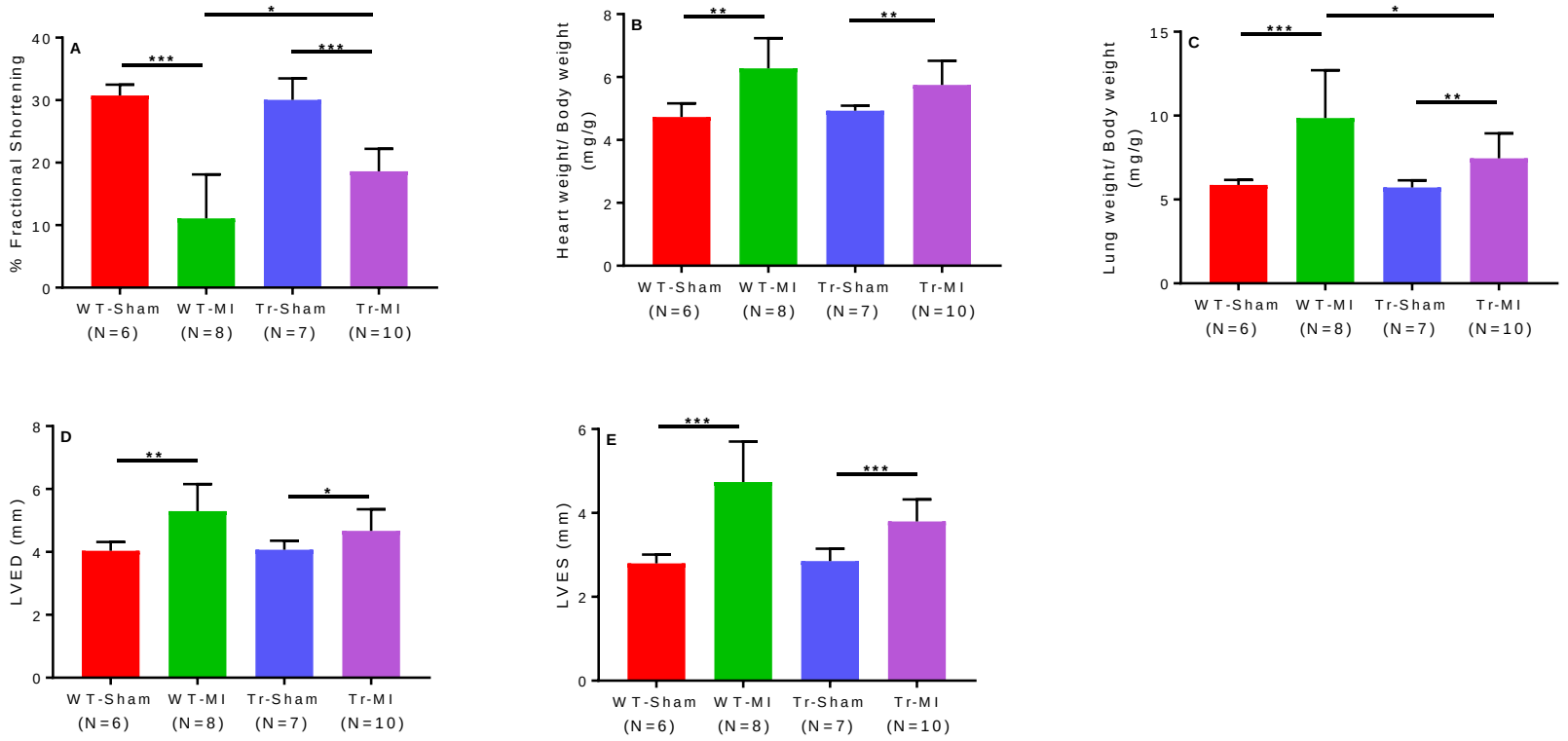

Figure 3.22. Echocardiographic data measurement to reflect left ventricular function. (A) % Fractional shortening (%FS), an indicator of function of left ventricle, (B) heart weight to body weight (HW/BW) ratio, (C) lung weight to body weight (LW/BW) ratio, (D). measurement of left ventricle dimensions at the end of diastole (the biggest cardiac dimension, LVED, D) and systole (the smallest cardiac dimension, LVES, E) were collected for all the mice subjected to sham or MI surgery.

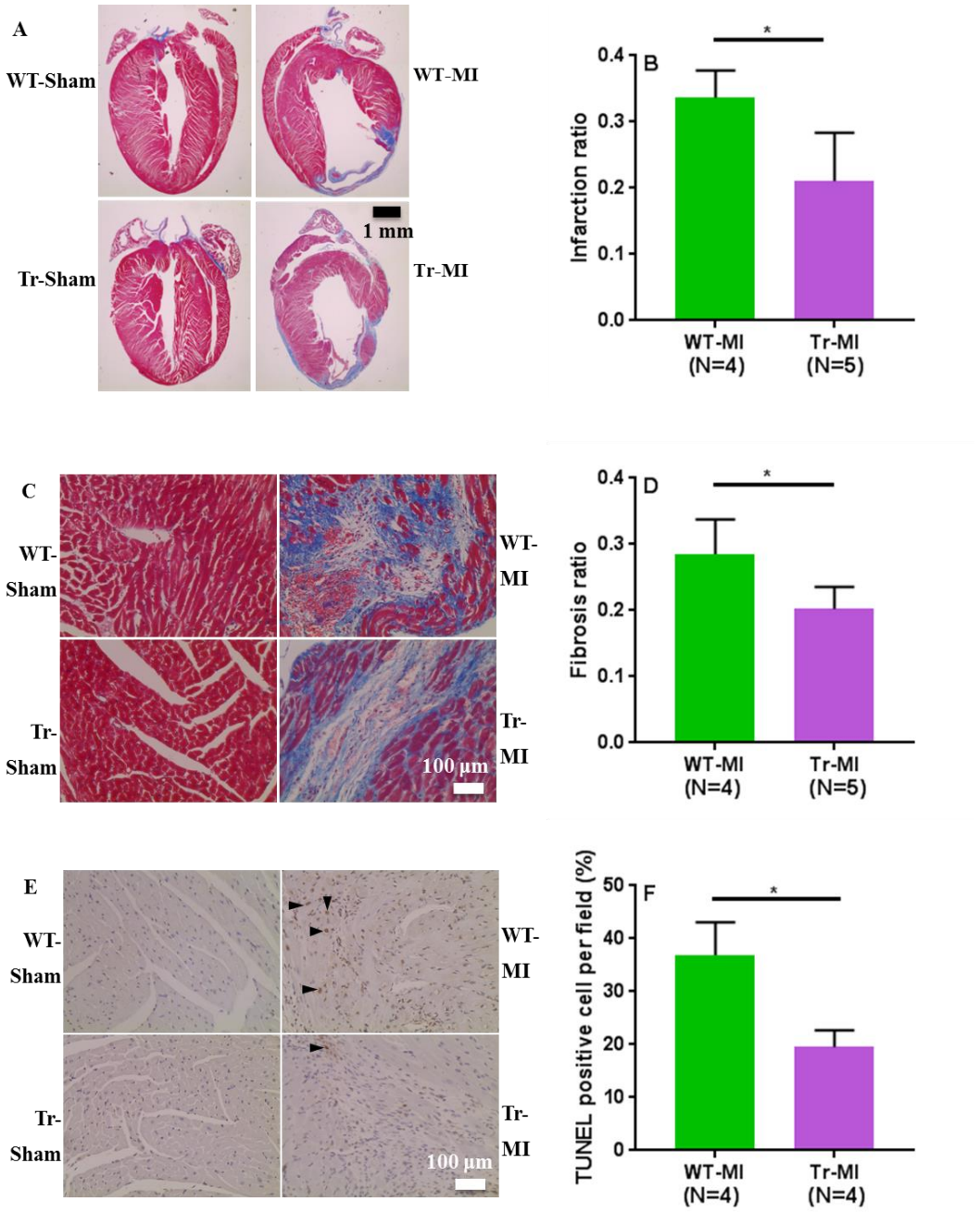

Figure 3.23. Overexpression of cardiac-specific CYP2J2 significantly minimizes the extent of infarction, fibrosis and apoptosis in mice following two-week MI. Paraffin-embedded cardiac sections of WT and Tr mice were stained using Masson's Trichrome (A and C). (A) shows whole slice of hearts while (C) shows only infarct zones. Blue area indicates myocardial fibrosis while red area indicates healthy muscle tissue. (B) Myocardial infarction size ratio and (D) myocardial fibrosis ratio were determined using MetaMorph software. (E) TUNEL-positive nuclei of paraffin-embedded sections from the mice hearts indicated in A. Apoptotic cells appeared brown while normal cells appeared blue. (F) Measurement of TUNEL-positive nuclei in cardiac sections from mice indicated in A. * indicates $p \leq 0.05$.

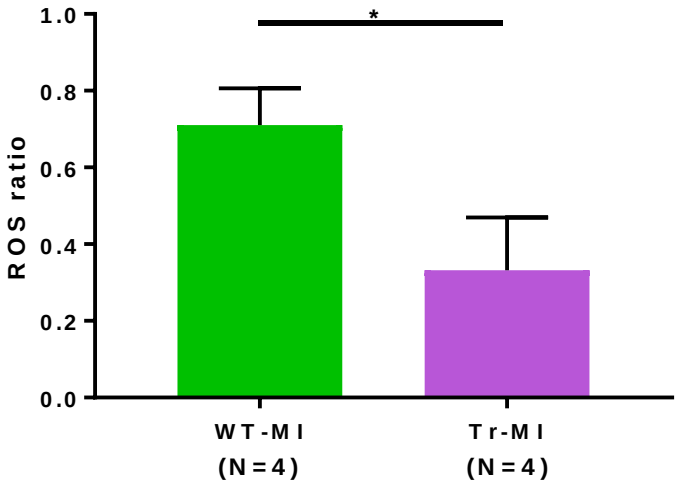

Figure 3.24. Overexpression of cardiac-specific CYP2J2 appears to reduce ROS production following two-week MI. Measurement of ROS ratio using CM-H2DCFDA staining from mice frozen cardiac sections. * indicates $p \leq 0.05$.

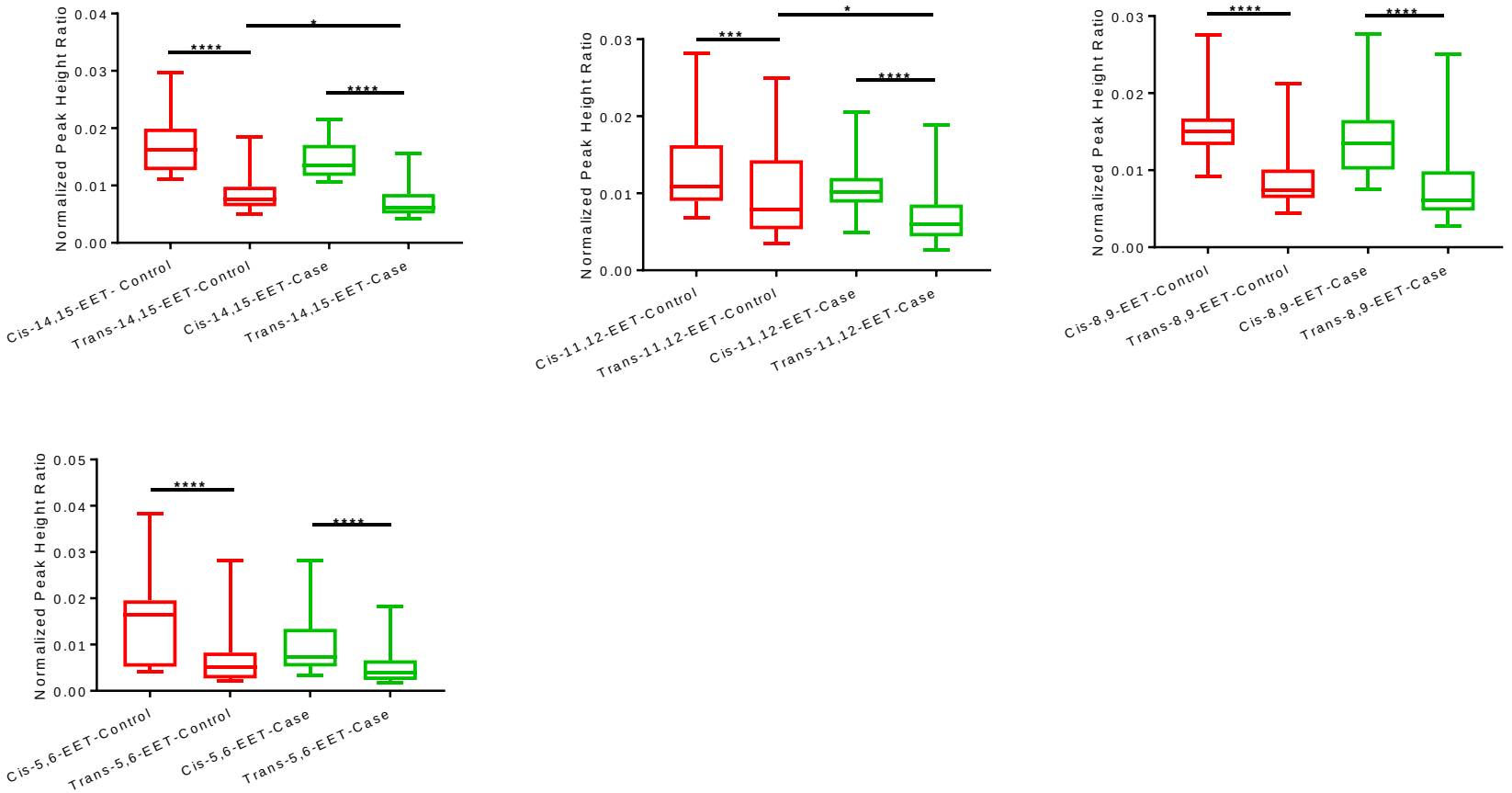

Figure 3.25. Comparison of *cis*- and *trans*-EET levels in erythrocyte membrane of control and SCA case (N=52) groups. Levels of *trans*-EETs in all of erythrocyte membrane of SCA cases are significantly lower than their *cis*-EETs counterparts. Levels of *trans*-14,15- and *trans*-11,12-EETs are significantly higher in control group which seems to drive the significant difference seen in the total *trans*-EETs between control and case groups. An individual regioisomer of *cis*-EET does not seem to show any significant difference between control and case groups. However, cumulatively *cis*-EETs were significantly higher in control than case groups. **** indicates $p \leq 0.0001$, *** indicates $p \leq 0.001$, and * indicates $p \leq 0.05$.

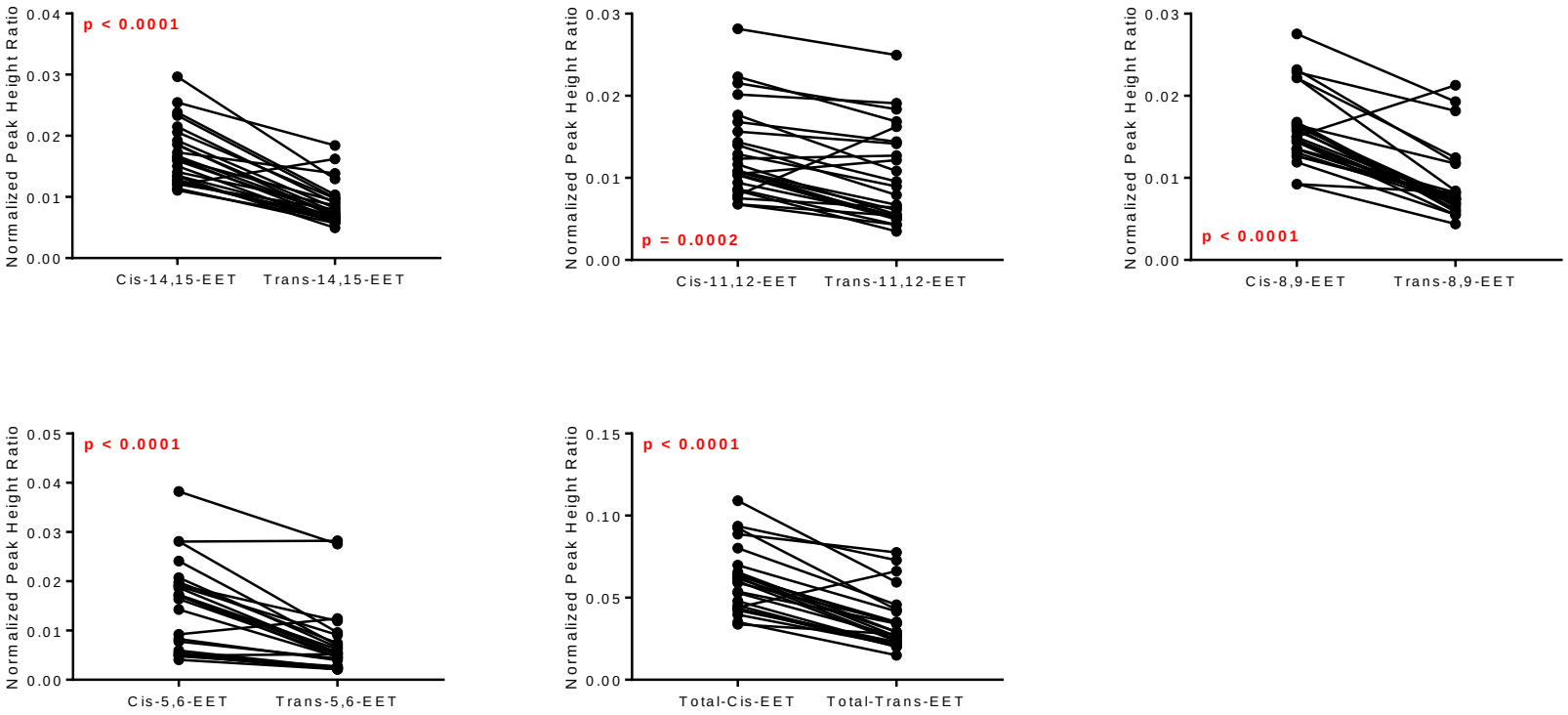

Figure 3.26. Comparison between total *cis*- and *trans*-EET levels extracted from erythrocyte membrane of control group. Each regioisomer and total *cis*-EETs extracted from erythrocyte membrane of control groups exhibited higher levels than their *trans*-EETs levels.

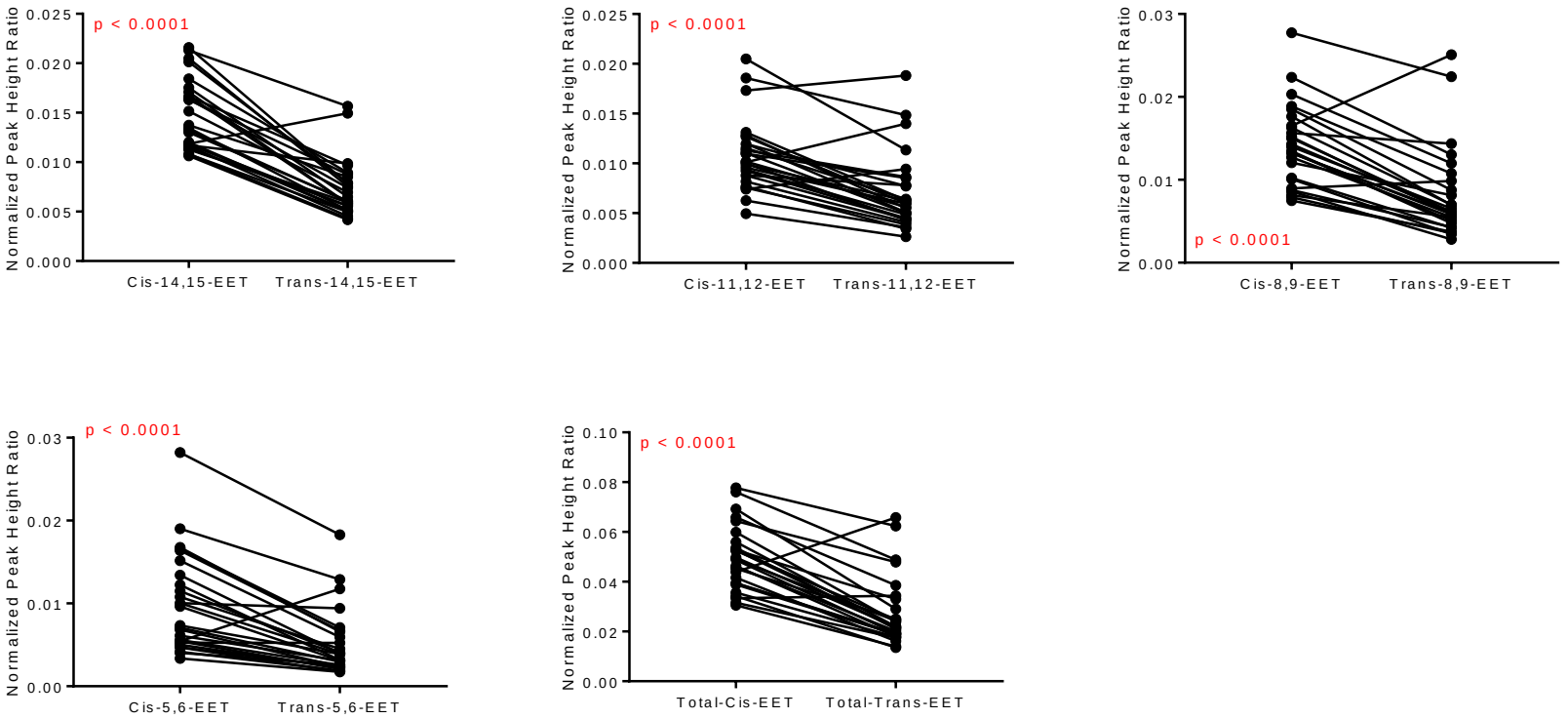

Figure 3.27. Comparison between total *cis*- and *trans*-EET levels extracted from erythrocyte membrane of SCA case group. Levels of *cis*-EETs among the different regioisomers were generally higher than levels of *trans*-EETs in erythrocyte membrane of SCA case group.

Table 3.1. Percent difference of each *cis*-EET in erythrocyte membrane of volunteer 1 when quantified using spiked RBC and PBS-based calibration curves.

	% difference when quantified using RBC-spiked and PBS-based calibration curves
14,15-EET	25.6%
11,12-EET	8.6%
8,9-EET	18.9%
5,6-EET	12.0%

Each concentration point and erythrocyte membrane of volunteer 1 were extracted as duplicate samples.

Table 3.2. Summary of ratio of each regioisomer of EETs in erythrocyte membrane and cardiac tissue of WT and Tr mice categorized by their age and geometric isomers.

	Cis		***Trans***	
	Young	Old	Young	Old
WT-RBC	1.8 : 1.0 : 4.3 : 7.2	2.2 : 3.3 : 1.0 : 1.4	1.0 : 1.0 : 2.4 : 3.2	1.4 : 3.1 : 1.0 : 1.1
Tr- RBC	1.8 : 1.0 : 4.1 : 6.6	2.2 : 3.3 : 1.0 : 1.4	1.2 : 1.0 : 2.9 : 4.7	1.8 : 3.5 : 1.0 : 1.3
WT-Heart	1.3 : 1.0 : 1.4 : 2.4	1.0 : 1.1: 1.0 : 1.1	1.1 : 1.0 : 3.0 : 3.8	0.8 : 1.3 : 2.0 : 1.0
Tr - Heart	1.4 : 1.0 : 1.3 : 2.7	1.0 : 1.1 : 1.0 :1.0	1.0 : 1.0 : 2.9 : 4.7	1.3 : 2.3 : 2.2 : 1.0

Each ratio is presented as ratio of 14,15-EET: 11,12-EET: 8,9-EET: 5,6-EET

Table 3.3. Summary of geometric isomers of individual regioisomer of EETs in cardiac tissue and RBC membrane of WT and Tr mice subjected to sham or MI surgery. There were 8 WT mice (4 female and 4 male mice) and 9 Tr mice (5 female and 4 male mice) subjected to sham surgery and 9 WT mice (4 female and 5 male mice) and 9 Tr mice (4 female and 5 male mice) subjected to MI surgery.

	Heart					**RBC**				
	trans-/cis- ratio					*cis-/trans-* ratio				
	14,15-EET	11,12-EET	8,9-EET	5,6-EET	Total	14,15-EET	11,12-EET	8,9-EET	5,6-EET	Total
WT-Sham	1.8 ± 0.5	1.6 ±0.3	2.3 ± 0.6	6.5 ±2.0	3.6 ± 0.6	2.2 ± 0.3	1.9 ± 0.2	2.4 ± 0.4	1.4 ± 0.2	1.8 ± 0.3
Tr-Sham	1.9 ± 0.2	1.3 ± 0.1	3.8 ± 0.5	9.0 ± 0.5	3.6 ± 0.2	2.2 ± 0.4	1.9 ± 0.2	1.8 ± 0.6	1.6 ± 0.3	1.8 ± 0.1
WT-MI	2.1 ± 0.4	1.7 ± 0.3	1.9 ± 0.4	2.8 ± 0.6	2.2 ± 0.4	2.0 ± 0.2	1.8 ± 0.2	2.6 ± 0.3	1.9 ± 0.2	2.0 ± 0.2
Tr-MI	2.1 ± 0.2	1.5 ± 0.3	4.1 ± 0.5	7.7 ± 0.7	3.5 ± 0.3	2.4 ± 0.2	1.8 ± 0.3	1.3 ± 0.4	1.5 ± 0.3	1.7 ± 0.2

Each entry is an average of eight to nine ratios of geometric isomers of EETs. Data are presented as mean ± S.D.

Table 3.4. Percentages of each regioisomer of *cis*-EET bound to various lipoproteins in human plasma.

	***cis*-14,15-EET**	***cis*-11,12-EET**	***cis*-8,9-EET**	***cis*-5,6-EET**
% in VLDL	4.3	4.2	5.2	7.5
% in LDL	77.6	77.3	72.2	68.0
% in HDL	18.2	18.5	22.6	24.5

Fractionated human plasma was extracted as duplicate samples.

REFERENCES

Aliwarga T, Raccor BS, Lemaitre RN, Sotoodehnia N, Gharib SA, Xu L, and Totah RA (2017) Enzymatic and free radical formation of cis- and trans- epoxyeicosatrienoic acids in vitro and in vivo. *Free Radic Biol Med* **112:**131-140.

Behm DJ, Ogbonna A, Wu C, Burns-Kurtis CL, and Douglas SA (2009) Epoxyeicosatrienoic acids function as selective, endogenous antagonists of native thromboxane receptors: identification of a novel mechanism of vasodilation. *J Pharmacol Exp Ther* **328:**231-239.

Bellien J, Joannides R, Richard V, and Thuillez C (2011) Modulation of cytochrome-derived epoxyeicosatrienoic acids pathway: a promising pharmacological approach to prevent endothelial dysfunction in cardiovascular diseases? *Pharmacol Ther* **131:**1-17.

Capdevila JH, Falck JR, and Harris RC (2000) Cytochrome P450 and arachidonic acid bioactivation. Molecular and functional properties of the arachidonate monooxygenase. *J Lipid Res* **41:**163-181.

Chaudhary KR, Zordoky BN, Edin ML, Alsaleh N, El-Kadi AO, Zeldin DC, and Seubert JM (2013) Differential effects of soluble epoxide hydrolase inhibition and CYP2J2 overexpression on postischemic cardiac function in aged mice. *Prostaglandins Other Lipid Mediat* **104-105:**8-17.

Franceschi C and Campisi J (2014) Chronic inflammation (inflammaging) and its potential contribution to age-associated diseases. *J Gerontol A Biol Sci Med Sci* **69 Suppl 1:**S4-9.

Goulitquer S, Dréano Y, Berthou F, Corcos L, and Lucas D (2008) Determination of epoxyeicosatrienoic acids in human red blood cells and plasma by GC/MS in the NICI mode. *J Chromatogr B Analyt Technol Biomed Life Sci* **876:**83-88.

Graves JP, Edin ML, Bradbury JA, Gruzdev A, Cheng J, Lih FB, Masinde TA, Qu W, Clayton NP, Morrison JP, Tomer KB, and Zeldin DC (2013) Characterization of four new mouse cytochrome P450 enzymes of the CYP2J subfamily. *Drug Metab Dispos* **41:**763-773.

Guo X, Yin H, Li L, Chen Y, Li J, Doan J, Steinmetz R, and Liu Q (2017) Cardioprotective Role of Tumor Necrosis Factor Receptor-Associated Factor 2 by Suppressing Apoptosis and Necroptosis. *Circulation* **136:**729-742.

Herse F, Lamarca B, Hubel CA, Kaartokallio T, Lokki AI, Ekholm E, Laivuori H, Gauster M, Huppertz B, Sugulle M, Ryan MJ, Novotny S, Brewer J, Park JK, Kacik M, Hoyer J, Verlohren S, Wallukat G, Rothe M, Luft FC, Muller DN, Schunck WH, Staff AC, and Dechend R (2012) Cytochrome P450 subfamily 2J polypeptide 2 expression and circulating epoxyeicosatrienoic metabolites in preeclampsia. *Circulation* **126:**2990-2999.

Jialal I, Devaraj S, and Venugopal SK (2004) C-reactive protein: risk marker or mediator in atherothrombosis? *Hypertension* **44:**6-11.

Jiang H, Anderson GD, and McGiff JC (2010) Red blood cells (RBCs), epoxyeicosatrienoic acids (EETs) and adenosine triphosphate (ATP). *Pharmacol Rep* **62:**468-474.

Jiang H, Quilley J, Reddy LM, Falck JR, Wong PY, and McGiff JC (2005) Red blood cells: reservoirs of cis- and trans-epoxyeicosatrienoic acids. *Prostaglandins Other Lipid Mediat* **75:**65-78.

Karara A, Wei S, Spady D, Swift L, Capdevila JH, and Falck JR (1992) Arachidonic acid epoxygenase: structural characterization and quantification of epoxyeicosatrienoates in plasma. *Biochem Biophys Res Commun* **182:**1320-1325.

Kaspera R and Totah RA (2009) Epoxyeicosatrienoic acids: formation, metabolism and potential role in tissue physiology and pathophysiology. *Expert Opin Drug Metab Toxicol* **5:**757-771.

Kinugawa S, Tsutsui H, Hayashidani S, Ide T, Suematsu N, Satoh S, Utsumi H, and Takeshita A (2000) Treatment with dimethylthiourea prevents left ventricular remodeling and failure after experimental myocardial infarction in mice: role of oxidative stress. *Circ Res* **87:**392-398.

Korff S, Katus HA, and Giannitsis E (2006) Differential diagnosis of elevated troponins. *Heart* **92:**987-993.

Lee CR, Imig JD, Edin ML, Foley J, DeGraff LM, Bradbury JA, Graves JP, Lih FB, Clark J, Myers P, Perrow AL, Lepp AN, Kannon MA, Ronnekleiv OK, Alkayed NJ, Falck JR, Tomer KB, and Zeldin DC (2010) Endothelial expression of human cytochrome P450 epoxygenases lowers blood pressure and attenuates hypertension-induced renal injury in mice. *FASEB J* **24:**3770-3781.

Li L, Guo X, Chen Y, Yin H, Li J, Doan J, and Liu Q (2016) Assessment of Cardiac Morphological and Functional Changes in Mouse Model of Transverse Aortic Constriction by Echocardiographic Imaging. *J Vis Exp*.

Lu T, Ye D, Wang X, Seubert JM, Graves JP, Bradbury JA, Zeldin DC, and Lee HC (2006) Cardiac and vascular KATP channels in rats are activated by endogenous epoxyeicosatrienoic acids through different mechanisms. *J Physiol* **575:**627-644.

Ma J, Bradbury JA, King L, Maronpot R, Davis LS, Breyer MD, and Zeldin DC (2002) Molecular cloning and characterization of mouse CYP2J6, an unstable cytochrome P450 isoform. *Biochem Pharmacol* **64:**1447-1460.

Ma J, Qu W, Scarborough PE, Tomer KB, Moomaw CR, Maronpot R, Davis LS, Breyer MD, and Zeldin DC (1999) Molecular cloning, enzymatic characterization, developmental expression, and cellular localization of a mouse cytochrome P450 highly expressed in kidney. *J Biol Chem* **274:**17777-17788.

Maisel A (2002) B-type natriuretic peptide levels: diagnostic and prognostic in congestive heart failure: what's next? *Circulation* **105:**2328-2331.

Marin-Garcia J, Goldenthal MJ, and Moe GW (2001) Mitochondrial pathology in cardiac failure. *Cardiovasc Res* **49:**17-26.

Morrow DA and Braunwald E (2003) Future of biomarkers in acute coronary syndromes: moving toward a multimarker strategy. *Circulation* **108:**250-252.

Oni-Orisan A, Edin ML, Lee JA, Wells MA, Christensen ES, Vendrov KC, Lih FB, Tomer KB, Bai X, Taylor JM, Stouffer GA, Zeldin DC, and Lee CR (2016) Cytochrome P450-

derived epoxyeicosatrienoic acids and coronary artery disease in humans: a targeted metabolomics study. *J Lipid Res* **57:**109-119.

Pearson TA, Mensah GA, Alexander RW, Anderson JL, Cannon RO, Criqui M, Fadl YY, Fortmann SP, Hong Y, Myers GL, Rifai N, Smith SC, Taubert K, Tracy RP, Vinicor F, Prevention CfDCa, and Association AH (2003) Markers of inflammation and cardiovascular disease: application to clinical and public health practice: A statement for healthcare professionals from the Centers for Disease Control and Prevention and the American Heart Association. *Circulation* **107:**499-511.

Qu W, Bradbury JA, Tsao CC, Maronpot R, Harry GJ, Parker CE, Davis LS, Breyer MD, Waalkes MP, Falck JR, Chen J, Rosenberg RL, and Zeldin DC (2001) Cytochrome P450 CYP2J9, a new mouse arachidonic acid omega-1 hydroxylase predominantly expressed in brain. *J Biol Chem* **276:**25467-25479.

Reardon CA, Blachowicz L, White T, Cabana V, Wang Y, Lukens J, Bluestone J, and Getz GS (2001) Effect of immune deficiency on lipoproteins and atherosclerosis in male apolipoprotein E-deficient mice. *Arterioscler Thromb Vasc Biol* **21:**1011-1016.

Schuck RN, Theken KN, Edin ML, Caughey M, Bass A, Ellis K, Tran B, Steele S, Simmons BP, Lih FB, Tomer KB, Wu MC, Hinderliter AL, Stouffer GA, Zeldin DC, and Lee CR (2013) Cytochrome P450-derived eicosanoids and vascular dysfunction in coronary artery disease patients. *Atherosclerosis* **227:**442-448.

Seubert J, Yang B, Bradbury JA, Graves J, Degraff LM, Gabel S, Gooch R, Foley J, Newman J, Mao L, Rockman HA, Hammock BD, Murphy E, and Zeldin DC (2004) Enhanced postischemic functional recovery in CYP2J2 transgenic hearts involves mitochondrial ATP-sensitive K+ channels and p42/p44 MAPK pathway. *Circ Res* **95:**506-514.

Shahabi P, Siest G, Meyer UA, and Visvikis-Siest S (2014) Human cytochrome P450 epoxygenases: variability in expression and role in inflammation-related disorders. *Pharmacol Ther* **144:**134-161.

Sun N, Youle RJ, and Finkel T (2016) The Mitochondrial Basis of Aging. *Mol Cell* **61:**654-666.

Theken KN, Schuck RN, Edin ML, Tran B, Ellis K, Bass A, Lih FB, Tomer KB, Poloyac SM, Wu MC, Hinderliter AL, Zeldin DC, Stouffer GA, and Lee CR (2012) Evaluation of cytochrome P450-derived eicosanoids in humans with stable atherosclerotic cardiovascular disease. *Atherosclerosis* **222:**530-536.

Webler AC, Michaelis UR, Popp R, Barbosa-Sicard E, Murugan A, Falck JR, Fisslthaler B, and Fleming I (2008) Epoxyeicosatrienoic acids are part of the VEGF-activated signaling cascade leading to angiogenesis. *Am J Physiol Cell Physiol* **295:**C1292-1301.

Weintraub NL, Fang X, Kaduce TL, VanRollins M, Chatterjee P, and Spector AA (1997) Potentiation of endothelium-dependent relaxation by epoxyeicosatrienoic acids. *Circ Res* **81:**258-267.

Wu S, Chen W, Murphy E, Gabel S, Tomer KB, Foley J, Steenbergen C, Falck JR, Moomaw CR, and Zeldin DC (1997) Molecular cloning, expression, and functional significance of a cytochrome P450 highly expressed in rat heart myocytes. *J Biol Chem* **272:**12551-12559.

Wu S, Moomaw CR, Tomer KB, Falck JR, and Zeldin DC (1996) Molecular cloning and expression of CYP2J2, a human cytochrome P450 arachidonic acid epoxygenase highly expressed in heart. *J Biol Chem* **271:**3460-3468.

Yu Z, Xu F, Huse LM, Morisseau C, Draper AJ, Newman JW, Parker C, Graham L, Engler MM, Hammock BD, Zeldin DC, and Kroetz DL (2000) Soluble epoxide hydrolase regulates hydrolysis of vasoactive epoxyeicosatrienoic acids. *Circ Res* **87:**992-998.

CHAPTER 4

EFFECTS OF CARDIOVASCULAR DISEASE ON EPOXYEICOSATRIENOIC ACID LEVELS AND PROTEINS INVOLVED IN THEIR BIOSYNTHESIS AND BIODEGRADATION

4.1. INTRODUCTION

Cardiovascular disease (CVD) remains the leading cause of mortality globally. The World Health Organization reported that 31% of global deaths in 2015 were due to CVD. Of these deaths, approximately 13% were caused by coronary artery disease (CAD). Based on the etiology of the disease, CVD is divided into two categories: ischemic and non-ischemic cardiomyopathies. Ischemic cardiomyopathy usually originates following CAD, where accumulation of plaque on coronary arteries is not properly controlled, leading to restriction of oxygenated blood flow to the heart. Non-ischemic cardiomyopathy, on the other hand, is historically described as alterations in morphology and function of the heart. Relatively recently, non-ischemic cardiomyopathy was defined as a complex disease of the myocardium associated with mechanical or electrical dysfunction that features abnormal ventricular hypertrophy or dilatation. It is considered a multifactorial disorder that is often genetic in nature (Maron et al., 2006).

Epoxyeicosatrienoic acids (EETs) are CYP mediated metabolites of arachidonic acid (AA). AA is usually found esterified at the *sn*-2 position of phospholipid membranes. Upon release by phospholipase A_2 (PLA_2), AA can be metabolized by cytochrome P450 (CYP) epoxygenases, notably CYP2 family members, e.g. CYP2J2 and others. There are several classes of phospholipase A_2, but calcium-dependent cytosolic PLA_2 type IVA ($cPLA_2\alpha$), encoded by *PLA2G4A*, is considered the major enzyme responsible for hydrolyzing AA from the membrane (Clark et al., 1991; Lin et al., 1993). Along with AA, most EETs are found esterified in the membrane and saponification or hydrolysis using PLA_2 is required to release them from this site (Karara et al., 1989; Wu et al., 1996; Goulitquer et al., 2008). Within the CYP catalytic cycle, there are two electron transfer steps from the cofactor, NADPH. It is well established that the

first electron transfer from NADPH, which reduces the ferric heme to ferrous, is catalyzed by NADPH-cytochrome P450 oxidoreductase (POR). Therefore, the rate of CYP mediated formation of EETs will depend, in part, on the expression and activity of POR in cardiac tissue.

Once formed, EETs are short lived and can be rapidly hydrolyzed to the less biologically active dihydroxyeicosatrienoic acids (DHETs) by soluble epoxide hydrolase (sEH), which is encoded by the *EPHX2* gene (Yu et al., 2000). EETs can also be re-esterified back into the phospholipid membrane for storage by acyl CoA synthase(s) (Weintraub et al., 1997). It is unclear which isoform(s) of acyl CoA synthase is responsible for the re-esterification of AA and EETs. However, based on a single nucleotide polymorphism association study of sudden cardiac arrest (SCA), *LPCAT1* and *PLA2G4A* were two of the few genes that were associated with incident SCA (Lemaitre et al., 2014). *LPCAT1* encodes for lysophosphotidylcholine acyltransferase 1 that is found mainly in phosphatidylcholine lipid droplets (Moessinger et al., 2011). LPCAT1 was shown to be protective against cytotoxicity induced by excess polyunsaturated fatty acids in HeLa cells by regulating the production of dipalmitoylphosphatidylcholine (Akagi et al., 2016). A different isoform of LPCAT, LPCAT3 was shown to be responsible for incorporating AA into glycerophospholipid during adipocyte differentiation, however, studies on LPCAT3's role in AA or EETs reincorporation into the membrane are lacking (Eto et al., 2012).

Numerous disease states can alter the expression of enzymes involved in the biosynthesis and degradation of EETs and consequently alter steady-state EET levels. Significantly higher total EETs were reported in both obese and non-obese CAD patients compared to healthy volunteers (Theken et al., 2012). While a follow up study by the same group reported that there were significantly lower levels of total plasma EETs in obstructive CAD patients compared to

healthy volunteers (Oni-Orisan et al., 2016). The authors suggested that the contradictory results from their studies were due to significant differences in sEH activity, as indicated by altered ratios of 14,15-EET to 14,15-DHET. Plasma levels of EETs were also significantly lower in subjects with renovascular disease compared to control subjects (Minuz et al., 2008). Transcripts for *EPHX2*, the gene that encodes sEH, were significantly lower in ischemic human heart failure patients compared to controls (Monti et al., 2008). Disease state also increases expression of the stress response protein, heme oxygenase 1 encoded by *HMOX1* (Deshane et al., 2005). Multiple animal studies have reported the upregulation of HMOX1 in atherosclerosis and myocardial infarction (MI) (Yet et al., 2001; Yet et al., 2003). In addition, lipoprotein-associated phospholipase A_2 (Lp-PLA_2) encoded by *PLA2G7* is reported to be abundant in coronary atherosclerotic plaques and elevated levels of this enzyme are associated with coronary heart disease events in healthy older adults (Kolodgie et al., 2006; Daniels et al., 2008). However, studies on the mechanism(s) by which POR, c$PLA_2\alpha$, and LPCAT1 are regulated in CVD are absent in literature. Since CYP2J2, POR, sEH, c$PLA_2\alpha$, and LPCAT1 are all involved in EETs biosynthesis and biodegradation, as summarized in Figure 4.1, it is important to investigate how CVD affects their protein expression. From prior unpublished studies in our lab, HMOX1 transcript seems to be responsive to EET levels and cell stress in general and should also be investigated. Therefore, we undertook a proteomics study to measure absolute levels of the proteins identified in Figure 4.1 and HMOX1 in control and diseased human ventricular heart tissues.

Mass spectrometric (MS)-based quantitative proteomics is a relatively new method to quantify proteins in biological samples. Although Western immunoblotting is still used widely to quantify proteins, there are several reasons why MS-based quantitative proteomics is

increasingly becoming the preferred method, including quality of assay, quality of results, and performance characteristics (Aebersold et al., 2013). Because Western blotting relies heavily on the quality of the primary antibody and its selectivity and sensitivity, poor characterization of that particular antibody can influence the quality of the results. In addition, proper quantification of proteins using Western blot depends on the successful separation of proteins of interest during gel electrophoresis and quality of protein sample preparation. In MS-based quantitative proteomics, two or more stable labelled reference peptides are used to quantify the protein of interest. Therefore, multiple peptides per protein, multiple measurements, and multiple mass transitions are used to measure level of protein of interest thereby reducing variability and measurement errors. Lastly, quantitative proteomics has the advantage of lower limits of detection, extended linear dynamic range, ability to multiplex, and higher reproducibility compared to immunoblotting.

In this study we quantified CYP2J2, POR, sEH, cPLA$_2\alpha$, and LPCAT1 because of their involvement in EET biosynthesis and degradation, in ventricular tissue from CVD patients vs. controls. We also measured *cis*- and *trans*-EETs in the same cardiac tissue homogenates. Finally, CYP2J2 activity, in the same homogenate, was determined using terfenadine (Figure 4.2) as the probe substrate.

4.2. MATERIALS AND METHODS

4.2.1. REAGENTS

Human heart S9 fractions were purchased from Sekisui Xenotech, LLC (Kansas City, KS). EDTA-free Halt protease inhibitor cocktail, and peptides of interest listed in Table 4.1 were obtained from Thermo Fisher Scientific (Waltham, MA) and used without further purification.

Dulbecco's phosphate buffered saline (DPBS, 10 ×), Pierce bicinchoninic acid (BCA) protein assay kit, sodium chloride, ammonium acetate, ACS-grade ethyl acetate, chloroform, optima-grade acetonitrile, water, methanol, and acetic acid were purchased from Fisher Scientific (Hampton, NH). Terfenadine, terfenadine alcohol, terfenadine acid hydrochloride, triphenylphosphine, azacyclonol, and phospholipase A_2 from *Naja mossambica mossambica* were obtained from Sigma-Aldrich (St. Louis, MO). A 1 mg/mL ethanolic solution of midazolam was purchased from Cerilliant Corporation (Round Rock, TX) and used as internal standard.

4.2.2. HUMAN CARDIAC TISSUE

Discarded, non-ischemic and ischemic human heart tissues were obtained from the University of Washington Medical Center as surgical waste during cardiac transplants and other procedures. Ventricular tissues were immediately flash-frozen in liquid nitrogen and stored at -80°C until further processing. Tissue was assigned as ischemic or non-ischemic based on diagnosis in the patient's chart by Dr. Jean C. Dinh and confirmed by the physician on the study, Dr. Nona Sotoodehnia. Control human heart tissues (N=17) were a gift from Dr. Scott Heyward at Bioreclamation IVT (Westbury, NY).

4.2.3. EETS EXTRACTION FROM CARDIAC TISSUE

EETs extraction from cardiac tissue followed the protocol in Chapter 2 section 2.7. 1 × EDTA-free Halt cocktail protease inhibitor was added to the remaining heart homogenate before further processing for proteomics analyses.

4.2.4. ABSOLUTE AND RELATIVE PROTEIN QUANTIFICATION

Absolute protein quantitation for CYP2J2, EPHX2, HMOX1 and POR and relative protein quantitation for LPCAT1, cPLA$_2\alpha$, and Lp-PLA$_2$ were carried out using a validated mass spectrometric proteomics method by members of Dr. Bhagwat Prasad's laboratory. At least one surrogate peptide for each protein was used for protein quantitation and their corresponding stable labelled peptides with [$^{13}C_6$, $^{15}N_4$]- arginine or [$^{13}C_6$, $^{15}N_2$]- lysine residues on their C-terminus were used as internal standard. The peptides used for the protein quantitation are listed in Table 4.1.

4.2.4.1. PROTEIN EXTRACTION AND TRYPSIN DIGESTION

Proteins from heart homogenates were solubilized, enriched, and extracted using Thermo Fisher Mem-PER^{TM} Plus membrane protein extraction kit following the manufacturer's protocol (Thermo Fisher Scientific, Waltham, MA). Membrane-bound proteins such as CYP2J2, POR, LPCAT1, and HMOX1 were analyzed using the pellet fraction while cytosolic proteins like EPHX2, cPLA$_2\alpha$ were analyzed using the supernatant fraction. Prior to sample preparation for proteomics analysis, total protein content was determined using BCA. The sample preparation for proteomics analysis followed the protocol published by Xu et al (Xu et al., 2017). Briefly, heart homogenates were diluted to 2 mg/mL total protein content. Microsomal or cytosolic proteins along with 0.7 mg/mL human serum albumin, 2.7 μg/mL bovine serum albumin were denatured and reduced with 20 mM ammonium bicarbonate buffer, pH 7.8 and 17 mM dithiothreitol at 95^{o}C for 10 minutes with gentle shaking at 300 rpm. After cooling to room temperature for 10 min, alkylation of denatured proteins was carried out by adding 59 mM of iodoacetamide and incubating the samples at room temperature in the dark for 30 min. Ice cold

methanol, chloroform, and water (5:1:4 ratio) were then added into each sample. After mixing and centrifugation at 16,000 × g for 5 min at 4^{o}C, the upper and lower layers were removed and the remaining pellets were dried at room temperature for 10 min. The pellets were washed with ice cold methanol followed by centrifugation at 8,000 × g for 5 min at 4^{o}C. After removal of the supernatant, the pellets were dried at room temperature for 30 min followed by resuspension in 60 μL of 50 mM ammonium bicarbonate buffer, pH 7.8. To initiate trypsin digestion, 0.04 μg of trypsin (desired protein:trypsin ratio was between 1:10 and 1:100) was added into each resuspended pellet and incubated at 37^{o}C for 18 hours for membrane protein or 16 hours for cytosolic protein with gentle mixing at 300 rpm. The reaction was quenched by flash freezing the samples in dry ice. Subsequently, 20 μL of a cold cocktail of stable labelled peptide internal standard (prepared in 80% acetonitrile containing 0.1% formic acid) and 10 μL of cold 80% acetonitrile containing 0.5% formic acid were added to the samples. The samples were vortexed and centrifuged at 4,000 x g for 5 min at 4^{o}C. The supernatants were collected and analyzed by mass spectrometry.

4.2.4.2. MASS SPECTROMETRIC ASSAY FOR PROTEIN QUANTIFICATION

Mass spectrometric assays to quantify proteins of interest were performed following the protocol by Xu et al (Xu et al., 2017). Briefly, samples were analyzed on an AB SCIEX Triple Quadrupole 6500 (PE SCIEX, Concord, ON, Canada) coupled to a Waters Acquity UPLC, I-class (Waters Technologies, Milford, MA) in ESI positive ionization mode. Mass spectrometer parameters for each protein of interest are summarized in Table 4.1. A Waters Acquity UPLC HSS T3, 1.8 μm, C18, 100 Å, 2.1 x100 mm column attached to a Phenomenex C18, 2 x 4 mm guard column was used to separate the different peptides with a gradient listed in Table 4.2. The

mobile phase for this assay consisted of water containing 0.1% acetic acid and acetonitrile containing 0.1% acetic acid.

4.2.5. TERFENADINE METABOLISM USING HEART HOMOGENATE AS PROTEIN SOURCE

Metabolic incubations were performed using 1 mg/mL total heart homogenate protein in the presence of 8 μM terfenadine in 100 mM potassium phosphate buffer, pH 7.4 (final volume 100 μL). Following addition of substrate, the samples were pre-equilibrated for 3 min at 37 ^{o}C after which the reaction was initiated with 1 mM NADPH. After 30 minutes, reactions were terminated with 100 μL ice cold acetonitrile containing internal standard (25 nM midazolam). The quenched reactions were vortexed followed by centrifugation at 3500 rpm at 4^{o}C for 10 min. The supernatant was transferred to a 96-well plate and analyzed using LC-MS/MS.

4.2.6. LIQUID CHROMATOGRAPHY AND MASS SPECTROMETRIC ASSAY TO MEASURE METABOLITES OF TERFENADINE

Measurement of terfenadine metabolites was performed on an AB SCIEX Triple Quadrupole 6500 (PE SCIEX, Concord, ON, Canada) coupled to a Waters Acquity UPLC, I-class (Waters Technologies, Milford, MA). Samples were analyzed in ESI positive ionization mode. Terfenadine alcohol, terfenadine acid, azacyclonol, and midazolam (internal standard) were separated on an Agilent Zorbax XDB C8, 5 μm, 2.1 x 50 column attached to a Phenomenex C18 guard column. The mobile phase consisted of: 10 mM ammonium acetate, pH 5.5 (solvent A) and 10 mM ammonium acetate in acetonitrile (solvent B). Midazolam and metabolites of terfenadine were separated using the following gradient: solvent B held at 20% from 0 to 1 min, then held at 100% from 2.5 to 4.5 min, followed by re-equilibration to 20% from 4.6 to 6.5 min.

Flow rate was constant at 0.35 mL/min throughout the run. For the first 1 min of runtime, 100% of the flow was diverted into waste. The mass spectrometer conditions are summarized in table 4.3. In order to prevent carry-over between samples, the injection needle was washed with 0.1% formic acid in acetonitrile after each sample injection.

4.2.7. DATA ANALYSIS

Mass spectrometry data for EET quantitation were analyzed using MassLynx 4.1 software while proteomics and terfenadine activity data were analyzed using Analyst 1.6.2. Statistical data analysis was performed using Prism 7.04 (GraphPad, La Jolla, CA) using non-parametric tests.

Absolute quantitation MS-based proteomics was achieved by establishing calibration curves using non-labeled peptides for proteins of interest. In contrast, relative quantitation was determined by comparing a protein level of an individual sample to a pooled sample of all the subjects (Prasad et al., 2014).

Terfenadine activity was determined by summating formation of terfenadine alcohol and terfenadine acid in all samples that were supplemented with NADPH. Ratio of each analyte to midazolam was calculated using the peak area ratio of samples with NADPH which was then subtracted from its corresponding peak area ratio of no NADPH control followed by summation of normalized peak area ratio of both terfenadine metabolites. These peak area ratios were then used to perform statistical analysis.

4.3. RESULTS

4.3.1. QUANTITATION OF EETS FROM HUMAN CARDIAC TISSUE

Control cardiac tissue (N=17) had significantly higher *cis*- and *trans*-EETs relative to diseased tissue (N= 31) (Figures 4.3 and 4.4). When the diseased cardiac tissues were separated into ischemic (N= 17) and non-ischemic (N= 14) samples and then analyzed, levels of *cis*-EETs in control cardiac tissue, with the exception of *cis*-5,6-EET, were significantly higher than non-ischemic cardiac tissues (Figure 4.3). Interestingly, diseased cardiac tissue, whether ischemic or non-ischemic, had significantly lower *trans*-EET levels for all regioisomers compared to control cardiac tissue (Figure 4.4). Total levels of *trans*-EETs in control cardiac tissue appeared to be slightly higher than their corresponding *cis*-EETs (Figure 4.5). Mixed trends were observed when analyzing total *cis*-EETs relative to total *trans*-EETs (Figure 4.6). Although not statistically significant, levels of total *trans*-EETs appeared to be mostly higher than those of *cis*-EETs in ischemic cardiac tissue (Figure 4.7) and mostly lower than *cis*-EETs in non-ischemic tissue (Figure 4.8).

4.3.2. PROTEIN QUANTITATION FROM HUMAN CARDIAC TISSUE

Protein levels of cPLA$_2\alpha$, Lp-PLA$_2$, LPCAT1, and HMOX1 for most of the samples were below the limit of quantitation. However, absolute quantitation of CYP2J2, POR, and EPHX2 were successful. In general, control cardiac tissues exhibited higher protein levels compared to diseased tissue (Figure 4.9). CYP2J2 protein levels were lower in non-ischemic cardiac tissue compared to control and ischemic tissue (Figure 4.9 A). POR levels were higher in control versus diseased cardiac tissue (Figure 4.9 B). Levels of EPHX2 in control cardiac tissue

were also found to be significantly higher than in diseased or in ischemic and non-ischemic cardiac tissues (Figure 4.9 C). In control cardiac tissue, the ratio of CYP2J2 to POR was approximately 1:12. Ratios of CYP2J2 to POR were about 1:12 in diseased cardiac tissue (1:11 in ischemic cardiac tissue, and 1:15 in non-ischemic cardiac tissue).

4.3.3. CYP2J2 SPECIFIC ACTIVITY IN HUMAN CARDIAC TISSUE USING TERFENADINE AS A PROBE SUBSTRATE

CYP2J2 in cardiac tissue oxidized terfenadine to the alcohol and acid metabolites (Figure 4.2). Formation of azacyclonol, a CYP3A4/5 specific metabolite was not observed in the cardiac tissue analyzed. Control cardiac tissue exhibited significantly higher CYP2J2 activity compared to diseased or ischemic cardiac tissues, as demonstrated in Figure 4.11.

4.4. DISCUSSION

A key finding from this study is that changes in EET levels are also accompanied by changes in CYP2J2, POR, and EPHX2 protein levels. In addition, there was a correlation between EET levels and CYP2J2 activity using terfenadine as a probe substrate. This is the first report demonstrating that disease state can alter EET levels as well as the proteins involved in their formation and degradation in human cardiac tissue.

In Chapter 2, we demonstrated that CYP2J2 metabolizes AA to exclusively four regioisomers of *cis*-EETs and that *trans*-EETs are not formed by CYP2J2. Based on the alteration of EET levels that we observed in the acute SCA cases in Chapter 3, we expected to see lower *cis*-EET levels in chronically diseased cardiac tissues. In this case, we have to take into consideration the type and progression of CVD in the subjects in this study. Our mouse MI study

(Chapter 3) only subjected mice to MI for 2 weeks (acute) which is similar to the SCA cases that had just suffered a massive cardiac event. In the diseased heart tissue, we show that both *cis*- and *trans*-EETs are lower in diseased cardiac tissue than control tissue (Figures 4.3 and 4.4). Our observation of higher *cis*-EET levels in controls are consistent with observations by Oni-Orisan et al. who reported significantly lower total plasma *cis*-EETs in obstructive CAD patients compared to healthy volunteers (Oni-Orisan et al., 2016). An unexpected observation was lower *trans*-EET levels in diseased cardiac tissue compared to control (Figure 4.4). Because we obtained the diseased ventricular tissues from left ventricular assist device (LVAD) or heart transplant patients, we assumed that these patients must have had failing hearts or nearly reached the end-stage of heart failure. A study by Saraste et al. demonstrated that the number of apoptotic cardiomyocytes significantly increased in both ischemic and non-ischemic cardiac tissues (Saraste et al., 1999). In the same study, they also showed the number of apoptotic cardiomyocytes increased significantly with progression of non-ischemic cardiac disease, while the increase in number of apoptotic cardiomyocytes in ischemic cardiac tissue was not statistically significant (Saraste et al., 1999). Because approximately 70-80% of heart tissue contains cardiomyocytes and 20-40% of cardiac tissue cellular volume accounts for mitochondria, the cumulative apoptotic cardiomyocytes in diseased tissue could be expected to produce less ROS (Marin-Garcia et al., 2001; Zhou et al., 2016), consistent with our observation of lower *trans*-EET levels in diseased cardiac tissue.

When closely examining different levels of *cis*- and *trans*-EETs in different groups, an unexpected observation was significantly lower *cis*-EETs compared to *trans*-EETs in control cardiac tissues (Figure 4.5). An increase in free radical oxidation, which is associated with pathology of many diseases, will lead to increase of predominantly *trans*-EETs (Chapter 2).

However, one factor that is easily overlooked in this case is the age of our subjects. About 90% of our cardiac tissue came from elderly patients. As described in Chapter 3, cardiac aging which is highly identified with mitochondrial aging (Marin-Garcia et al., 2001), is associated with increase ROS production and reduced mitochondrial respiratory capacity as indicated by a reduced level of phosphocreatine recovery time (Sun et al., 2016). This elevated production of ROS would be expected to lead to an increase in production of *trans*-EETs relative to cis-EETs in our control cardiac tissues as seen in Figure 4.5. In diseased tissue, *cis*-EET levels are not significantly different than *trans*-EET levels (Figure 4.6). Although there was no significant difference between *cis*- and *trans*-EETs levels in diseased cardiac tissues, we could tease out some trends when samples were further categorized into ischemic and non-ischemic cardiac tissues. The relative levels of *cis*- to *trans*-EETs within ischemic and non-ischemic sub-groups displayed an inverse relationship (Figures 4.7 and 4.8). An earlier study in human cardiac tissue showed that non-ischemic cardiac tissue possessed a higher number of apoptotic cardiomyocytes than ischemic cardiac tissue (Saraste et al., 1999). Therefore, it is plausible that in non-ischemic cardiac tissue, where sections of the hearts were dysfunctional, ROS production during mitochondrial respiration could be less. With reduced ROS production, it is anticipated that formation of *trans*-EETs, which are mediated by free radical oxidation, should also be lower (Figure 4.8) (Aliwarga et al., 2017). On the other hand, in ischemic cardiac tissue, the blockage of oxygenated blood flow into the heart followed by reperfusion could lead to a greater release of ROS (de Groot and Rauen, 2007). This excessive formation of ROS could lead to more *trans*-EETs, compared to *cis*, which is what we observed in Figure 4.7.

Although not statistically significant, control cardiac tissue generally exhibited higher CYP2J2 levels compared to diseased or ischemic or non-ischemic cardiac tissue (Figure 4.9 A)

when using absolute quantification. Statistical significance, however, was achieved in the relative quantification dataset (Figure 4.10). Since disease state can affect both protein levels and enzyme activity, we sought to determine the CYP2J2 activity in the same heart homogenates used for protein quantification and EET analysis using terfenadine as a probe substrate to provide a functional readout. Higher EETs were associated with higher CYP2J2 activity in control tissue vs. diseased (Figure 4.11). To our knowledge this is the first report of terfenadine, or any drug, metabolism in control and diseased cardiac tissue. It is important to note the azacylonal, the major metabolite formed by CYP3A4/5 and CYP4Fs was not observed in our study confirming that the major metabolic activity cardiac tissue is attributed to CYP2J2.

When examining ischemic or non-ischemic cardiac tissue separately, only CYP2J2 protein levels showed a significant difference (Figure 4.9 A). Non-ischemic cardiac tissue had significantly lower CYP2J2 compared to ischemic cardiac tissue (Figure 4.9 A). Considering localization of CYP2J2 protein in the cardiomyocytes (Delozier et al., 2007) and the nature of non-ischemic cardiomyopathy being associated with mechanical, electrical or morphological dysfunction of the myocardium, it is expected that we would observe lower levels of CYP2J2 in non-ischemic tissue compared to control and ischemic tissue.

In untreated rat liver microsomes, the ratio of total CYPs to POR is reported to be approximately 23:1 (Estabrook et al., 1971). In a different study using rat liver microsomes, Reed et al. immunochemically measured the ratio of total CYPs to POR to be about 5:1 (Reed et al., 2011). In this study, control human cardiac tissue, the ratio of CYP2J2 to POR was approximately 1:12 which was similar to the ratio in ischemic cardiac tissue (1:11) and non-ischemic cardiac tissue (1:15). Functions of POR in cardiac tissue remain largely unknown. Loss of POR in mouse was shown to be lethal during embryogenesis (Shen et al., 2002). However,

conditional knockout of cardiomyocyte-specific POR mice did not prove to be lethal (Fang et al., 2008). Because of the maintenance of POR levels in cardiac tissue, one might infer that POR possesses important roles in cardiac homeostasis in addition to metabolism.

Looking at sEH levels, control cardiac tissue has significantly higher sEH (encoded by *EPHX2*) than diseased tissue (Figure 4.9 C). Due to cardioprotective function of EETs, lower EPHX2 protein in diseased cardiac tissue leads to higher EET levels and less degradation to the less active DHETs. This result is consistent with the lower level of EPHX2 transcripts observed in ischemic human heart failure (Monti et al., 2008).

4.5. CONCLUSION

Measurement of *cis*-EETs in cardiac tissue was consistent with the trend observed in erythrocyte membrane of control vs. SCA patients where control tissue had significantly higher *cis*-EETs compared to diseased tissue. Significantly lower *trans*-EET levels in diseased cardiac tissue relative to control tissue were observed due likely to cumulative apoptotic cardiomyocytes that led to an increasing loss of mitochondria. Mitochondria are the main source of cellular ROS (Lenaz, 2001). Quantitation of proteins involved in biosynthesis and biodegradation of EETs showed that control tissue generally had significantly higher protein levels of POR and EPHX2 than in diseased tissues. The role of POR in altering EET levels remains unclear given that it is expressed at higher levels than CYP2J2 and therefore unlikely to be the limiting factor in CYP2J2 catalytic turnover. We expected lower EPHX2 protein levels in diseased cardiac tissue in order to prevent further hydrolysis of EETs and to prolong their cardioprotective duration of action and our data is supportive of this hypothesis (Widstrom et al., 2001).

Unfortunately, quantitation of a few proteins involved in formation and degradation of EETs, such as cPLA$_2\alpha$, Lp-PLA$_2$, and LPCAT1 and a stress-marker protein, HMOX1 were not fruitful due to levels being under the limits of detection. Furthermore, the native structures of these proteins need to be considered carefully for mass spectral determination. If post-translational modifications occur in these proteins, especially in the peptides used for quantification, then such modifications could alter protein yield during the protein isolation steps. To achieve optimal results, protein isolation steps might have to be optimized for each protein.

There are several limitations in this study. Of note, there was a lack of information available on the disease state of each heart tissue and the assumption that all auxiliary enzymes involved in biosynthesis and biodegradation of EETs were not changing with disease state. In terms of the disease progression of our heart tissue, we assumed they were close to the end-stage since the patients were undergoing a heart transplant or an LVAD. However, better information regarding the severity of CVD progression could potentially explain some of the variability observed in both EET and protein levels. Finally, while data obtained with the *trans*-EETs are very interesting, and their levels seem to vary with disease state, further work is necessary to determine the role *trans*-EETs play in cardiac health and disease.

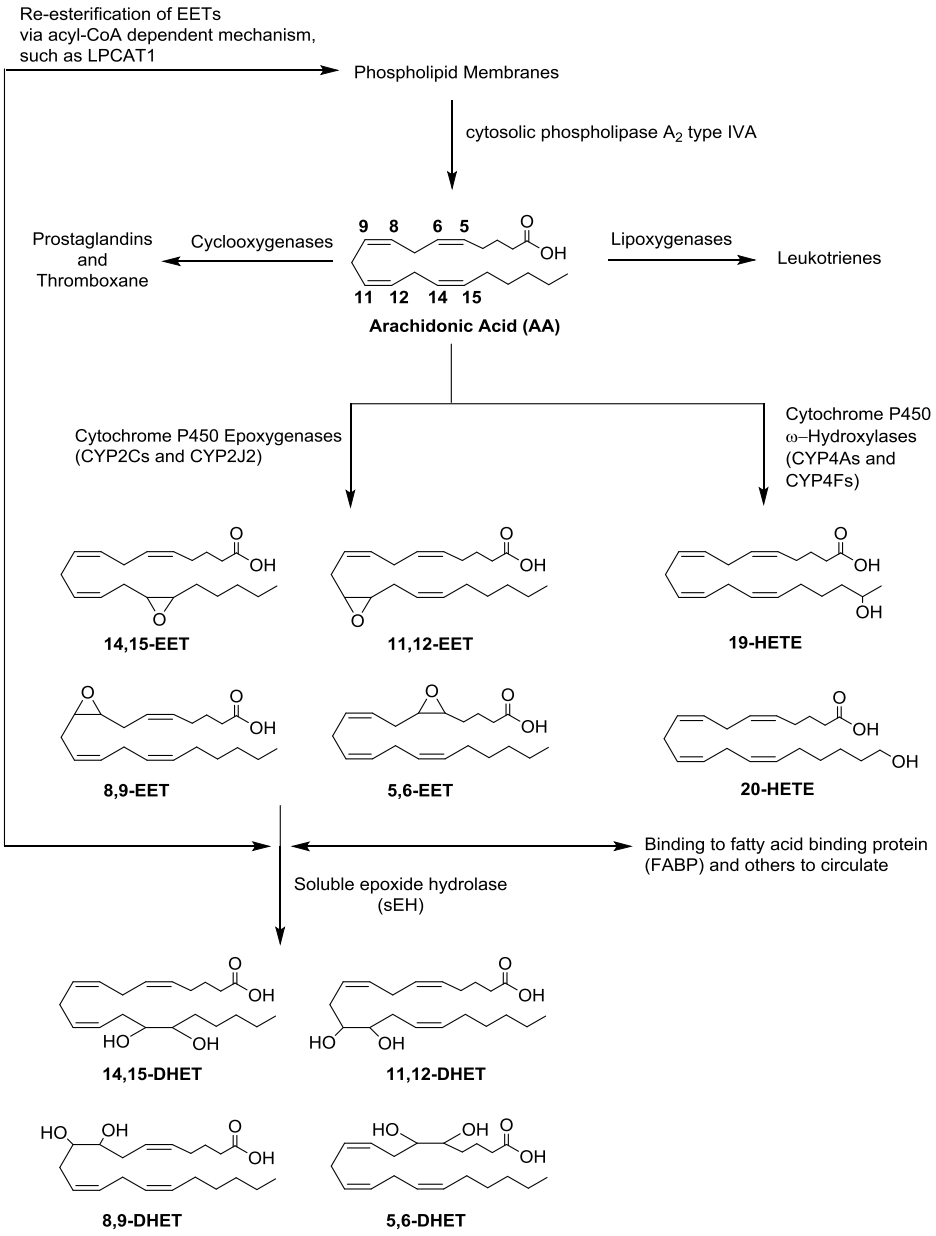

Figure 4.1. AA metabolic pathway focused on the formation of CYP mediated eicosanoids. Upon activation of cPLA$_2\alpha$ (encoded by *PLA2G4A*), AA is released from the phospholipid membrane. AA can be metabolized by cyclooxygenases to generate prostaglandins and thromboxane or by lipoxygenases to form leukotrienes. CYPs require NADPH-Cytochrome P450 Oxidoreductase (*POR*) to transfer electrons to initiate their catalytic cycle. CYP epoxygenases notably CYP2Cs and CYP2J2 will mediate biotransformation of AA to exclusively four regioisomers of *cis*-EETs. Once formed, EETs can either be incorporated back into the phospholipid membrane via acyl-CoA such as lysophosphatidylcholine acyltransferase 1 (*LPCAT1*), bound to other proteins to circulate or hydrolyzed by sEH to generate DHETs.

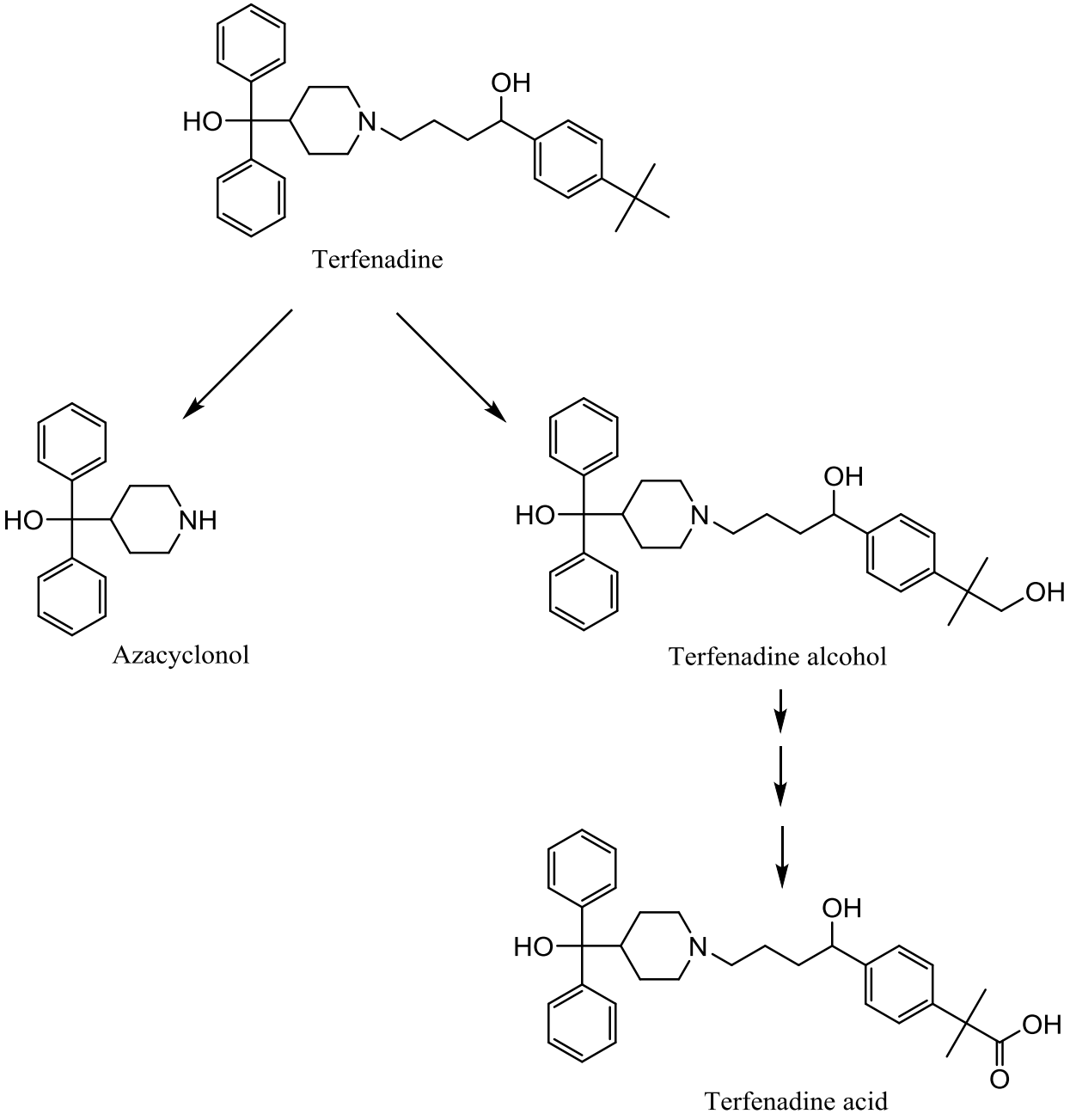

Figure 4.2. CYP-mediated terfenadine metabolic pathway.

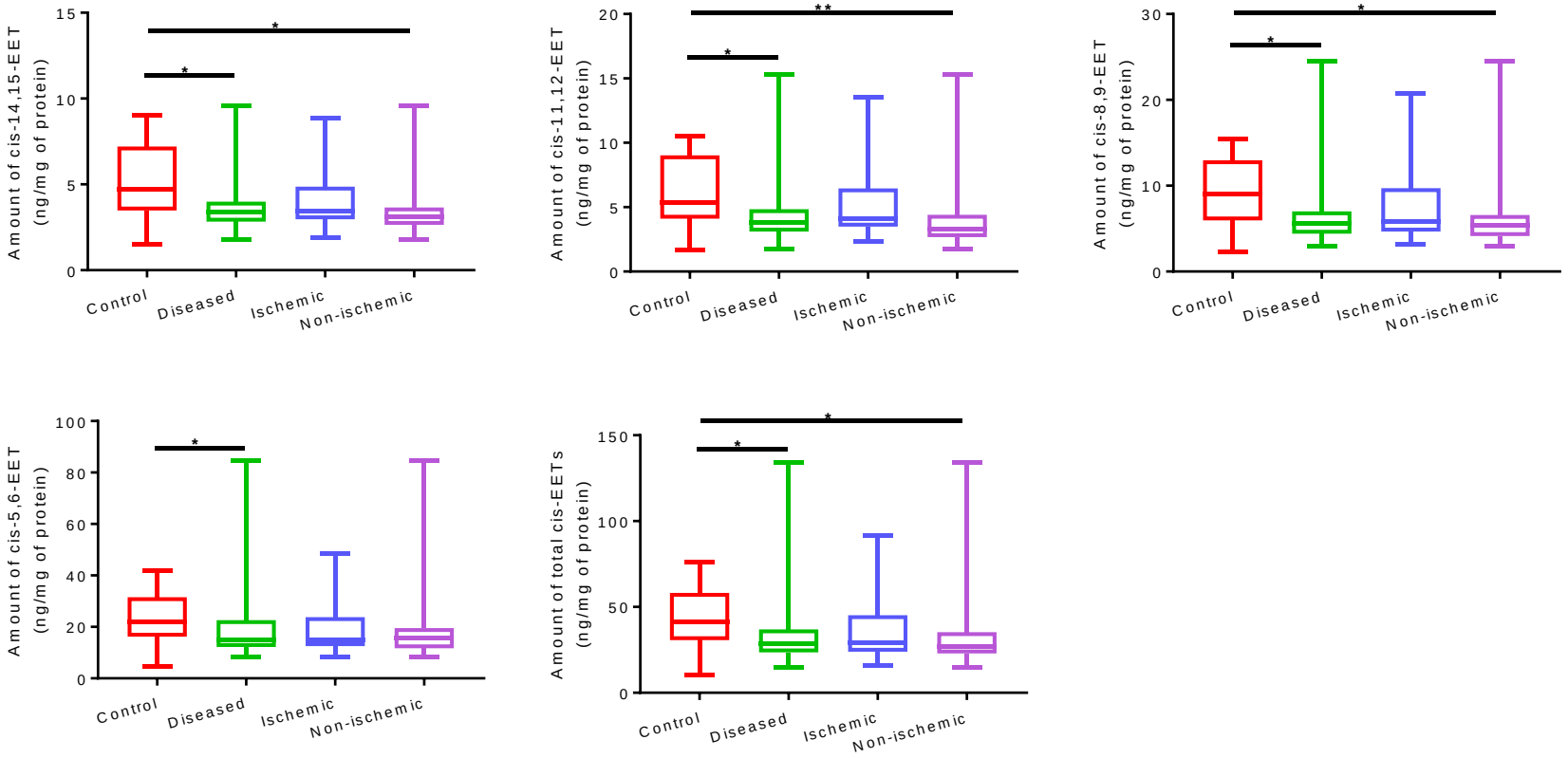

Figure 4.3. Amount of each *cis*- EET and total *cis*-EETs extracted from control and diseased human cardiac tissues. ** indicates $p \leq 0.01$, and * indicates $p \leq 0.05$.

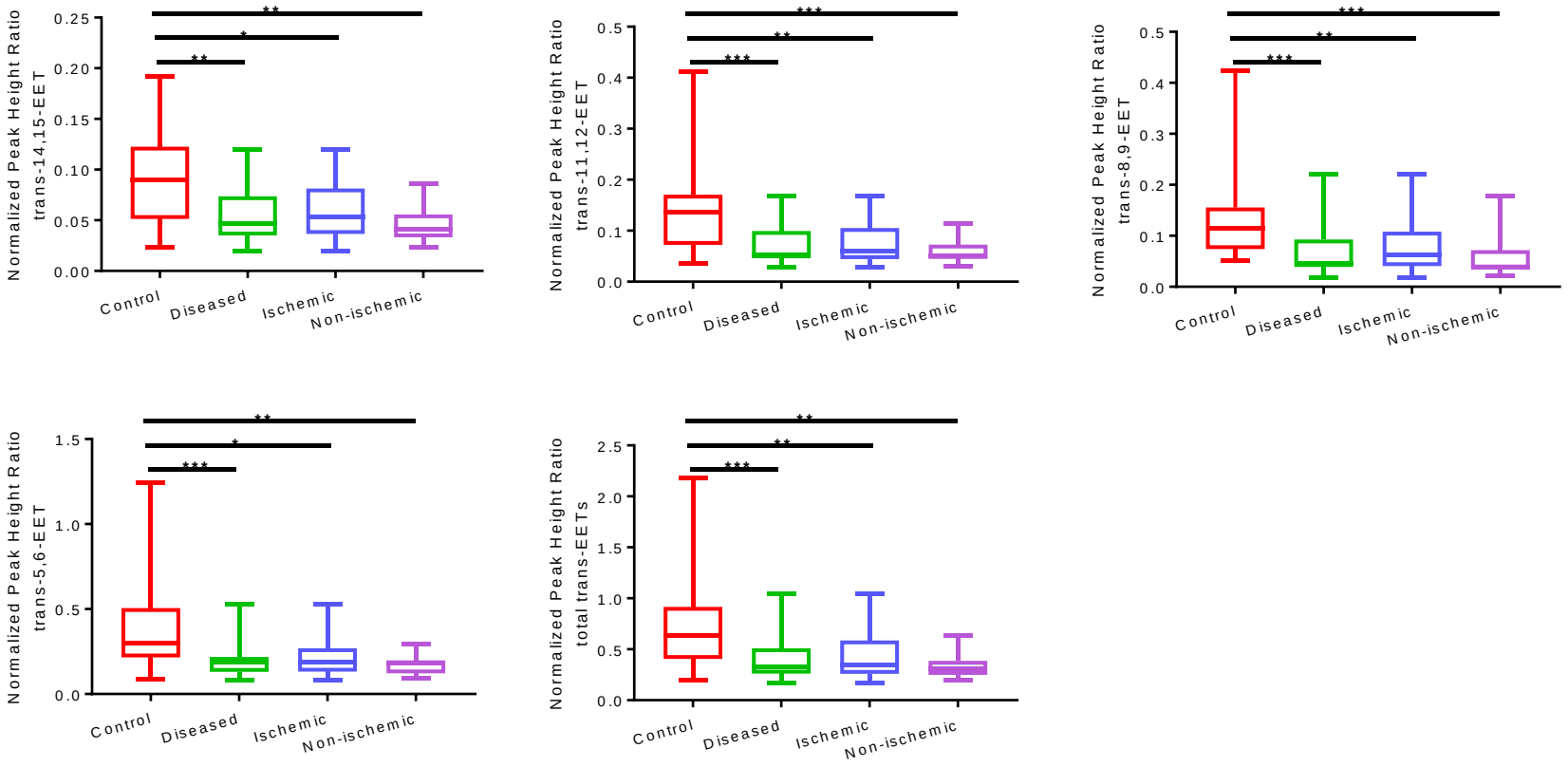

Figure 4.4. Normalized peak height ratio of each *trans*-regioisomer of EETs and total *trans*-EETs extracted from control and diseased human cardiac tissues. *** indicates $p \leq 0.001$, ** indicates $p \leq 0.01$, and * indicates $p \leq 0.05$.

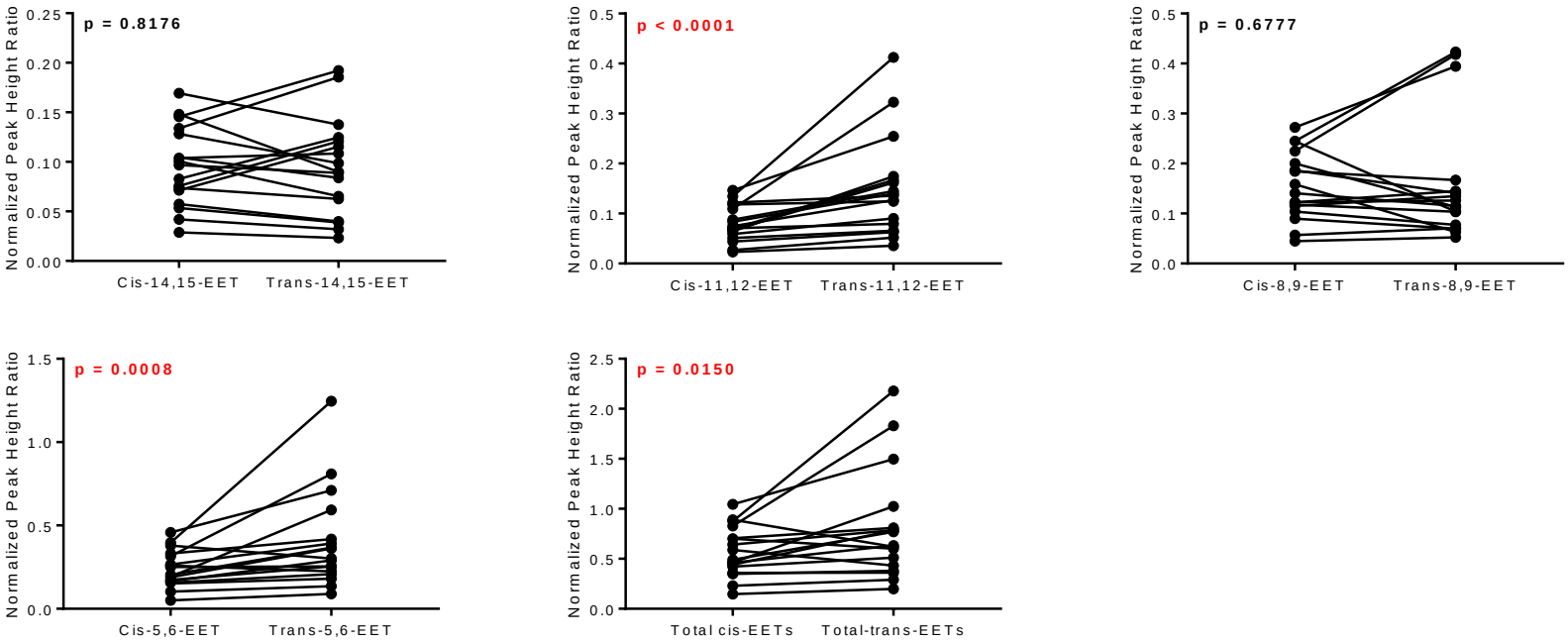

Figure 4.5. Levels of *cis*-EETs and trans-EETs among the different regioisomers in control cardiac tissue.

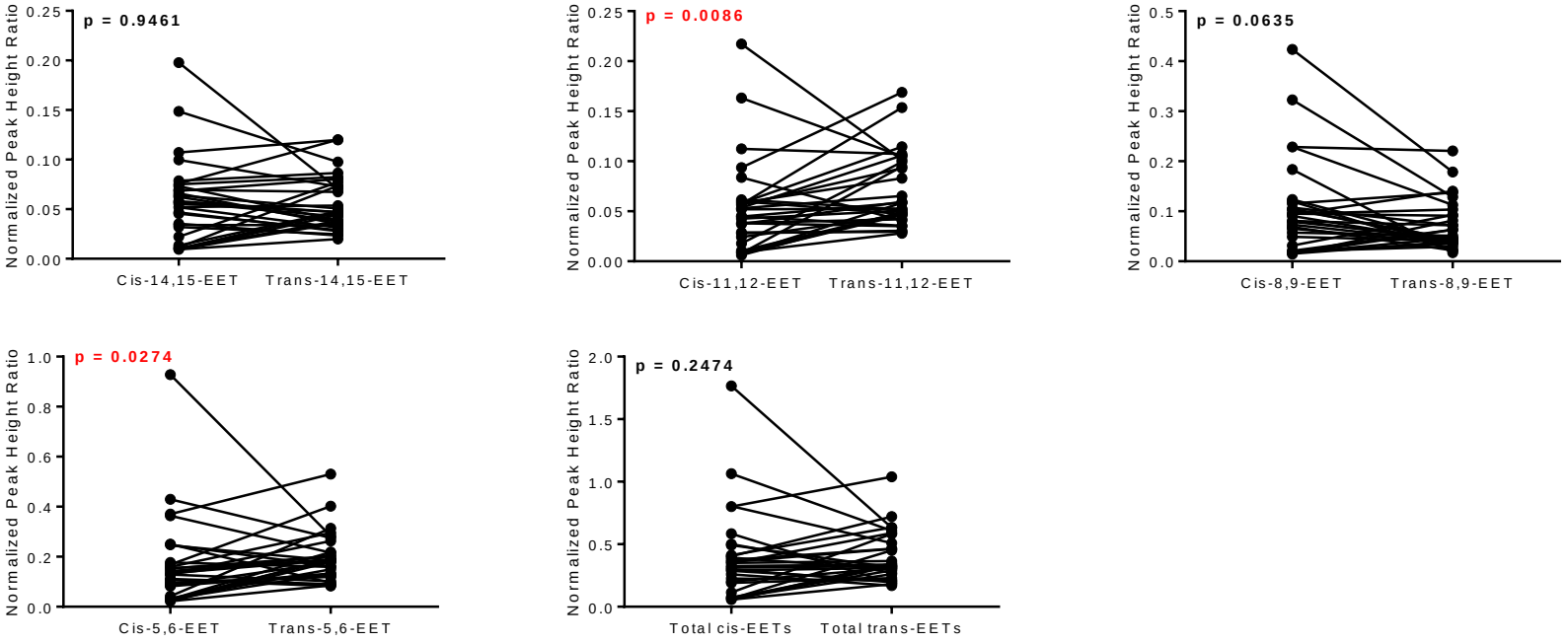

Figure 4.6. Levels of *cis*-EETs and corresponding *trans*-EETs in diseased cardiac tissue.

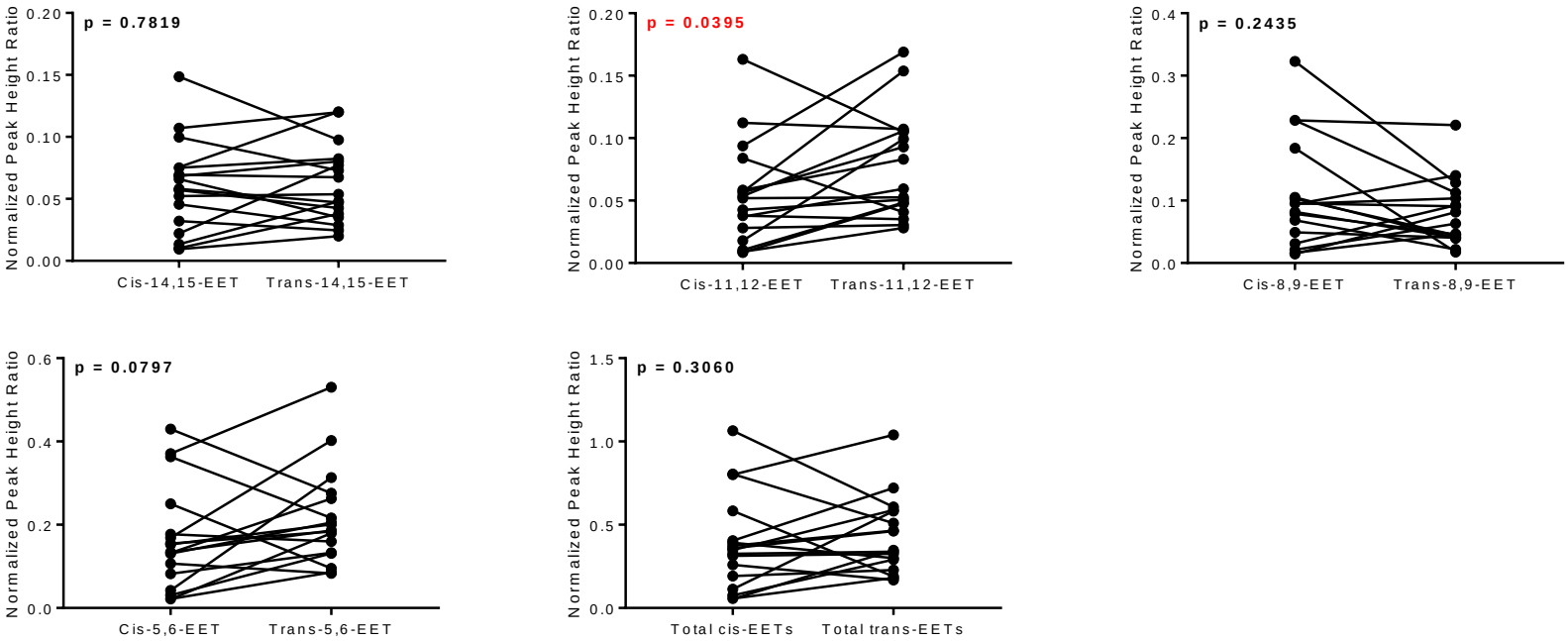

Figure 4.7. Levels of individual *cis*-EETs compared to the corresponding individual *trans*-EETs in ischemic cardiac tissue.

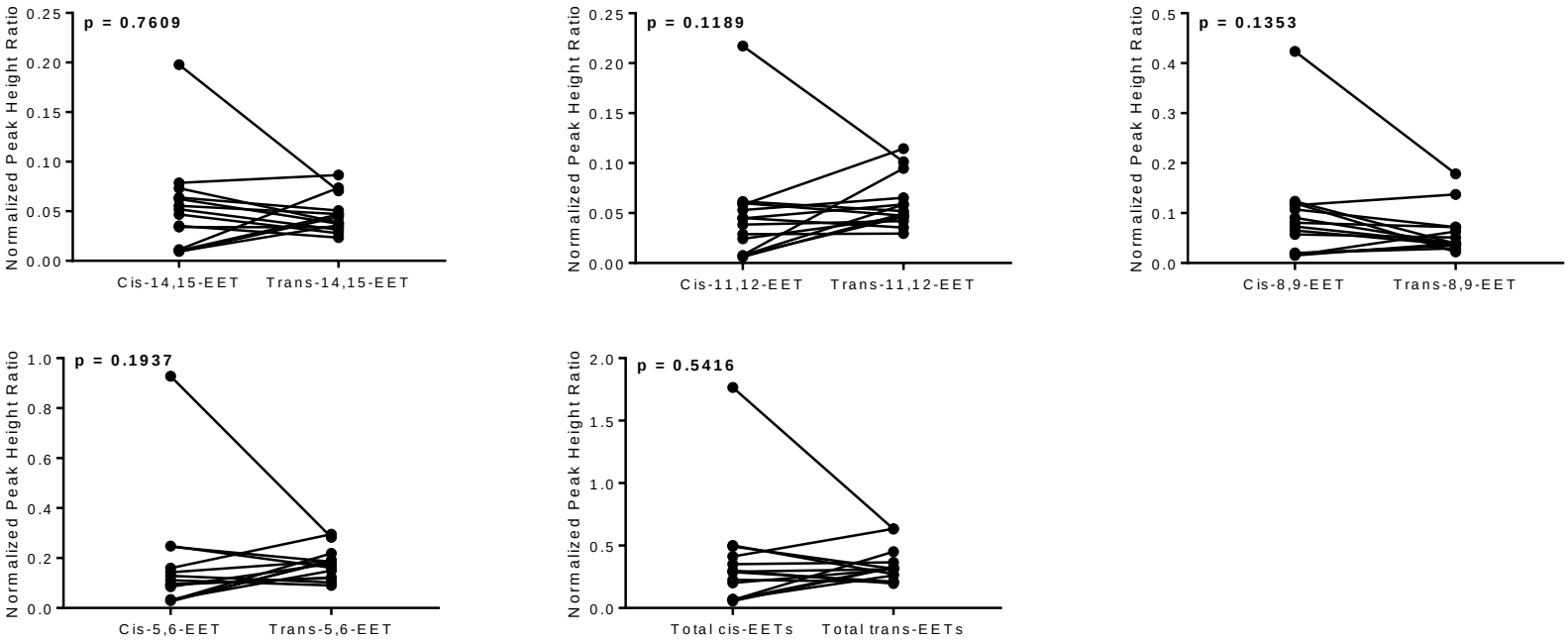

Figure 4.8. Levels of individual *cis*-EET and corresponding *trans*-EET regioisomers in non-ischemic cardiac tissue.

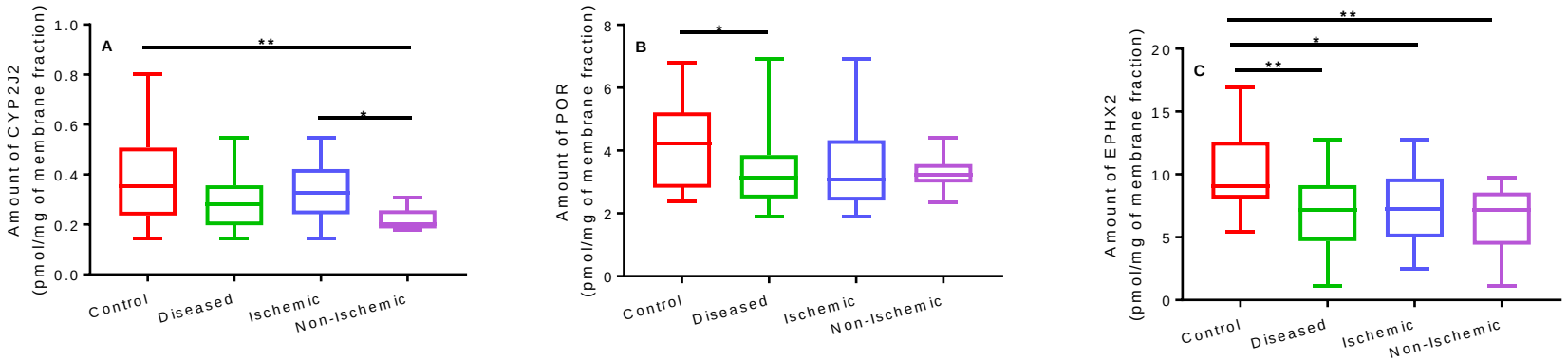

Figure 4.9. Quantitation of proteins involved in biosynthesis and biodegradation of EETs. Amount of (A) CYP2J2, (B) POR, and (C) EPHX2 proteins extracted from human cardiac tissue (N = 17 for control tissue, N = 17 for ischemic tissue, N = 11 for non-ischemic tissue, and diseased tissue was the sum of ischemic and non-ischemic tissue).

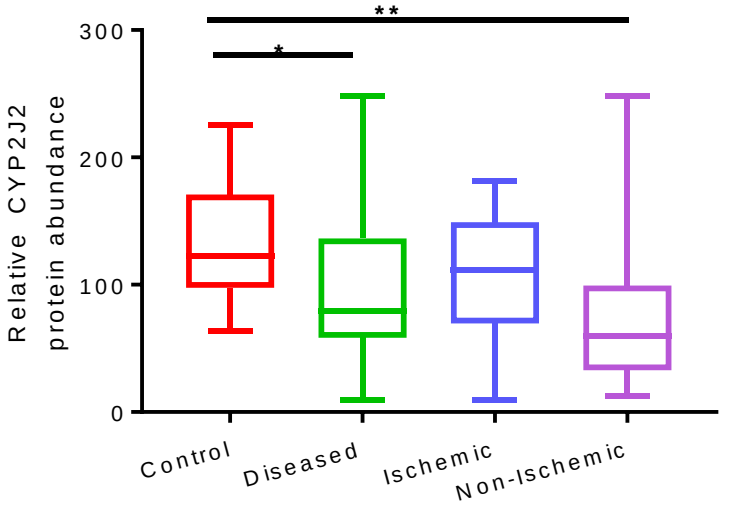

Figure 4.10. Relative CYP2J2 abundance extracted from human cardiac tissue.

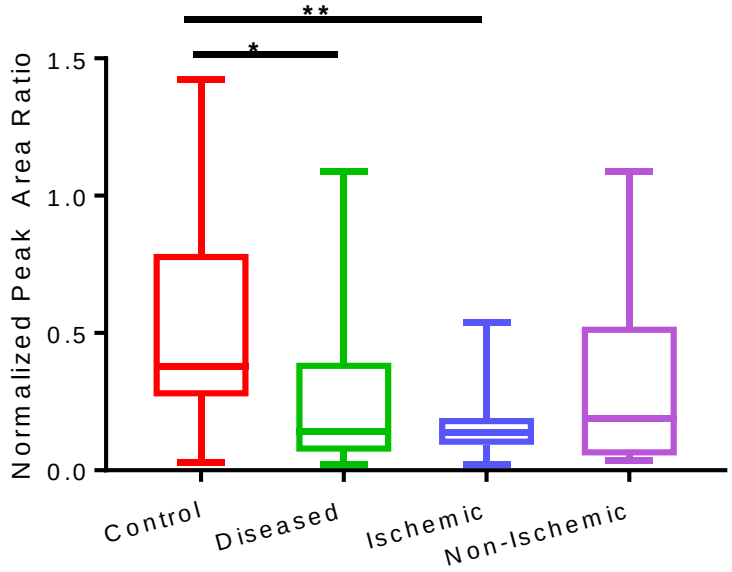

Figure 4.11. Total terfenadine metabolites (alcohol + acid) formed using control and diseased cardiac tissue homogenates.
** indicates $p \leq 0.01$ and * indicates $p \leq 0.05$.

Table 4.1. List of peptides and mass spectrometric parameters for CYP2J2, EPHX2, POR, PLA2G4A, PLA2G7, and HMOX1 protein quantification.

Protein	Peptide sequence	Light/Heavy	Parent ion	Product ion	Retention time (min)	CE (eV)	DP (V)
CYP2J2	VIGQGQQPSTAAR	Light	656.85	915.46	8.3	32.5	69
				730.38			
				602.33			
		Heavy	661.86	925.47			
				740.39			
				612.33			81.1
	EVTVDTTLAGYHLPK	Light	548.63	785.43	14.2	22.4	61.1
				714.39			
				608.32			
		Heavy	551.3	793.44			
				722.41			
				612.33			71.5
	LLDEVTYLEASK	Light	690.87	910.49	14.8	33.7	71.5
				811.42			

				710.37			
		Heavy	694.87	918.5			
				819.43			
				718.39			70.9
EPHX2	VC[CAM]EAGGLFVNSPEEPSLSR	Light	683.33	914.46	14.5	30	70.9
				559.32			
				457.73			
		Heavy	686.67	924.47			
				569.33			
				462.74			57.8
	GLLNDAFQK	Light	503.27	835.43	13.9	22	57.8
				722.35			
				608.3			
		Heavy	507.28	843.45			
				730.36			
				616.32			72.2
	ASPSEVVFLDDIGANLKPAR	Light	700.38	764.93	17.4	30.7	72.2

				715.39			
				647.69			
		Heavy	703.71	769.93			
				720.4			
				651.02			55.9
POR	FAVFGLGNK	Light	476.77	734.42	15.5	21	55.9
				635.35			
				488.28			
		Heavy	480.77	742.43			
				643.37			
				496.3			57.8
	YYSIASSSK	Light	503.25	842.43	9.7	25	57.8
				679.36			
				592.33			
		Heavy	507.26	850.44			
				687.38			
				600.34			61.4

LPCAT1	NPALYASNVR	Light	552.79	893.48	10.4	61.4	28.8
				822.45			
				709.36			
		Heavy	557.80	903.49			
				832.46			
				719.37		48	28.8
	TC[CAM]LITFKPGAFIPGAPVQPVVLR	Light	827.81	1132.68	18.3	81.5	37.6
				907.57			
			827.81	566.85			
		Heavy	831.14	1142.69			
				917.58			
				571.85		58.5	
PLA2G4A	IDPYVFDR	Light	512.76	796.40	13.7	58.5	22.3
				536.28			
				398.70			
		Heavy	517.76	806.41			
				546.29			

				403.71		83.1	
PLA2G7	YPLVVFSHGLGAFR	Light	521.62	651.87	17.3	59.1	26
			521.62	595.33			
			521.62	467.27			
		Heavy	524.96	656.87			
			524.96	600.33			
			524.96	470.60		53.1	
	.ASLAFLQK	Light	439.26	719.45	13.7	53.1	20
			439.26	606.36			
			439.26	535.32			
		Heavy	443.27	727.46			
			443.27	614.38			
			443.27	543.34		75.8	
HMOX1	TEPELLVAHAYTR	Light	750.40	930.52	13	75.8	35.9
			750.40	817.43			
			750.40	635.35			
		Heavy	755.40	940.52			

			755.40	827.44			
			755.40	640.36		79.2	
BSA	AEFVEVTK	Light	461.75	722.41	10.7	21.5	54.8
				575.34			
				476.27			
		Heavy	465.75	730.42			
				583.35			
				484.29			63.6
	LVNELTEFAK	Light	582.32	951.48	14.4	25	63.6
				595.31			
				218.15			
		Heavy	586.33	959.49			
				603.32			
				226.16			51.3
NaKATPase	AAVPDAVGK	Light	414.23	685.39	8.9	23.8	51.3
				586.32			
				489.27			

		Heavy	418.24	693.4 594.33 497.28			 45
	LSLDELHR	Light Heavy	328.18 331.52	435.23 391.71 440.23 396.72	11.7	15.4	45 48.2
LDH	LNLVQR	Light Heavy	371.73 376.74	515.33 228.13 525.34 228.13	10.3	22.2	48.2 56.1
	FIIPQIVK	Light Heavy	479.31 483.32	697.46 584.38 705.47 592.39	16.4	21.1	56.1

Table 4.2. Liquid chromatography gradient used to separate different peptides from digested protein of interest.

Time (min)	Flow rate (mL/min)	% A	% B
0	0.3	97	3
4.0	0.3	97	3
8.0	0.3	87	13
18.0	0.3	70	30
22.9	0.3	60	40
23.0	0.3	40	60
23.1	0.3	97	3
27	0.3	97	3

Table 4.3. Mass transitions and mass spectrometer parameters for terfenadine metabolites and internal standard, midazolam.

	Mass transition	DP (V)	CE (V)
Terfenadine alcohol	488.3 > 452.2	100	40
Terfenadine acid	502.4 > 466.3	50	30
Azacyclonol	267.8 > 91.15	91	39
Midazolam	326.0 > 291.2	90	40

REFERENCES

Aebersold R, Burlingame AL, and Bradshaw RA (2013) Western blots versus selected reaction monitoring assays: time to turn the tables? *Mol Cell Proteomics* **12:**2381-2382.

Akagi S, Kono N, Ariyama H, Shindou H, Shimizu T, and Arai H (2016) Lysophosphatidylcholine acyltransferase 1 protects against cytotoxicity induced by polyunsaturated fatty acids. *FASEB J* **30:**2027-2039.

Aliwarga T, Raccor BS, Lemaitre RN, Sotoodehnia N, Gharib SA, Xu L, and Totah RA (2017) Enzymatic and free radical formation of cis- and trans- epoxyeicosatrienoic acids in vitro and in vivo. *Free Radic Biol Med* **112:**131-140.

Clark JD, Lin LL, Kriz RW, Ramesha CS, Sultzman LA, Lin AY, Milona N, and Knopf JL (1991) A novel arachidonic acid-selective cytosolic PLA2 contains a Ca(2+)-dependent translocation domain with homology to PKC and GAP. *Cell* **65:**1043-1051.

Daniels LB, Laughlin GA, Sarno MJ, Bettencourt R, Wolfert RL, and Barrett-Connor E (2008) Lipoprotein-associated phospholipase A2 is an independent predictor of incident coronary heart disease in an apparently healthy older population: the Rancho Bernardo Study. *J Am Coll Cardiol* **51:**913-919.

de Groot H and Rauen U (2007) Ischemia-reperfusion injury: processes in pathogenetic networks: a review. *Transplant Proc* **39:**481-484.

Delozier TC, Kissling GE, Coulter SJ, Dai D, Foley JF, Bradbury JA, Murphy E, Steenbergen C, Zeldin DC, and Goldstein JA (2007) Detection of human CYP2C8, CYP2C9, and CYP2J2 in cardiovascular tissues. *Drug Metab Dispos* **35:**682-688.

Deshane J, Wright M, and Agarwal A (2005) Heme oxygenase-1 expression in disease states. *Acta Biochim Pol* **52:**273-284.

Estabrook RW, Franklin MR, Cohen B, Shigamatzu A, and Hildebrandt AG (1971) Biochemical and genetic factors influencing drug metabolism. Influence of hepatic microsomal mixed function oxidation reactions on cellular metabolic control. *Metabolism* **20:**187-199.

Eto M, Shindou H, Koeberle A, Harayama T, Yanagida K, and Shimizu T (2012) Lysophosphatidylcholine acyltransferase 3 is the key enzyme for incorporating arachidonic acid into glycerophospholipids during adipocyte differentiation. *Int J Mol Sci* **13:**16267-16280.

Fang C, Gu J, Xie F, Behr M, Yang W, Abel ED, and Ding X (2008) Deletion of the NADPH-cytochrome P450 reductase gene in cardiomyocytes does not protect mice against doxorubicin-mediated acute cardiac toxicity. *Drug Metab Dispos* **36:**1722-1728.

Goulitquer S, Dréano Y, Berthou F, Corcos L, and Lucas D (2008) Determination of epoxyeicosatrienoic acids in human red blood cells and plasma by GC/MS in the NICI mode. *J Chromatogr B Analyt Technol Biomed Life Sci* **876:**83-88.

Karara A, Dishman E, Blair I, Falck JR, and Capdevila JH (1989) Endogenous epoxyeicosatrienoic acids. Cytochrome P-450 controlled stereoselectivity of the hepatic arachidonic acid epoxygenase. *J Biol Chem* **264:**19822-19827.

Kolodgie FD, Burke AP, Skorija KS, Ladich E, Kutys R, Makuria AT, and Virmani R (2006) Lipoprotein-associated phospholipase A2 protein expression in the natural progression of human coronary atherosclerosis. *Arterioscler Thromb Vasc Biol* **26:**2523-2529.

Lemaitre RN, Johnson CO, Hesselson S, Sotoodehnia N, Sotoodhenia N, McKnight B, Sitlani CM, Rea TD, King IB, Kwok PY, Mak A, Li G, Brody J, Larson E, Mozaffarian D, Psaty BM, Huertas-Vazquez A, Tardif JC, Albert CM, Lyytikäinen LP, Arking DE, Kääb S, Huikuri HV, Krijthe BP, Eijgelsheim M, Wang YA, Reinier K, Lehtimäki T, Pulit SL, Brugada R, Müller-Nurasyid M, Newton-Cheh CH, Karhunen PJ, Stricker BH, Goyette P, Rotter JI, Chugh SS, Chakravarti A, Jouven X, and Siscovick DS (2014) Common variation in fatty acid metabolic genes and risk of incident sudden cardiac arrest. *Heart Rhythm* **11:**471-477.

Lenaz G (2001) The mitochondrial production of reactive oxygen species: mechanisms and implications in human pathology. *IUBMB Life* **52:**159-164.

Lin LL, Wartmann M, Lin AY, Knopf JL, Seth A, and Davis RJ (1993) cPLA2 is phosphorylated and activated by MAP kinase. *Cell* **72:**269-278.

Marin-Garcia J, Goldenthal MJ, and Moe GW (2001) Mitochondrial pathology in cardiac failure. *Cardiovasc Res* **49:**17-26.

Maron BJ, Towbin JA, Thiene G, Antzelevitch C, Corrado D, Arnett D, Moss AJ, Seidman CE, Young JB, Association AH, Council on Clinical Cardiology HaFaTC, Groups QoCaORaFGaTBIW, and Prevention CoEa (2006) Contemporary definitions and classification of the cardiomyopathies: an American Heart Association Scientific Statement from the Council on Clinical Cardiology, Heart Failure and Transplantation Committee; Quality of Care and Outcomes Research and Functional Genomics and Translational Biology Interdisciplinary Working Groups; and Council on Epidemiology and Prevention. *Circulation* **113:**1807-1816.

Minuz P, Jiang H, Fava C, Turolo L, Tacconelli S, Ricci M, Patrignani P, Morganti A, Lechi A, and McGiff JC (2008) Altered release of cytochrome p450 metabolites of arachidonic acid in renovascular disease. *Hypertension* **51:**1379-1385.

Moessinger C, Kuerschner L, Spandl J, Shevchenko A, and Thiele C (2011) Human lysophosphatidylcholine acyltransferases 1 and 2 are located in lipid droplets where they catalyze the formation of phosphatidylcholine. *J Biol Chem* **286:**21330-21339.

Monti J, Fischer J, Paskas S, Heinig M, Schulz H, Gösele C, Heuser A, Fischer R, Schmidt C, Schirdewan A, Gross V, Hummel O, Maatz H, Patone G, Saar K, Vingron M, Weldon SM, Lindpaintner K, Hammock BD, Rohde K, Dietz R, Cook SA, Schunck WH, Luft FC, and Hubner N (2008) Soluble epoxide hydrolase is a susceptibility factor for heart failure in a rat model of human disease. *Nat Genet* **40:**529-537.

Oni-Orisan A, Edin ML, Lee JA, Wells MA, Christensen ES, Vendrov KC, Lih FB, Tomer KB, Bai X, Taylor JM, Stouffer GA, Zeldin DC, and Lee CR (2016) Cytochrome P450-derived epoxyeicosatrienoic acids and coronary artery disease in humans: a targeted metabolomics study. *J Lipid Res* **57:**109-119.

Prasad B, Evers R, Gupta A, Hop CE, Salphati L, Shukla S, Ambudkar SV, and Unadkat JD (2014) Interindividual variability in hepatic organic anion-transporting polypeptides and P-glycoprotein (ABCB1) protein expression: quantification by liquid chromatography

tandem mass spectroscopy and influence of genotype, age, and sex. *Drug Metab Dispos* **42:**78-88.

Reed JR, Cawley GF, and Backes WL (2011) Inhibition of cytochrome P450 1A2-mediated metabolism and production of reactive oxygen species by heme oxygenase-1 in rat liver microsomes. *Drug Metab Lett* **5:**6-16.

Saraste A, Pulkki K, Kallajoki M, Heikkilä P, Laine P, Mattila S, Nieminen MS, Parvinen M, and Voipio-Pulkki LM (1999) Cardiomyocyte apoptosis and progression of heart failure to transplantation. *Eur J Clin Invest* **29:**380-386.

Shen AL, O'Leary KA, and Kasper CB (2002) Association of multiple developmental defects and embryonic lethality with loss of microsomal NADPH-cytochrome P450 oxidoreductase. *J Biol Chem* **277:**6536-6541.

Sun N, Youle RJ, and Finkel T (2016) The Mitochondrial Basis of Aging. *Mol Cell* **61:**654-666.

Theken KN, Schuck RN, Edin ML, Tran B, Ellis K, Bass A, Lih FB, Tomer KB, Poloyac SM, Wu MC, Hinderliter AL, Zeldin DC, Stouffer GA, and Lee CR (2012) Evaluation of cytochrome P450-derived eicosanoids in humans with stable atherosclerotic cardiovascular disease. *Atherosclerosis* **222:**530-536.

Weintraub NL, Fang X, Kaduce TL, VanRollins M, Chatterjee P, and Spector AA (1997) Potentiation of endothelium-dependent relaxation by epoxyeicosatrienoic acids. *Circ Res* **81:**258-267.

Widstrom RL, Norris AW, and Spector AA (2001) Binding of cytochrome P450 monooxygenase and lipoxygenase pathway products by heart fatty acid-binding protein. *Biochemistry* **40:**1070-1076.

Wu S, Moomaw CR, Tomer KB, Falck JR, and Zeldin DC (1996) Molecular cloning and expression of CYP2J2, a human cytochrome P450 arachidonic acid epoxygenase highly expressed in heart. *J Biol Chem* **271:**3460-3468.

Xu M, Bhatt DK, Yeung CK, Claw KG, Chaudhry AS, Gaedigk A, Pearce RE, Broeckel U, Gaedigk R, Nickerson D, Schuetz E, Rettie AE, Leeder S, Thummel KE, and Prasad B

(2017) Genetic and Non-genetic Factors Associated with Protein Abundance of Flavin-containing Monooxygenase 3 in Human Liver. *Journal of Pharmacology and Experimental Therapeutics*.

Yet SF, Layne MD, Liu X, Chen YH, Ith B, Sibinga NE, and Perrella MA (2003) Absence of heme oxygenase-1 exacerbates atherosclerotic lesion formation and vascular remodeling. *FASEB J* **17:**1759-1761.

Yet SF, Tian R, Layne MD, Wang ZY, Maemura K, Solovyeva M, Ith B, Melo LG, Zhang L, Ingwall JS, Dzau VJ, Lee ME, and Perrella MA (2001) Cardiac-specific expression of heme oxygenase-1 protects against ischemia and reperfusion injury in transgenic mice. *Circ Res* **89:**168-173.

Yu Z, Xu F, Huse LM, Morisseau C, Draper AJ, Newman JW, Parker C, Graham L, Engler MM, Hammock BD, Zeldin DC, and Kroetz DL (2000) Soluble epoxide hydrolase regulates hydrolysis of vasoactive epoxyeicosatrienoic acids. *Circ Res* **87:**992-998.

Zhou J, Ahmad F, Parikh S, Hoffman NE, Rajan S, Verma VK, Song J, Yuan A, Shanmughapriya S, Guo Y, Gao E, Koch W, Woodgett JR, Madesh M, Kishore R, Lal H, and Force T (2016) Loss of Adult Cardiac Myocyte GSK-3 Leads to Mitotic Catastrophe Resulting in Fatal Dilated Cardiomyopathy. *Circ Res* **118:**1208-1222.

Chapter 5

GENERAL CONCLUSIONS AND FUTURE DIRECTIONS

5.1. GENERAL CONCLUSIONS

The overarching goal of this dissertation was to elucidate the protective role of epoxyeicosatrienoic acids (EETs) in ischemic cardiomyopathy. A cardiac-specific CYP2J2-overexpressing transgenic (Tr) mouse model, sudden cardiac arrest (SCA) patients and controls, and cardiac tissue from patients with cardiovascular disease (CVD) and controls were used to achieve this goal. In addition, formation of enzymatic and non-enzymatic EETs was explored in *in vitro* studies in both benzene and liposomes. Due to the susceptibility of arachidonic acid (AA) to autoxidation by both light and air, an optimized *in vitro* protocol for AA incubations in reconstituted recombinant Cytochrome P450 2J2J (CYP2J2) was developed to minimize non-enzymatic oxidation during P450 catalysis.

The *in vitro* studies revealed that metabolism of AA by recombinant CYP2J2 formed exclusively *cis*-EETs while both *cis*- and *trans*-EETs were generated by autoxidation. Free radical oxidation of AA in both benzene and liposomes exhibited time- and AA concentration-dependent formation of both *cis*- and *trans*-EETs with preference for *trans*-EETs. AA readily autoxidizes with light and air and posed a challenge when trying to minimize oxidation under air in CYP incubations. The catalytic cycle of P450 involves incorporation of molecular oxygen; therefore, performing the incubation anaerobically was not an option. Addition of catalase and superoxide dismutase did not reduce non-enzymatic oxidation products of AA. However, addition of the iron chelating agent, DETAPAC, and the hydrogen peroxide scavenger, pyruvate, proved to be successful in minimizing non-enzymatic production of *cis*-EETs (< 8%, except 5,6-EET that is intrinsically unstable). AA also adsorbs to many surfaces which posed another challenge in making accurate dilutions. Dilutions of AA had to be made directly from the AA stock solution into polypropylene tubes because AA adheres least to polypropylene surface

compared to glass or silanized glass surface. Additionally, autoxidation of AA is minimal in 0.06% ethanolic solution.

Cardiac-specific CYP2J2-overexpression in our mouse model led to significantly higher levels of cardiac *cis*- and *trans*-EETs in Tr mice compared to their wild-type (WT) counterparts. A significant positive correlation between total *cis*-EETs in cardiac tissue and erythrocyte membranes, established in our Tr mouse model, indicated that CYP2J2-mediated *cis*-EETs could potentially report on cardiac events. With age as a stressor, EET levels were altered. Independent of mouse genotype, both *cis*- and *trans*-EETs extracted from erythrocyte membranes increased with age. Cardiac *cis*- and *trans*-EETs were also altered with age, but this appeared to be regioisomer-specific. The age range for our mouse population in this study was relatively narrow and it would be preferable to have a study with multiple mice at varying ages to better ascertain the effect of age on EET levels.

When our mouse model was exposed to an experimentally-induced two-week myocardial infarction (MI), cardiac-specific overexpressing CYP2J2 Tr mice exhibited higher *cis*-EETs compared to their WT-MI counterparts and were better protected from the consequences of MI. This finding was corroborated with echocardiographic and histological data that demonstrated significantly better cardiac contractility, significantly less pulmonary edema, smaller infarction size, lower myocardial fibrosis, lower number of apoptotic cells, and reduced reactive oxygen species (ROS) formation in Tr-MI mice. An interesting observation was that levels of *cis*-EETs in both sham and MI groups were significantly higher than their corresponding *trans*-EETs. While the *trans*-EETs findings are interesting, it was quite unexpected to observe their levels mirror the *cis*-EETs and more research in the future is needed to elucidate the importance of the *trans*-EETs and their role in tissue protection, if any.

Alteration in EET levels was also explored in human subjects. In a model of the acute cardiac condition, SCA, total erythrocyte membrane *cis*- and *trans*-EETs in control subjects were significantly higher than SCA cases. Similar to observations in our mouse model exposed to acute MI, levels of *trans*-EETs in erythrocyte membrane of both control and SCA groups were significantly lower than that of *cis*-EETs. To model chronic cardiac conditions, we extracted EETs from the ventricular cardiac tissue of control and diseased subjects. Control cardiac tissue had significantly higher *cis*- and *trans*-EETs than diseased cardiac tissue. From our *in vitro* studies, we found that *trans*-EETs were generated primarily through free radical oxidation. *In vivo*, free radical oxidation could be mediated by ROS produced through mitochondrial respiration. It was quite unexpected to observe lower *trans*-EET levels in diseased cardiac tissue compared to controls and we speculate that this is due perhaps to cumulative apoptotic cardiomyocytes associated with the disease state, which leads to cumulative mitochondrial loss. This loss of mitochondria, the main source of cellular ROS, could lead to lower ROS formation that in turn leads to lower *trans*-EET formation. Although not statistically significant, ischemic cardiac tissue appears to have elevated *trans*-EET levels, while non-ischemic cardiac tissue appears to be the opposite. A plausible explanation is possibly due to the nature of the cardiac disease. Ischemic cardiomyopathy involves blockage of oxygenated blood flow into the heart due to accumulation of plaque. On the other hand, non-ischemic cardiomyopathy involves electrical, mechanical, or morphological dysfunction of myocardium that will lead to more apoptosis of cardiomyocytes. Contingent on the type and progression of the disease, it has been reported that the number of apoptotic cardiomyocytes increases in both ischemic and non-ischemic cardiac tissue (Saraste et al., 1999).

Diseased tissue had lower protein levels of CYP2J2, EPHX2, and POR, which are enzymes involved in the biotransformation and biodegradation of EETs. When assessing the specific activity of CYP2J2 with terfenadine as the probe substrate, diseased tissue had lower CYP2J2 specific activity, the main cardiac AA epoxygenase. Lower protein levels of sEH was expected and observed, in diseased cardiac tissue to prevent further hydrolysis of EETs and to prolong their cardioprotective action (Widstrom et al., 2001).

5.2. Future Directions

Further studies are needed to validate the correlation between *cis*-EETs in erythrocyte membranes and cardiac tissue using specific CYP2J2 inhibitors. Mice overexpressing CYP2J2 in their cardiac tissue can be administered a specific CYP2J2 inhibitor followed by the measurement of EETs both in cardiac tissue and in erythrocyte membranes to establish if reduction in cardiac CYP2J2 function would also reduce EET levels in both tissues. However, this study is currently not feasible due to absence of CYP2J2 specific inhibitors that are useful as *in vivo* probes.

Another study is needed to systematically establish more accurately the effect of age on EET levels and associate them with vital signs at a wide range of age. As the mice get older, they may develop cardiovascular disease and other aging-related disease that we did not account for in our current studies. Because EETs appeared to be altered with age and CYP2J2 is not inducible by canonical CYP inducers, it would be interesting to determine if inflammation markers that increase with age could induce CYP2J2 expression and activity. In investigating the effect of age and disease in our mouse model, we found that individual regioisomers of EETs

were altered differentially. It will be useful in the future to explore the functions of each regioisomer of EETs in normal and diseased tissue and tease out the role for each epoxide.

To evalute alterations of EET levels in ischemic and non-ischemic cardiac tissues, additional tissue with a complete medical history including medication use is necessary. Only then is it possible to assess progression of the disease as well as other existing conditions that might impact EET levels, e.g. diabetes, hypertension etc. Finally, reports on the function of *trans*-EETs *in vivo* are scarce in the literature. Future studies should focus on the role that trans-EETs play in healthy and diseased tissue compared to cis-EETs and determine which geometric isomers are more important in maintaining cell function.

REFERENCES

Saraste A, Pulkki K, Kallajoki M, Heikkilä P, Laine P, Mattila S, Nieminen MS, Parvinen M, and Voipio-Pulkki LM (1999) Cardiomyocyte apoptosis and progression of heart failure to transplantation. *Eur J Clin Invest* **29:**380-386.

Widstrom RL, Norris AW, and Spector AA (2001) Binding of cytochrome P450 monooxygenase and lipoxygenase pathway products by heart fatty acid-binding protein. *Biochemistry* **40:**1070-1076.

VITA

Theresa Aliwarga was born in Jakarta, Indonesia. In 2004, she graduated from the University of Washington with a dual baccalaureate degree in Biochemistry and Chemistry. She then earned her M.S. degree in Medicinal Chemistry under the mentorship of Dr. Rory P. Remmel. Theresa then joined the Department of Medicinal Chemistry at the University of Washington as a graduate student, and joined Dr. Rheem A.Totah's laboratory in 2012.